Advancing Hydrogen Deuterium Exchange Mass Spectrometry Through the development of Novel Internal Exchange Reporters

Taylor Murphree

A dissertation submitted in partial fulfillment of the requirements for the degree of

Doctor of Philosophy

University of Washington

2023

Reading Committee members:

Miklos Guttman, Chair

Libin Xu

Gaurav Bhardwaj

Program Authorized to Offer Degree:

Medicinal Chemistry

University of Washington

Abstract

Advancing Hydrogen Deuterium Exchange Mass Spectrometry Through the development of Novel Internal Exchange Reporters

Taylor Murphree

Chair of the Supervisory Committee:

Miklos Guttman

Department of Medicinal Chemistry

Hydrogen deuterium exchange mass spectrometry (HDX-MS) is a powerful tool for protein structure analysis. The remarkable versatility and sensitivity of HDX-MS renders the technique uniquely well suited to probing challenging biological systems. Over the last two decades advancements in mass spectrometers, sample handling techniques, and software tools have brought HDX-MS into the mainstream by dramatically improving data quality. Despite this renaissance, HDX-MS measurements remain very challenging to reproduce. The strong solution dependence of the chemical process underlying amide HDX contributes significantly to irreproducibility; even small variations in temperature or pH can have a pronounced effect on the deuterium uptake by a protein. As a result, a myriad of controls have been developed to help the investigator identify and address variations in solution conditions. Among these controls are compounds which directly monitor the conditions under which amide exchange takes place. These compounds, referred to as internal exchange reporters (IERs), have been the focus of my graduate work in the Guttman Lab at the University of Washington. When my work in the area began, the concept of reporting controls had been well established. However, the reporters themselves, small unstructured peptides, were of limited utility. Under the guidance of Dr. Miklos Guttman and with the assistance of many brilliant and rather patient friends and colleagues I have been able to develop novel imidazolium based IERs. This document will describe the design, validation and subsequent refinement of these compounds through the discussion of previously published and ongoing work.

Contents

Chapter 1

overview

1.1 Introduction to HDX-MS

Hydrogen/deuterium exchange mass spectrometry (HDX-MS) exploits the natural exchange of hydrogens that occurs at backbone amides within proteins[63, 62, 35] In a folded protein, the exchange kinetics for individual amides are strongly influenced by the local electronic environment, the higher-order structure and solvent. The incorporated deuterium acts as a label along the backbone that can reveal information about each amide's relative accessibility in protein under the experimental conditions. The tools for measuring amide hydrogen exchange evolved considerably over the years[30, 33]. The pioneering experiments that provided the foundational theory of H/D exchange in proteins were accomplished using sensitive densitometry measurements of intact proteins in solution[63]. Initially using tritium instead of deuterium to do hydrogen/tritium exchange the technique was refined through the incorperation of proteolysis to localize exchange at the peptide level [34, 102, 29]. The foundational work and principles established from these early studies allowed HDX to be effectively coupled to mass spectrometry (MS) and offered advantages over previous methods of detection[71, 133]. The approach for most HDX-MS studies remains relatively simple. A protein, typically under native conditions, is transferred from an aqueous buffer to a deuterium-rich buffer and allowed to undergo exchange. The exchange process is then slowed and the levels of deuterium incorporation are readily measured with MS, thanks to the approximately one Dalton mass difference between the mass of a protium (1H) and a deuterium (2H) 1.2.

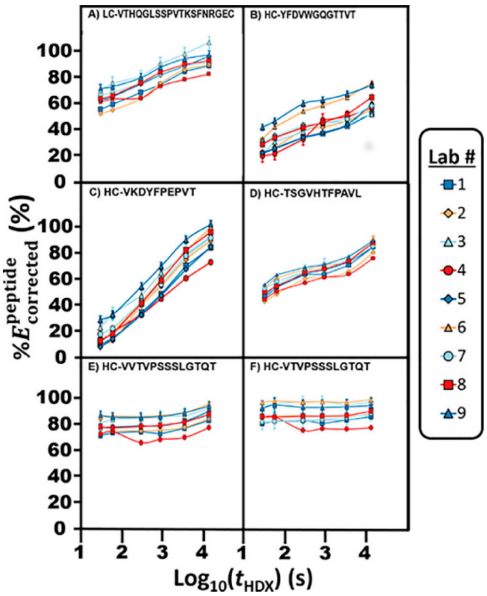

Figure 1.1: Various peptides from an interlab comparative HDX-MS study that controlled sample and labeling/quench buffers. Results for the same peptide from nine different laboratories are plotted to illustrate the interlab variability in the study. Reproduced with permission from [60]. Copyright 2019 American Chemical Society.

While the experimental concept is simple, there are many considerations necessary for obtaining and interpreting HDX-MS data sets. One of the reasons HDX-MS has been so successful is its inherent versatility; it can be applied to nearly any protein system, many of which are too large, flexible, heterogeneous, or sample limited to be analyzed by other existing structural tools. For instance, in 2011 Houde et. al. demonstrated how HDX-MS could be a valuable tool for establishing comparability in biopharmaceuticals by using the technique to map the effects of small structural defects on a protein with accuracy exceeding many more established techniques[58]. This study and many others since have noted considerable variation in HDX-MS measurements separated by extended periods of time or collected at different locations [60, 22, 134, 10, 109,

89]. In this chapter we will discuss the reasons underlying variability in HDX-MS data and the controls which have been developed to mitigate it. The tools and methods discussed here and in subsequent chapters have been developed for "bottom-up" HDX-MS experiments. In these experiments the deuterium labeled protein is cleaved into smaller peptides typically with an acid active non-specific protease like pepsin [84]. The resulting peptides are analyzed using liquid chromatography mass spectrometry (LC-MS) allowing for the resolution of global deuterium uptake at the peptide level.

1.2 Understanding the Analytical Performance of HDX-MS

In response to the widespread use and growing interest for regulatory filings, numerous studies have focused on the analytical performance of HDX-MS. Particular attention has been directed towards the assessment of the repeatability and reproducibility of HDX-MS studies. HDX-MS experiments conducted within in single lab on the same day often report very high precision, as little as 1% variation in deuterium uptake; as one would expect, when measurements are made over an extended period of time or carried out in different laboratories, variability increases [11, 10, 60]. Automated sample handling systems offer one way to reduce some of the variables and have been implemented in efforts to increase reproducibility of HDX-MS [10, 134]. Cummins et. al. demonstrated the potential of improving reproducibility by reporting impressively comparable HDX-MS data collected in two different labs[22]. In this particular study, the reagents and analyses were rigorously harmonized, and identical automated systems were used to eliminate platform dependency and provide better control over each step in the HDX-MS experiment. This example represents the highest possible level of reproducibility but requires a level of harmonization that cannot be realistically achieved by the majority of laboratories.

A study carried out by the National Institute of Standards and Technology (NIST) sought to provide a more practical indication of analytical performance by comparing HDX-MS data collected on a wide variety of platforms by a large group of independent investigators [60]. Participants in this study were provided with a kit containing buffer components, a fragment of a standardized monoclonal antibody designed and produced by NIST, in addition to explicit instructions. In doing so, NIST sought to minimize error arising from the forward exchange reaction as much as possible. Moreover, the study required numerous controls including a system-specific back-exchange correction (1.1). In spite of these precautions, deuterium incorporation varied by as much as 9% between laboratories. Much of this variability was attributed to processes such as digestion, liquid chromatography, and instrument specific parameters. More broadly, this study like many other demonstrates that there are many sources of variability in the HDX-MS experiment, and that available controls are unable to facilitate comparison of disparate datasets[134, 10, 109, 89, 35, 84]. In the next section we will look more closely at some of the most widely utilized controls for HDX-MS, why they are necessary, the associated limitations, and how they can be improved.

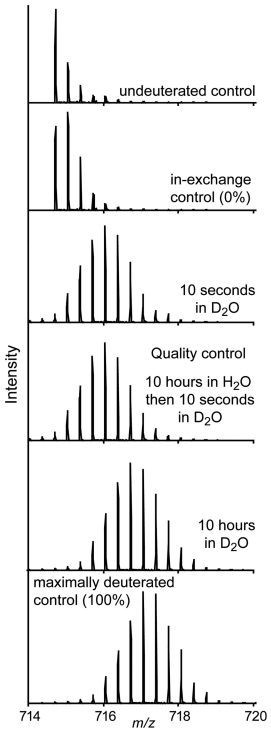

Figure 1.2: Example peptide spectra as undeuterated, 0% (in-exchange control), after 10 s labeling in D2O, after 10 h of labeling in D2O, and 100% exchanged control (top to bottom). The quality control in the middle is used to verify that the protein has not been perturbed during the 10hrs incubation by verifying that the spectra looks identical to the first 10 s time point.

1.3 Controls for HDX-MS

As the conclusions we draw from HDX-MS measurements rely solely on our interpretation of the observed accumulation of deuterium by a protein, it is critical that we have a comprehensive understanding of how these structures gain and lose deuterium over the course of the entire experiment. Due to the complexity of amide exchange processes, it is necessary to approach this

challenge practically, through the development of robust controls. We can break the HDX-MS experiment into two phases: labeling or forward exchange and downstream processing, in other words, the uptake and loss of deuterium. From that perspective it becomes clear that we need controls to provide the maximum and minimum extent of deuterium uptake as well as controls to provide some means of comparing the conditions of deuterium uptake and downstream loss. Much effort has been directed towards developing appropriate control for HDX-MS, in this section we will briefly discuss some of these concepts in an effort to provide necessary context for the work described in later chapters.

An undeuterated sample is a necessary starting point for HDX-MS studies as it is used to establish sample handling conditions, identify peptides via MS/MS, and serve as a reference for calculation of deuterium content in the deuterated samples. This sample is prepared identically to all deuterated samples, except that the D_2O in the labeling step is replaced with H_2O. For comparative HDX-MS studies that seek to identify changes within two states of a protein, for example a side-by-side comparison of two protein samples or to map changes associated with binding, an undeuterated control may be all that is necessary [120]. On the other hand, using HDX-MS to probe fine structural changes or quantitative dynamics requires more elaborate controls, as it is necessary to account for more variables.

An inherent variable common to any HDX-MS analysis is the extent of back-exchange that occurs throughout all downstream processes after the labeling step. Consistent conditions that yield reproducible back-exchange are crucial to the comparability of HDX-MS data. With bottom-up HDX-MS, reducing the back-exchange itself can limit variability. Many factors have been optimized to minimize back-exchange during digestion and separation [107, 117, 126, 73, 129, 121] and within the mass spectrometer (e.g., ion source temperature [121, 15]). However, reducing overall back-exchange only limits this inherent variation, it does not alleviate the problem. One of the most useful controls to include for HDX-MS is a maximally deuterated standard [133, 55]. This control serves as the most accurate way of measuring levels of back-exchange during analysis, an important metric for evaluating the platform suitability for reliable HDX measurements [84]. Using a maximally deuterated control is also the most accurate approach for determining the maximal deuteration point in calculating extents of labeling and exchange kinetics (1.2). The importance of this control can be illustrated using the highlighted range of the data in 1.3 panel D. Without the 100% reference standard we might (wrongly) infer that the peptide has fully exchanged by the time point, as its plateaued final observed exchange is close to what we would expect based on the deuterium incorporation for a certain number of amides. Having the 100% reference here reveals that there are actually a few amides within the peptide that are highly protected even at very long time points.

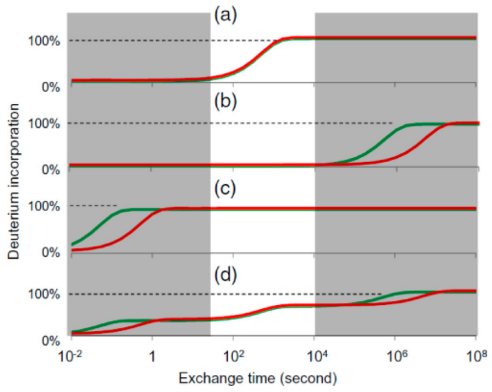

Figure 1.3: Amide exchange kinetics in proteins vary over 8 orders of magnitude. Comparative studies that sample only a limited temporal range can lead to missed information. Plots a—d show various kinetics for two states of a protein (red and green). Only in plot a is the comparison truly the same for all exchange times. Plots b—d have actual difference in exchange rates, but they are invisible due to the limited temporal sampling (highlighted region of the plot). Reproduced with permission from ref [86]. Copyright 2017 American Chemical Society.

In practice, the preparation of an appropriate maximally deuterated standard can be challenging. Historically, preparation of a maximally deuterated standard was accomplished by heating the protein (e.g., $75°C$ for several hours) in the presence of $D_2O$to equilibrate all amides with deuterium [133]. However, some proteins are prone to aggregation or may be too stable to maximally exchange even with such exhaustive conditions [120]. Furthermore, high temperatures can lead to exchange of the C2 proton on histidine sidechains, which will inflate the levels of observed deuterium uptake observed [85]. Additionally, there are reports that under exhaustive deuterium exchange other carbon-protons can start to exchange, and chemical modification of the protein become more common, both of which may further distort the level of deuterium[27, 5, 113]. A safer approach is to incubate the protein for a long period of time (12-24 hours) at a low pH (between 2.5 and 4) at room temperature in the presence of denaturants such as guanidine or urea [84, 111]. In spite of such precautions there is always a level of uncertainty with regard to whether a maximally deuterated control

is in fact actually completely deuterated. An alternative approach for obtaining a fully deuterated control is to prepare a pre-digested sample that is dried, and resuspended in deuterium, before being quenched to mimic all other samples [56]. Though practically very useful, this strategy can generated confounding results due to variation in back-exchange rates between quenched free peptides and peptides in the context of full protein[6, 50, 56, 55, 26].

During the entire downstream processing of proteins, the deuterium labeled species continues to equilibrate to the final percentage of deuterium in solution. For example, if the labeling reaction was 90% deuterium, and quenching was accomplished with a 1:1 dilution into a H_2O quench buffer at $0°C$, then the peptides will experience 45% deuterium upon the quench. They can equilibrate towards a maximum of 45% until trapping, desalting and chromatography further reduces the % D. This can cause peptides that were natively completely undeuterated during the labeling step to take on deuterium, and peptides that were maximally deuterated to loose it, even at $0°C$within the few minutes it takes a quenched sample to thaw before injection[56]. Although it is possible to mitigate this effect, it has become routine to include peptides which are not derived from the system being studied such as Bradykinin and Angiotensen II to act as back-exchange reporters[67]. Back-exchange reporters are incorporated into the D_2Obuffer prior to mixing with the protein stock during the labeling step. During labeling, these compounds equilibrate to the % D of the exchange reaction. Downstream, Bradykinin and Angiotensen II undergo relatively rapid back-exchange making them highly sensitive to changes in sample handling conditions[122, 134].

Through the use of an undeuterated sample, a well-matched maximally deuterated sample, and back-exchange reporter such as Bradykinin or Angiotensen II very high precision HDX-MS measurements can be made[124, 84, 56, 125]. However, it was noted from well-harmonized comparisons, that these tools are not adequate for the comparison of data generated in different labs or on different days[22, 60]. Burkitt et al. attributed day-to-day variation to instrument conditions, inconsistent chromatography, and sample concentration [10]. Other studies implicated ambient lab temperature and the shift in the pH of buffers over time as possible contributors to this kind of variability [22]. There is also evidence of different ionization methods and mass analyzers complicating the comparison HDX-MS data[11]. Ultimately, this suggests that for comparative HDX-MS studies to be truly robust, all samples should be prepared as close together as possible using the same set of reagants and analyzed using the same system. Despite the many compounding factors underlying this apparent limitation interest in HDX-MS grows and efforts continue to improve reproducibility. One of the more promising methods of improving the comparability of HDX-MS data involves looking at how variation in the labeling conditions impacts observed deuterium uptake[84, 121, 109].

Changes in the labeling solution conditions i.e., pH, temperature, salt concentration and solvent composition influence deuterium uptake or forward exchange by acting on both the intrinsic rate of amide exchange (k_{ch}) and protein structure. The sensitivity of proteins toward these changes is what allows HDX-MS to resolve subtle structural variations and weak binding interactions. As previously discussed it is virtually impossible match conditions precisely enough from day-to-day and lab-to-lab to avoid ambiguity, so strategies have been developed to help account for change in the labeling conditions[58, 45, 13, 22, 10, 123]. In general, it is assumed that the vast majority of forward exchange variation arises from changes in pH or temperature. As a result, the most widely utilized method for addressing forward exchange variation is to adjust time points according the measured temperature and pD by assuming only k_{ch}changes and in a manner that is 1st order with respect to the hydroxide ion in solution[50]. While this is a useful assumption, a means of verifying solution changes is necessary or corrections may yield misleading results.

Recently, internal exchange reporter (IER) based strategies have been developed in effort to make forward exchange correction more robust. The IER is designed to exchange alongside the protein and respond more predictably to changes in the exchange reaction conditions. Several groups have proposed the use of small unstructured peptides as IERs [134, 115, 92]. Small peptide IERs have a single slowly exchanging C-terminal amide that exchanges in a time regime relevant to most HDX-MS studies, the slow exchanging site losses deuterium downstream at slightly slower rate than most peptides. The lack of higher order structure for these IERs means that the exchange behavior is theoretically governed only by the electronic effects inherent to the structure. In other words, because no large scale structural movements are necessary to render the amide exchange competent, observed k_{ch}can be used to more directly review reaction conditions. Furthermore, these IERs are efficiently ionized and sufficiently retained under most relevant chromatographic conditions, making them relatively simple to incorporate into a wide variety of HDX-MS experiments. The use of these compounds has been shown to facilitate more robust comparisons where solution conditions are not

matched, for example looking at the effects of high concentrations of chaotropes or buffer additives on the structural dynamics of proteins[92, 115, 134](1.4). One notable limitation of using the C-terminal amide as a reporter is that this site undergoes acid catalyzed exchange at higher pH than other sites, which reduces sensitivity towards changes in pH potentially leading to misrepresentation of actual reaction conditions[130, 90]. Moreover, these reporters cannot accurately report on reaction deuterium content which has a significant impact on observed exchange.

Variations in the percent deuterium ($\%D$) of the labeling solution can occur from sample to sample either through dispensing error or by changes in the quality of the deuterium buffer (e.g., deuterium solutions open to air will exchange with atmospheric moisture and slowly lose $\%D$ over time). In an effort to reduce variation attributed to changes in $\%D$, Sheff et. al., developed an approach wherein the addition of known quantities of light and heavy isotopically labeled caffeine to the protein solution and deuterium labeling solution can be used to estimate the relative proportions of D2O and H2O in each sample [109]. In this study, the incorporation of the caffeine dispensing standards was able to improve the precision of deuterium measurements across multiple replicates. While this application is both clever and highly useful, it can be difficult to implement and is incapable of accounting for several sources of $\%D$. In essence, the concepts necessary to make robust comparisons between labeling conditions from day-to-day and lab-to-lab are well established in literature, but the chemical tools available are inadequate. The overarching goal of this document is to describe the development and validation of novel chemical tools which utilize these concepts to facilitate much more robust comparison of HDX-MS data.

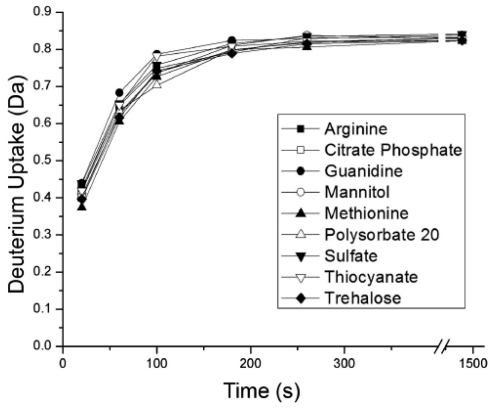

Figure 1.4: Deuterium uptake kinetics for the tripeptide YPI are shown in the presence of various buffer additives. The offset in the exchange profiles can be used to correct for the offset to the k_{ch}in the different solution, thereby enabling robust comparisons for proteins in the various solutions. Reproduced with permission from [114]. Copyright 2017 American Chemical Society.

Chapter 2

Imidazolium Internal Exchange Reporters: **Adapted from previously published work[90]**

2.1 Internal Exchange Reporters for HDX-MS

Hydrogen-deuterium exchange mass spectrometry (HDX-MS) is a widely utilized technique for the rapid assessment of protein structure and local dynamics. By observing deuterium uptake of back-bone amides via mass spectrometry it is possible to gain information about the local structural stability throughout a protein, map protein-protein and protein-ligand interactions, and monitor allosteric effects[69]. Recent advancements have made HDX-MS amenable to the analysis of large molecule biopharmaceuticals and the FDA now recommends HDX-MS as a tool for establishing "equivalence" between existing biologics and emerging biosimilars[57]. Despite the many advantages of HDX-MS for biophysical evaluation, poor reproducibility has limited its widespread use. The most notable issues pertaining to poor reproducibility are inconsistent sample handling and variation in the exchange reaction conditions[59].

The development of automated HDX-MS systems has made significant progress towards minimizing variation in sample handling, but even with these systems variation in deuterium uptake can vary by as much as 5.4% for a given peptide observed in different laboratories[60]. This persistent variability is a consequence of the strong solution dependence on backbone amide exchange. Even a small change in the reaction conditions (i.e., temperature, deuterium content, or pH) can have a pronounced effect on the observed exchange[134]. Furthermore, solution conditions can drastically affect both the protein conformational dynamics and the rate of amide intrinsic exchange (k_{ch}, the exchange rate of an unstructured amide) deferentially. This means that without some means of accounting for altered reaction conditions, any difference in deuterium incorporation observed over two separate experiments could be due to variation in protein dynamics, amide intrinsic exchange, or both[114]. As a result, correcting for variation in reaction conditions has been a focal point among groups trying to improve the reproducibility of HDX-MS [134, 114].

Another challenging aspect of studying proteins by HDX-MS is that the exchange of backbone amides can occur over a massive time window, from 10-2 s to 1010 s under standard conditions[48]7 Performing HDX experiments over this time scale is impractical, not only from a logistical standpoint, but also because many proteins may not be stable enough in solution beyond 104 s. Incomplete coverage of this large time window can significantly limit the ability of HDX-MS to monitor protein dynamics and discern structural perturbations. To overcome this limitation, techniques have been developed to artificially expand the time window for HDX-MS experiments, most often accomplished through the preparation of multiple HDX reaction buffers at different pH values [45, 84]. These approaches attempt to modify HDX reaction conditions to accelerate or decelerate kch while minimizing the impact on the conformational dynamics of the protein being studied. This approach, although informative, can provide misleading results if measures are not taken to accurately monitor HDX reaction conditions.

Small peptide internal exchange reporters (IERs) have been developed to monitor HDX reaction conditions. These compounds lack secondary structure and feature a relatively slow exchanging c-terminal amide. When added to the reaction mixture with the analyte protein, these small peptides undergo exchange under the same conditions as the analyte. Thus, variation in the deuterium uptake by the small peptide IER from run to run can be used to correct for variation in the deuterium uptake by the analyte protein[134, 114]. Al-

though these compounds can improve reproducibility, they have limited benefit. For instance, peptide IERs, such as YPI, become fully deuterated within a few minutes at neutral pH and $25°C$, making it ineffective for monitoring exchange at longer time points. Additionally, it was recently reported that C-terminal amides exhibit complex pH dependent exchange behavior within physiologically relevant systems[130]. The limitations of existing small peptides IERs encouraged us to explore alternative chemistries capable of extending the utility of IERs in HDX-MS.

The term pD is used in frequently in this chapter and throughout the rest of the document. The term pD is synonomous with pH in that both describe activity of the acidic form of water (D_3O^+, H_3O^+) as a decimal logarithm. It is necessary to differentiate the two terms because the activity of the $D_3O^+$and H_3O^+ions are different, and it is therefore necessary to apply a correction to the measured activity of a D_2Osolution as observed using a combined glass electrode calibrated in an H_2Osolution (pH*). There is a certain amount of error assocaited with the conversion of pH* to pD. In an effort to minimize this, experimental pH* is measured for all conditions using the same probe and calibration solutions on the same day. Where a pD value is provided, it has been calculated from pH* using the empirically derived equation 2.1[19, 20, 44].

$$pD = ((pH^* \cdot 0.929) + 0.41) \cdot 1.076 \tag{2.1}$$

2.2 Exploring Different Chemistries in Persuit of Suitable pH Dependent Kinetics

The currently available small peptide internal exchange reporters (i.e. the tripeptide: YPI and the tetrapeptide: PPPI) rely on the observed exchange at the C-terminal amide to correct for variation in HDX reaction conditions[134, 114]. To better understand the exchange kinetics of the C-terminal amide, the HDX of YPI was probed under a variety of conditions by time resolved NMR. The spectra show the loss of the isoleucine amide resonance for YPI, over time, as a result of H-D exchange with the buffered NMR solvent (D_2O). The HDX kinetics were monitored at different pD values, and in all cases the signal decay could be fit to a single exponential to reveal the exchange rate (2.1, panel A). The change in the log rate versus pD for YPI shows a linear relationship, but interestingly, the slope of the fit for these data is only 0.195 (2.1, panel B). This slope deviates significantly from the notion that the intrinsic exchange of backbone amides exhibits a first order relationship with the concentration of hydroxide in solution above the pH_{min}(i.e. the slope of the linear fit for the log rate versus pH above the $pH_{min}$is expected to be near 1)[32]. The shallow slope suggests, that within the observed pH range, HDX at this site cannot be adequately described by a simple base catalyzed mechanism. These findings are consistent with a recent report that the c-terminal amide exhibits complex solution dependent exchange behavior and are ill-suited for empirical exchange correction of data collected at different pH[130].

In response to these findings, we sought to identify alternative chemistries which exhibit pH dependent exchange behavior which more closely reflects that of backbone amides. This search was further refined by considering the conditions and time points relevant to solution HDX-MS studies (i.e. $1^{01} - 1^{0}4s$ near neutral pH and $25°C$). From extensive screening, it was determined that imidazolium containing compounds such as 1,3-dimethylimidazolium are ideal IERs for HDX-MS studies. Although imidazolium IERs convey many advantages over peptides, the comparative simplicity of the moiety's exchange kinetics is perhaps the most important. The HDX at the C-2 position of the imidazolium ion has been thoroughly investigated and is understood to proceed through base catalyzed hydrogen transfer followed by deuteration of the anionic C-2 of the imidazol-2-yl carbene, which occurs at the rate of solvent reorganization (2.1, panel D)[2]. It should be noted that exchange at the C-2 position can within certain confines be considered irreversible in comparison to backbone amides. This property of C-2 HDX has been utilized to investigate side chain accessibility of histidine residues[53]. However, it should be noted that imidazole by itself is not desirable as an IER, because the rapid exchange of the nitrogens at positions 1 and 3 strongly influences the observed rate of HDX at the 2 position effectively reducing the sensitivity of this position to changes in pH[9].

To test the potential of imidazolium derivatives to act as IERs the pH dependent exchange behavior of 1,3-dimethylimidazolium was probed by hydrogen deuterium exchange nuclear magnetic resonance spectroscopy (HDX-NMR). The comparison revealed that the slope of the change in the log rate as a function of pH is nearly 1 (m=1.05) across a range from pH 6-8 (2.1, panel B), and therefore the exchange at the C-2 proton

is first order with respect to hydroxide concentration. Unfortunately, the overall exchange rate was too slow to be useful as a reporter within the typical time window used for HDX-MS experiments (t1/2 30 hours at pD 7.02 and 25°C). Fortunately, conjugated azolium ions are notable for being highly efficient in the transmission of substituent effects to groups bonded to the C-2 position[4]. This observation suggested that it would be possible to accelerate HDX at the C-2 through the addition of electron withdrawing substituents to the ring system. Through the study of numerous imidazolium derivatives, a very strong correlation emerged making it possible to relate the rate of C-2 HDX to the chemical shift of the C-2 proton in D_2O(2.2, panel E). This relationship has considerable value as a basis for more rapidly understanding the extent to which imidazolium structures can be tuned to achieve exchange over a wider temporal window.

Several C-5 substituted 1,3-dimethylbenzimidazolium derivatives were synthesized and the pH dependence of exchange was measured by HDX-NMR (2.2). We focused mainly on three variants: "TM-68", "TM-65", "TM-85" (2.2, panels A-C). TM85 contains a highly electron withdrawing nitro group and exchanges relatively quickly with a rate of $1.59x10^2s^{-1}$ (t1/2 = 41 s) at pD 7.16. TM65 contains a less electron withdrawing ester group and exchanges around 10-fold slower than TM85 with a rate of $2.38x10^{-3}s^{-1}$ (t1/2 = 4.8 min) at pD 7.23. The slowest compound TM68 contains a weakly electron donating C-5 methyl group. The addition of this group results in a nearly 100-fold reduction in the rate of exchange compared to TM85, with a rate of $1.25x10^{-4}s^{-1}$ (t1/2 = 1.5 hrs) at pD 7.19. For each of these compounds there was a clear linear relationship between the reaction pD and the log of the exchange rate with a slope near 1 (2.2, panel D). The HDX of these compounds was also probed at low pH (approx. pD 3.0), where C-2 exchange was observed to be negligible (2.2, panels A-C). In contrast, the YPI showed considerable exchange within tens of minutes at the same pH (2.1, panel A). These data suggest that imidazolium compounds are likely to retain more deuterium than peptides following the quench and downstream processing, which is highly desirable as any downstream deuterium loss will complicate correction of deuterium uptake by the analyte. We also tested a saturated 1,3-dimethylbenimidazolium-5-methyl ester derivative where positions 3a,4,5,6,7 and 7a were hydrogenated (TM-91). This compound exhibited extremely slow C-2 exchange with a rate of $8.45x10^{-6}s^{-1}$ (t1/2 = 22 hrs) at pD 8.04. While this compound may have been suitable for probing long time scales, we found that the ester was hydrolyzed at both high and low pH. The hydrolyzed product, containing a free carboxylic acid, had altered exchange kinetics and was therefore not considered further. NMR spectra confirmed that this type of hydrolysis was unique to TM-91 as none of the other compounds showed any form of degradation under any condition tested even after extensive incubation. Fortunately, TM-91 was rendered unnecessary by TM-65, TM-68 and TM-85, which together provided ample coverage of the typical HDX-MS time window[48].

2.3 Temperature Dependent Exchange Kinetics

Temperature variation during or between HDX-MS experiments is a significant source of day to day and lab to lab variability. Although large variations in temperature are unusual within climate-controlled lab spaces, it is understood that the rate of back-bone amide exchange is exponentially related to the temperature of the exchange reaction[32]. Therefore, even a small change in temperature could have a significant impact on the observed deuterium uptake by a protein. The change in the rate of amide intrinsic exchange as a function of temperature is a consequence of the temperature dependence of the equilibrium ionization of water and is therefore predictable within physiologically relevant boundaries[35]. To assess how temperature influences HDX of imidazolium compounds, we observed the exchange of TM-85, TM-68, and TM-65 BY HDX-NMR at 12, 23 and 40C while maintaining constant solution pH, ionic strength, and solvent composition (2.3, panel A). In all cases there was a linear relationship between the natural log of the exchange rate ($ln_{k_{ex}}$) and the inverse temperature ($1/K$), which is typical of compounds exhibiting first order exchange kinetics [50]. Using the Arrhenius equation the activation energies of TM-85, TM-68, and TM-65 in the PBS buffer were 27.54, 29.44 and 30.84 $Kcal/mol$, respectively. We note that the methyl ester present in compound TM-65 did not undergo any measurable hydrolysis even after an hour at 40C. These data demonstrate that imidazolium compounds respond predicatbly to changes in solution temperature and are therefore capable of acting as robust IERs in HDX-MS experiments where temperature is a variable.

2.4 Solution ionic strength Dependent Exchange Kinetics

The rate of amide intrinsic exchange(k_{ch}) is influenced by electrostatic interactions with neighboring groups and with solvated ions. These interactions are implicated in the complex exchange behavior of amides in high salt solutions[116, 14]. However, to understand the impact of dissolved salts on amide HDX, one must also consider how the salts themselves interact with hydroxide (OH^-) and hydonium (H_3O^+) ions. For instance, it is understood that the addition of sub molar quantities of neutral salts, such as sodium chloride, to a phosphate or citric acid buffered solution results in an apparent decrease in pH[119, 21]. This apparent change in solution pH is manifests primarily through alteration of $OH^-$and H_3O^+ion activities(source). As the extent to which salts modulate $k_{ch}$is not necessarily related to the aforementioned impact on the water and its ions, modeling salt effects on amide HDX is challenging (sources). This effect is somewhat dramatically represented in (2.5) wherein YPI exhibits a more than 2-fold increase in the rate of HDX in the presence of 0.5 M sodium chloride. This behavior is striking as this quantity of sodium chloride has a proportionately small effect on the apparent pH of the buffered solution and suggests that the local electronic environment surrounding the C-terminal amide is significantly perturbed by the presence of the salt. To test how dissolved salts influence the HDX of benzimidazolium compounds, HDX-NMR was used to observe the exchange behavior of TM-85 as a function of solution ionic strength (i) (2.3, panel B). The small decrease in the observed HDX rate at higher i is consistent with the theoretical rate calculated by accounting for the effects of salt on the ionization of the reaction buffer. This behavior is highly desirable for an IER, because it suggests that the kinetics of exchange are more strongly dependent on the ionization of the solvent than by interactions with dissolved salts. In other words, the salt dependent exchange behavior of benzimidazolium based IERs is a consequence of the effect of the salt on the ionization of the reaction buffer, not the effect of the salt on the electronic structure of the compound.

2.5 Influence of Organic Solvents on Exchange Kinetics

HDX-MS studies are often performed with an organic co-solvent to help solubilize hydrophobic peptides or small molecule ligands. The addition of miscible organic solvents to water interferes with the bonded structure of water thereby altering the solvated structures of proteins and ions alike, such changes are understood to significantly impact exchange processes in ways that are challenging to model[128, 29]. However, in general it is assumed that the addition of organic co-solvents depresses the rate amide HDX [50, 35]. This assumption though apparently problematic given our understanding proton transfer processes in buffered hydroorganic systems, has received very little scrutiny within the HDX-MS community. That is to say, the addition of acetonitrile to a phosphate buffered aqueous solution is expected to raise the observed pH of the solution through modulating the activity of the OH^-ion, which should increase the rate of exchange under most circumstances. In an attempt to better understand how organic co-solvents impact exchange kinetics we carried out HDX-NMR studies involving TM-68 and YPI in the presence of two commonly used organic co-solvents: acetonitrile (ACN) and dimethylsulfoxide (DMSO). As with the previously discussed studies only a single solution condition was varied within the sample set; in this case, the mole fraction of organic solvent (ACN or DMSO).

From 2.3, panel C it is clear that there was a strong positive correlation between the log of the exchange rate and the mole fraction of organic solvent. While the rate of HDX for TM-68 increases rapidly with the mole fraction of both co-solvents, it is notable that the rate of HDX increases more rapidly in the presence of DMSO than ACN. This is consistent with the difference in the activities of ions in the two solvent systems[99, 3]. These data further suggest that imidazolium compounds respond directly to changes in the activity of the OH^-ion. While not within the scope of this study, further evaluation of this relationship may prove a valuable tool in understanding the complexity of amide HDX in hydroorgnaic buffer systems. It should be noted that this effect does not represent a practical limitation for the use of the proposed IERs, because even under chromatographic conditions, where the mole fraction of the organic component is highest, the combined effects of low pH and low temperature will suppress the exchange rate to a much greater extent. For example, the calculated half-life for compound TM-85 under HDX-MS chromatographic conditions (pH 2.5, $0°C$and 15% ACN) is estimated to be in excess of 50 hours. This estimate is corroborated by the lack of any observable back exchange from multiple LC-MS studies performed using compounds TM-85, TM-68, and TM-65.

2.6 Suitability of imidazolium compounds for HDX-MS studies

Following the assessment of the exchange behavior of the proposed Alternative IERs, we incorporated these compounds along with other previously published controls into a multi-condition HDX-MS experiment with Equine Cytochrome C (CytC). the purpose being to determine if imidazolium compounds could serve as useful IERs. TM-65, TM-68, and TM-85 at micromolar concentrations were spiked into a solution of CytC and HDX was measured at various time points from 3 seconds to 20 hours. Among the additional controls included in this experiment was YPI, which like the proposed benzimidazolium compounds can be used to monitor variation in exchange reaction conditions, and bradykinin, which is another samll peptide regularly used to detect variaitons in downstream processes[84]. In this study, two groups of exchanges were carried out side-by-side at $22°C$ in a standard phosphate buffered saline solution adjusted to pD 7.80 and 7.30. Resulting peptides were analyzed for deuterium content along with TM-85, TM-68, TM-65 and YPI and bradykinin. The imidazolium IERs were easily detected by MS due to their fixed positive charge. The uptake of a single deuterium by each IER was evident across the different HDX time points (2.6). We note that the maximum deuterium uptake for all IERs was between 0.85 and 0.90 Da, consistent with the total deuterium content during the HDX reaction (85% D). Some of the deuterium content may be exaggerated due to intensity distortions of isobaric peaks in FT-MS instrumentation[11]. This indicates that back-exchange for imidazolium based IERs under HDX quench conditions is not significant. In contrast, YPI showed a maximum shift of 0.60 +/- 0.03 Da consistent with a high degree of back-exchange. Furthermore, the difference in the exchange of the pepsin derived peptides of CytC between pD 7.80 and pD 7.30 (2.4, panels B and C left) is paralleled by the observed exchange for all three imidazolium IERs, and data from bradykinin suggest that downstream variation was negligible (2.4, panel A).

To test whether the offset in the exchange kinetics at the two pH conditions could be corrected, we shifted the time-axis for the low pD dataset to account for the difference in the kch between the high and low pH datasets 8,25 (see methods). The pH-based time shifting results in overlays which are still visibly offset (2.4, panels B and C middle). As an alternative approach, we tried utilizing the exchange kinetics of the IERs to time shift the pD 7.30 data. The exchange for each of the IERs was fit to a single exponential function (2.4, insets). The ratio of the exchange rate for each imidazolium compound at the high and low pH conditions was fairly consistent (TM-85: 2.3; TM-65: 2.2; TM-68: 2.5), but notably lower for the YPI (1.3). The average ratio from all three imidazolium compounds (2.3) was applied to time-shift all the peptides in the data set (see methods). The IER-based time adjusted overlays look remarkably consistent, suggesting that using the IER is an accurate approach for time adjustment (2.4, panels B and C right). The improvement in time adjustment can be attributed to several things. First, the benzimidazolium based IERs detect reaction buffer pH directly. This insight overcomes some of the error inherent to calculating exchange reaction pD from the reaction buffer pH* [77]. Second, the proposed IERs are sensitive to changes in solution conditions beyond pH. For instance, if there was a subtle offset in temperature or salt concentration between the two samples the benzimidazolium IERs would be able to detect it whereas the pH probe alone would not.

2.7 Overall utility of imidazolium IERs

The proposed benzimidazolium compounds have several advantages that make them ideal IERs for HDX-MS studies: 1) Exchange exclusively through base-catalysis, rendering their exchange rates highly responsive to pH; 2) Exhibit high solubility in water, making it possible to create very concentrated stocks ($>$ 10 mM); 3) Are highly stable in aqueous solvent, so they can be used for long incubations without the risk of degradation; 4) The combination of the three proposed compounds provides coverage of a wide time scale; ranging from seconds to hours at pH 7 and $25°C$) The compounds have a fixed positive charge, making them easily detectable by MS; 6) Will not react with protein side-chains[2]. Additionally, these compounds exhibit negligible back-exchange under HDX quench conditions, making it possible to use their maximum deuterium uptake to directly detect the total deuterium content during the exchange reaction.

Beyond these desirable properties a few limitations were observed. Compounds 85, 68 and 65 have exact masses of 192.08, 161.11, 205.10 Da, respectively, which are outside of the mass window typically observed in HDX-MS studies (300 - 2000 m/z). Therefore, in order to detect these compounds the m/z window was expanded, which can impact sensitivity for some MS instrumentation [106]. A second limitation is poor retention during the LC-MS step. All three compounds were only effectively trapped on C18 columns

at $0°C$when loaded with a buffer containing less than 2% ACN. None of the compounds were effectively retained on C4 or C8 columns. We note that TM-85, the most polar of the proposed compounds, was poorly retained even by C18 chromatography. For this reason, we had to use a nearly 100 times greater concentration of TM85, compared to TM-65 and TM-68, to obtain sufficient signal. This is not an effect of diminished ionization efficiency for TM-85, as direct infusion of all three compounds produced the same signal intensity. TM-65 and TM-68 on the other hand were easily detectable at starting concentrations lower than the protein being studied. Even if the protein had a strong affinity for the IERs, which is an inevitable caveat of any internal standard, only a fraction of the protein would be bound thereby minimizing the effects on the observed HDX data. Further optimization of imidazolium-based compounds will likely alleviate the aforementioned caveats.

Despite the current limitations of the three proposed benzimidazolium based IERs, these compounds are capable of making meaningful exchange corrections under a wide variety of experimental conditions. The immediate benefit of the proposed IERs is making comparative studies more robust. Currently, biocomparability studies by HDX-MS are known to be highly variable and only datasets collected and analyzed in parallel provide rigorous comparative power[58]. More recent studies have revealed that HDX-MS studies carried out under carefully matched conditions on an identical protein sample can still vary considerably[60]. Through the use of the proposed benzimidazolium based IERs we were able to effectively compare HDX-MS data collected for a protein under different reaction conditions (Fig. 4B). We believe that the inclusion of imidazolium based IERs could make it possible to accurately reference HDX-MS data collected on different days or even in different labs to a benchmark condition. Currently, HDX-MS studies include specific information on reaction exchange conditions (pH, temp, buffer etc), but this information is largely self-reported, and is therefore of limited utility for rigorous comparison of disparate data sets. Incorporation of IERs like the proposed benzimidazolium compounds could provide a chemical exchange “stamp” that could facilitate more robust comparison of exchange reaction conditons regardless of when and where the data was actually collected. To be clear, this proposed ”stamp” approach cannot be utilized to isolate variation in specific solution parameters like pH or temperature, but rather to improve the statistical power of comparative studies by allowing for a more robust distinction between effects on the protein structure and dynamics vs. global offsets to intrinsic exchange rates arising from altered reaction conditions.

2.8 Methods

2.8.1 Reagents

D2O, deuterated ACN, and deuterated DMSO were purchased from Cambridge Isotope Labs (Tewksbury, MA, USA). Methyl iodide 99.9%, potassium carbonate, Methyl 3a, 4,5,5,6,7,7a-hexahydro-1H-1,3-benzodiazole-5carboxylate 98%, and 1-methylimidazole 98% were purchased from sigma Aldrich (St. Louis, MO, USA). 5-mehtylbenzimidazole 98%, and 5-nitrobenzimidazole 98+% were purchased through Alfa Aesar (Haverhill, MA, USA). Benzimdazole 98% was purchased from Acros organics (Geel, Belgium). 1-methylbenzimdazole-5-carboxylic acid was purchased from Maybridge chemicals (Altrincham, UK). Before use in alkylation reactions the solvents were dried via distillation over activated 3A molecular sieves. Chromatography solvents were purchased from Fisher Scientific (Hampton, NH, USA).

2.8.2 HDX kinetics by NMR (HDX-NMR)

Dried samples were re-suspended in an aqueous reaction buffer containing sodium phosphate (50 mM), 3-(Trimethylsilyl)-1-propanesulfonic acid (DSS) (0.104 mM), and 10% D2O (final volume 600 μL). This aqueous buffer was adjusted to specific pH using small additions of NaOH or HCl. Prior to NMR analysis, the adjusted samples were dried fully by speedvac. The resulting solid was re-suspended in D2O (99.96%), mixed vigorously for approximately 15 seconds, transferred into a NMR tube, and rapidly loaded into the NMR. For experiments with organic co-solvents, pH adjusted samples were resuspended in a mixture of D2O and either deuterated DMSO or ACN at a specific ratio. All NMR experiments were performed on a 499.73 MHz Agilent DD2 spectrometer equipped with a 5 mm triple-resonance 1H(13C/15N), z-axis pulsed-field gradient probe head. Course shim values were briefly manually adjusted prior to beginning arrayed 1H NMR experiments. Array HDX-NMR studies consisted of identical experiments featuring Watergate

solvent suppression separated by a pre-acquisition delay between experiments to allow access to different time scales. The duration of the delay was chosen to allow for the observation of 3 half-lives over 500 total experiments. The dead-time between resuspension and NMR acquisition for each sample was in the range of 45 to 90 seconds. The preparation and adjustment steps necessary for all the replicates of a particular sample set were carried out in the same day. All experiments were conducted at 298 K except for the temperature dependence studies which were sampled at 313 and 285 K. Actual experimental temperatures were determined using solvent chemical shift values as described by Gottlieb et al29. Exact pH* was measured for each sample after collection of the NMR kinetic data. Using an empirically derived equation, the pH* value was used to calculate the sample pD26 (see supporting methods). For experiments carried out at elevated temperature, pH* measurements were made at the experimental temperature via the use of a recirculating water bath. NMR data was processed using SpinWorks version 4.2.8. Spectra were referenced to DSS (0 ppm) to ensure consistent reporting of chemical shifts. The disappearance of the C-2 1H peak (or C-terminal NH peak for YPI) was analyzed relative to the intensity of a nearby well-resolved aromatic resonance; this was to account for any changes in the total signal intensity during the experiment. The change in the ratio of integrations as a function of exchange in the experiment time was fitted using an exponential function. For ionic strength comparisons a sample of TM85 was prepared at pH 5.5, separated into three identical aliquots, and dried by speedvac. The aliquots were resuspended in 600 μL of either pure water, 250 mM NaCl, or 500 mM NaCl. Each sample was dried again and resuspended in D2O for HDX measurements. Prior to each NMR measurement a blank containing deuterated reaction buffer or with sodium chloride (250mM or 500mM) was used to roughly tune, lock, and shim the spectrometer for each ionic strength. Corrections to the reaction buffer pD were made using literature values corresponding the to the activity of phosphate buffered water in the presence of sodium chloride (see supporting information).

2.8.3 Compounds Stability measurements

To assess the solution stability of the proposed benzimidazolium IERs, samples of purified TM85, TM68 and TM65 were reconstituted in D2O (99.9%), transferred into NMR tubes and sealed with parafilm. The sealed samples were analyzed by 1H NMR immediately after preparation and again after two months of storage at room temperature on the benchtop.

2.8.4 HDX-MS

Equine Cytochrome C (Sigma Aldrich) was resuspended in PBS (20 mM sodium phosphate 150 mM NaCl, 2 mM DTT) to a concentration of 0.1 mg/mL and adjusted to either pH 7.39 or 7.94 (corresponding to a calculated pD of 7.3 and 7.8, respectively) with small additions of HCl and NaOH. Internal exchange reporters were added to each solution for a final concentration of 6.5 μM TM65, 6.5 μM TM68, and 20 mM TM85. 10 μL of the protein solution was diluted 10-fold into deuterated buffer (for a final content of 85% D2O) and incubated at $22°C$ for 3 sec, 15 sec, 1 min, 5 min, 30 min, 4 hrs, or 20 hrs. Exchanged samples were added to an equal volume (100 μL) of ice-cold quench buffer (8 M Urea, 0.2% formic acid) for a final pH of 2.5. Samples were flash frozen in an ethanol-dry ice bath ($-60°C$) and subsequently stored at $-80°C$until LC-MS analysis. The exact pH* during the deuterium reaction was measured using an identical sample in D2O, without protein and used to calculate the pD as described for the NMR methods. Frozen samples were thawed on a $5°C$block for 4 minutes prior to injection onto a loading loop. The loaded sample was passed over a custom packed pepsin column (2.1 x 50 mm) kept at $8°C$ with a flow of 0.1% trifluoroacetic acid (TFA) at 200 μL/min (Cite pepsin column). Digested peptic fragments were trapped onto a Waters BEH trap column (2.1 x 5 mm, 1.7 μm). After 5 minutes of loading, digestion, and trapping, peptides were resolved on an analytical column (Waters CSH 1 x 100 mm, 1.7μm, 130Å) using a gradient of 3% to 40% solvent B for 9 minutes (A: 0.1% FA, 0.025% TFA, 2% ACN; B) 0.1% FA in ACN). The LC system was coupled to a Thermo Orbitrap performing full scans over the m/z range of 150 - 1500 with a resolution setting of 30,000. During the analytical separation step, a series of 250 μL injections were used to clean the pepsin column: 1) 0.1% Fos-12 with 0.1% TFA; 2) 2 M GndHCl in 0.1% TFA; 3) 10% acetic acid, 10% acetonitrile, 5% IPA[80, 51]. After each gradient the trapping column was washed with a series of 250 μL injections: 1) 10% FA; 2) 30% trifluoroethanol; 3) 80% MeOH; 4) 66% isopropanol, 34% ACN; 5) 80% ACN. During the trap washes the analytical column was cleaned with three rapid gradients[39]. These cleaning steps were necessary to

ensured that the level of carry-over was below 5% for each peptide analyzed. Undeuterated samples were used to collect MS/MS spectra using data-dependent acquisition. Peptic peptides were identified by exact mass and tandem mass spectrometry (MS/MS) spectra using Byonic (Protein Metrics). Mass shifts were determined using HD-Examiner V2 (Sierra Analytics) and HX-Express v2[46]. The exchange kinetics for each IER were calculated by fitting the data to a single exponential.

2.8.5 Time shifting HDX-MS Data

Time shifting of the pD 7.30 data was first achieved by assuming a ten-fold increase in the intrinsic amide exchange rate for a pH increase of 1.0. By this criterion, the time axis of the pD 7.30 data set was shifted down by a factor of 10(7.94-7.39) or 3.54. Time-shifting using the exchange offset as observed by the benzimidazolium IERs was accomplished by first calculating the difference in exchange rate between the pD 7.80 and 7.30 data sets and then using the average ratio between the rates (average factor of 2.3) to scale the time points of the pD 7.30 data set. For example, the 1 minute time point was shifted down to 26 seconds.

2.8.6 Alkylation of Imidazole Derivatives

To an oven dried round bottom flask containing a magnetic stir bar benzimidazole (0.84mmol, 1.0 eq) and potassium carbonate (1.26mmol, 1.5 eq) were added. The vessel was fitted with a rubber septum and flushed with Argon (g). Approximately 30ml of dried acetonitrile was added via cannula to the vessel via argon pressure. Next the mixture was set to stir and methyl iodide (4,23mmol, 5.0 eq) was added dropwise to the stirring solution. The vessel was then fitted with a liquid cooled reflux condenser and heated to reflux. The mixture was allowed to stir at this temperature for approximately 12 hours or until all starting material appeared to be consumed by TLC. Excess solvent was removed under reduced pressure. The residue was resuspended in mobile phase (9:1 H2O:ACN w/ 0.1% TFA) and filtered using a syringe driven filter (0.22μM). The effluent was purified via reverse phase HPLC (gradient elution: 15-95% ACN in H2O with 0.1% TFA), to yield 1,3-dimethlybenzimidazolium (TM-39) as a yellowish solid, 89%.

2.8.7 Synthesis 1,3-dimethlybenzimidazolium (TM-39)

See Alkylation of Imidazole Derivatives, no changes made to procedure. Purified by HPLC (gradient elution: 15-95% ACN in H2O with 0.1% TFA) to yield yellowish solid 89%, 73% yield; 1H NMR (499.73 MHz, D2O, ppm): 9.17 (S, 1H),7.79 (D, 4H) 4.09 (S, 6H); MS (ESI) calcd for C9H11N2: 147.09, found: 147.1

2.8.8 Synthesis 1,3-dimethylimidazolium (TM-31)

See Alkylation of Imidazole Derivatives, no changes made to procedure. Isolated via filtration to yield white solid 97%, 90% yield; 1H NMR (499.73 MHz, D2O, ppm): 8.64 (S, 1H), 7.41 (S, 2H), 3.884 (S, 6H)

2.8.9 Synthesis 1,3-dimethylbenzimidazolium-5-methyl ester (TM-65)

See Alkylation of Imidazole Derivatives, no changes made to procedure. Purified via HPLC (isocratic elution: 10% ACN in H2O with 0.1% TFA) to yield white solid 98%, 40% yield; 1H NMR (499.73 MHz, D2O, ppm): 9.36 (S, 1H), 8.57 (S, 1H), 8.325 (D, 1H), 7.96 (D, 1H), 4.14 (6H, SS), 4.01 (S, 3H); MS (ESI) calcd for C9H13N2O2: 205.10, found: 205.10

2.8.10 Synthesis 1,3,5-triimethylbenzimdazolium (TM68)

See Alkylation of Imidazole Derivatives, no changes made to procedure. Purified via HPLC (gradient elution: 15-95% ACN in H2O with 0.1% TFA) to yield white solid 95%, 68% yield; 1H NMR (499.73 MHz, D2O, ppm): 9.07ppm (S, 1H), 7.67 (S, 1H), 7.55 (D, 1H), 7.72 (D, 1H), 4.05 (S, 6H), 2.56 (S, 3H); MS (ESI) calcd for C10H13N2: 161.11, found: 161.11

2.8.11 Synthesis 5-nitro-1,3-dimethlybenzimidazolium (TM-85)

See Alkylation of Imidazole Derivatives, no changes made to procedure. Purified via HPLC (isocratic elution: 20% ACN in H2O with 0.1% TFA) to yield yellow solid 98%, 65% yield; 1H NMR (499.73 MHz, D2O, ppm): 9.51 (S, 1H), 8.92 (S, 1H), 8.58 (D, 1H), 8.08 (D, 1H), 4.19 (S, 3H), 4.17 (S, 3H); MS (ESI) calcd for C9H10N3O2: 192.08, found: 192.08

2.8.12 Synthesis 3a,4,5,6,7,7a-hexahydro-1,3-dimethylbenzimidazolium-5-methyl ester (TM-91)

See Alkylation of Imidazole Derivatives, no changes made to procedure. Purified via HPLC (gradient elution: 10-95% ACN in H2O) to yield white solid 98%, 85% yield; 1H NMR (499.73 MHz, D2O, ppm): 8.46 (S, 1H), 3.74-3.70 (9H, SSS), 3.08-3.02 (m, 1H) 2.95-2.83 (m, 3H), 2.69- 2.66 (m, 3H), 2.28-2.22 (m, 1H), 2.07-1.99 (m, 1H); MS (ESI) calcd for C9H19N2O2: 211.14, found: 211.1

2.8.13 Solid Phase Peptide Synthesis of YPI

In a glass fritted 2 port solid state synthesis vessel 300mg of chlorotrityl resin preloaded with Fmoc-L-isoleucine (approx. 0.1mmol) was allowed to swell in 5ml of dried DMF under an N2 atmosphere with gentle agitation for 30 minutes. Next the residual DMF was pushed through the frit using N2 gas pressure. The beads were then resuspended in approximately 5ml of 20% piperidine in Dry DMF. The beads were agitated under a nitrogen atmosphere for 5 minutes, before the solvent was removed via gas pressure. This step was repeated until cleavage of the Fmoc group was complete by ninhydrin assay (Kaiser test). Following successful FMOC cleavage, the solvent was pushed out via gas pressure and the beads were washed with several 5ml portions of dry DMF. While washing the beads, the coupling reaction mixture containing Fmoc-proline (0.5mmol) was set to stir in dry DMF with HATU (0.51mmol) and triethylamine (1.0mmol) in a separate vessel. The coupling reaction mixture was added to the gas dried beads and agitated under a nitrogen atmosphere for approximately 8 hours. Washing, cleavage and couplings steps were repeated for the addition of Fmoc-O-tert butyl-L-tyrosine with no changes made to the reaction stoichiometry. After completing the coupling of tyrosine, simultaneous deprotection of the tyrosine O-tertbutyl and Fmoc protecting groups and cleavage was achieved by agitating the bead bound peptide in 5ml of 95% trifluoroacetic acid (TFA) for approximately 1 hour at room temperature. The cleaved crude tripeptide, YPI, was recovered via vacuum filtration. The effluent was concentrated under reduced pressure and purified via HPLC (gradient elution 2ml/min 10-95% ACN in H2O with 0.1% TFA). The resulting white solid was characterized via mass spectrometry and proton NMR. tyrosine-proline-isoleucine (YPI) purified via HPLC (gradient elution: 5-95% ACN in H2O with 0.1% TFA) to yield white solid 98%, 35% yield (calculated overall); 1H NMR (499.73 MHz, D2O, ppm): 7.81 (m, 0.5H), 7.24-7.17 (m, 2.5), 6.907 (m, 2H), 4.10-3.04 (m, 6H), 2.29 (m,1H), 1.99-1.77 (m, 6H), 1.47 (m, 1H) 1.28 (m, 1H), 0.95-0.88 (m, 8H); MS (ESI) calcd for C19H27N3O5: 391.21, found 392.21

2.9 Conclusions

Benzimidazolium based IERs exhibit solution dependent HDX behavior ideal for monitoring changes in pH, temperature, salt concentration, or levels of organic co-solvent, and over a wide range of time scales. The use of the IERs proposed in this publication served as a proof of concept, effectively demonstrating that forward exchange controls can significantly improve data quality in comparative HDX-MS studies. While carrying out this work we also learned how to manipulate the electronic properties of imidazolium containing compounds to overcome some of the caveats associated with the three compounds proposed here. The next chapter will cover the process of designing and testing a 2nd generation of imidazolium IERs.

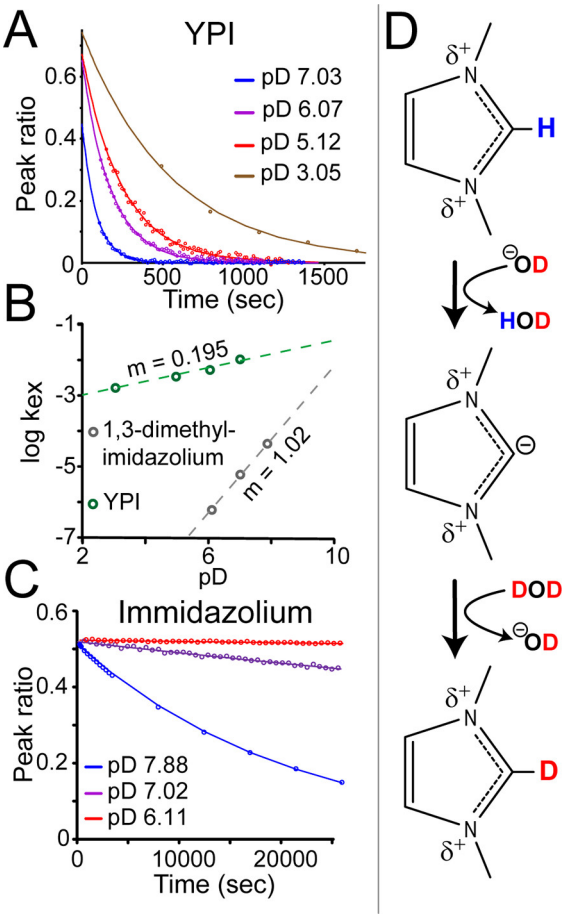

Figure 2.1: (A) HDX rates for the C-terminal isoleucine in peptide YPI measured by NMR at various pD. Solid lines represent fits of exponential decay functions. (B) Plot of the log of the exchange rate, log(kex), as a function of pD for both YPI (green) and 1,3-dimethylimidazolium (gray). The slopes (m) of the lines are shown next to the linear fit. (C) pD dependence of HDX at the C-2 proton for 1,3-dimethylimidazolium measured by NMR at various pD. (D) General mechanism for HDX at the C-2 proton for 1,3-dimethylimidazolium.

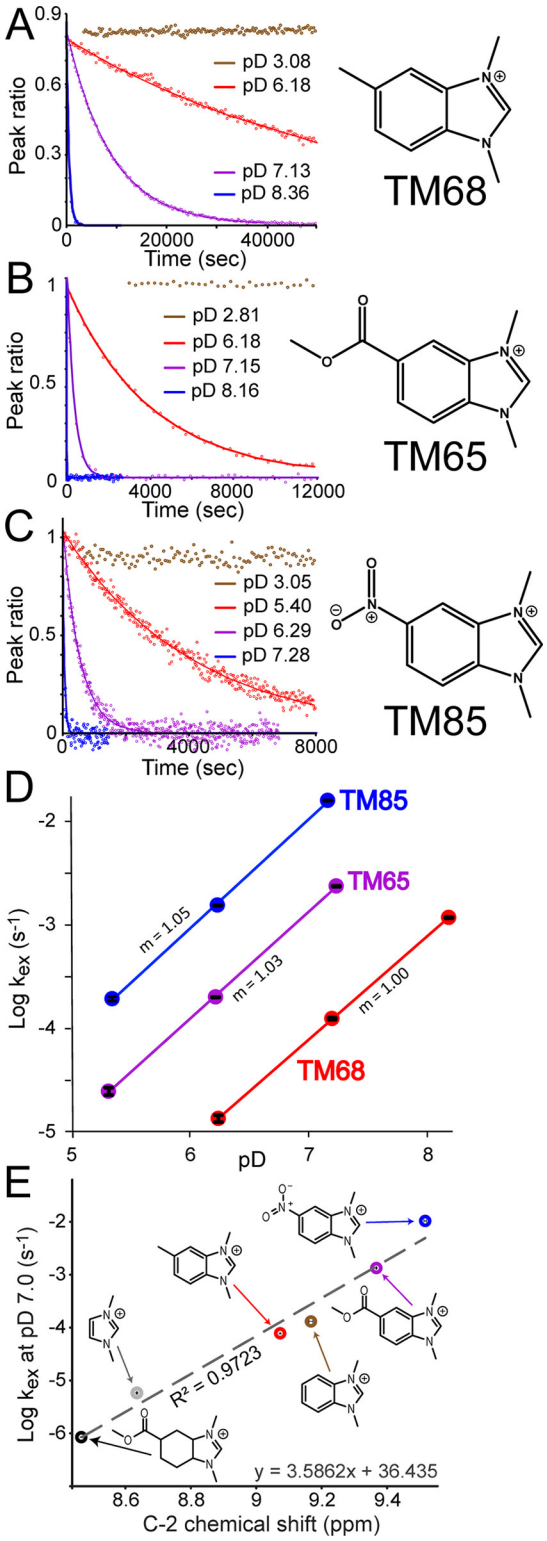

Figure 2.2: pD dependence of HDX rates for the C-2 proton in TM68 (A), TM65 (B), and TM85 (C) measured by HDX-NMR. Chemical structures are shown on the right. (D) The observed log rate of exchange (kex) for compounds TM85 (blue), TM68 (red), and TM65 (purple) as a function of pD. The slope of each line (m) is indicated next to the linear fit. (E) The rate of exchange for compounds TM85 (blue), TM68 (red), TM65 (purple), TM39 (brown), TM31 (gray), and TM91 (black) at pD 7.0 as a function of C-2 chemical shift (ppm). Error bars show standard deviations from triplicate measurements.

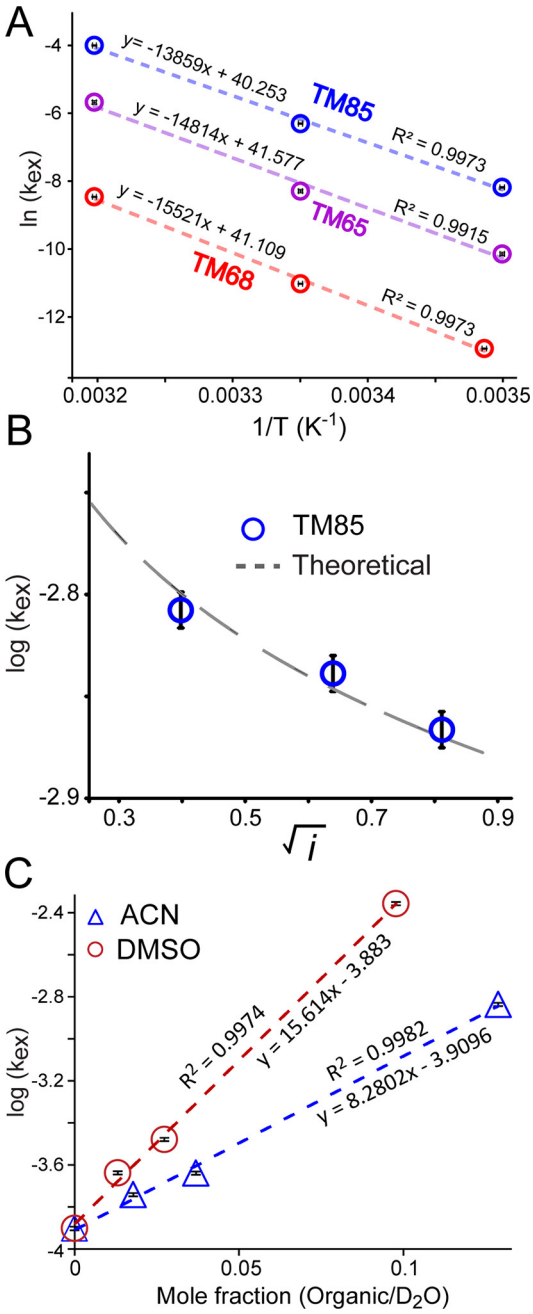

Figure 2.3: (A) Arrhenius plots showing the temperature dependence on the HDX rates of compounds TM85 (blue), TM68 (red), and TM65 (purple). The equations for the linear fits and R2 values are shown above each line. (B) The observed rate of exchange for TM85 as a function of the square root of the solution of ionic strength (0.0 M, i = 0.158 M, 0.250 M, i = 0.408 and 0.50 M, i = 0.658 M) (blue circles). The dashed line corresponds to the theoretical rate of exchange (log10) for compound TM85 as a function of the solution ionic strength. (C) The observed rate of exchange for TM68 as a function of the fraction of organic solvent in the D2O reaction buffer with either DMSO (red) or ACN (blue). Equations for the linear fits are shown below each line.

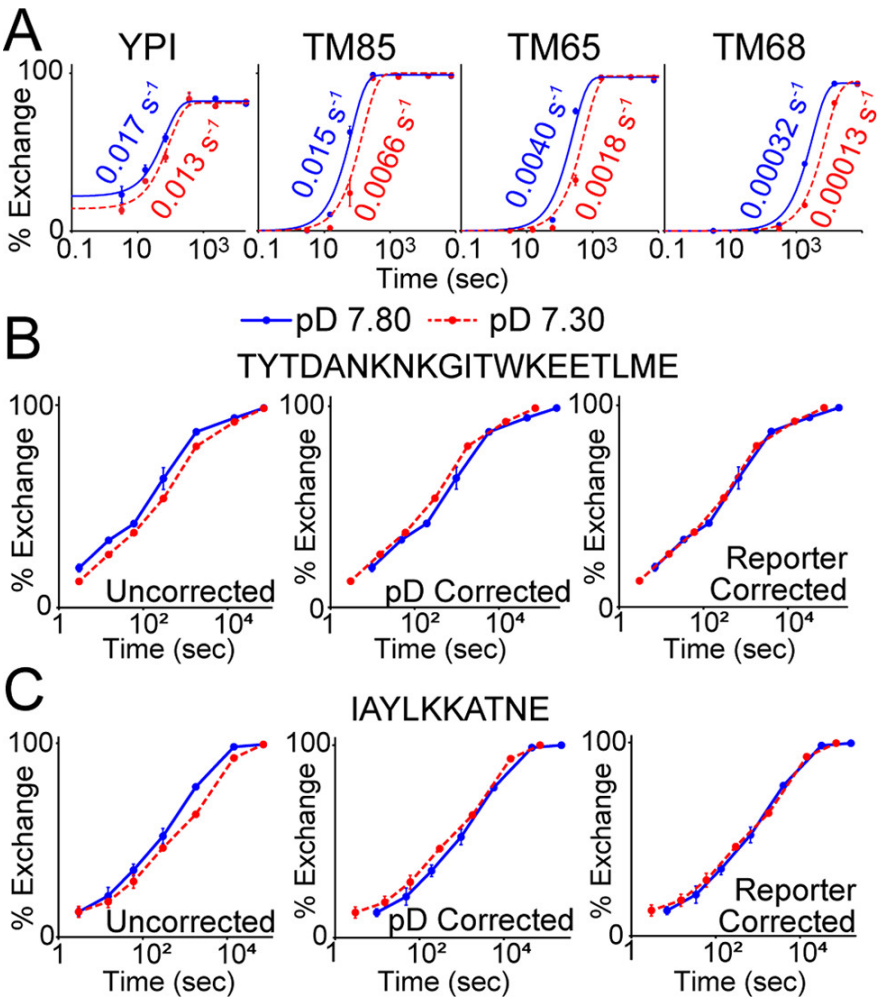

Figure 2.4: Solution HDX-MS data for cytochrome C and internal exchange reporters. (A) Deuterium uptake plots for YPI, TM85, TM65, and TM68 is shown for various time points at pD 7.8 (blue) and 7.3 (red). Solid and dashed lines show a single exponential fit. Example deuterium uptake plots for two peptides of cytochrome C: TYTDANKNKGITWKEETLME (B) and IAYLKKATNE (C) are shown. (B, C) The plots on the left show the uncorrected deuterium uptake at pD 7.8 (blue) and 7.3 (red). The plots in the center show the deuterium uptake after time-shifting the pD 7.8 data to match the exchange conditions based on the pD difference. The plots on the right show the deuterium uptake after time-shifting the pD 7.8 data based on the difference in rates measured using the exchange rates of the exchange reporters TM85, TH65, and TM 68 shown in part A. Additional examples are shown in Figure S7, and data for all peptides are provided in Supporting Information.

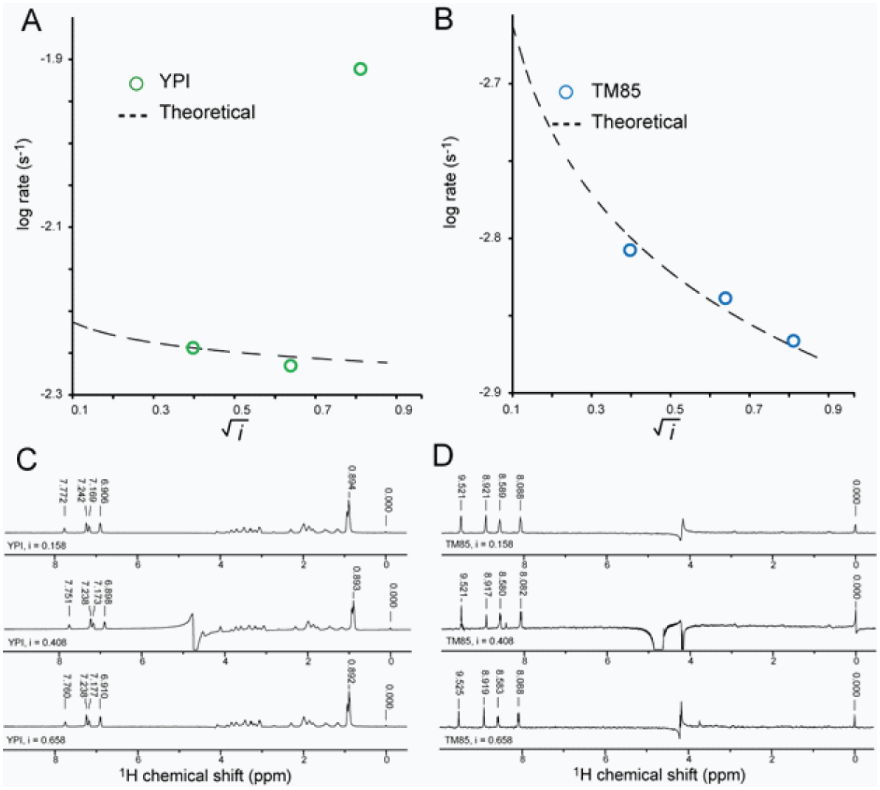

Figure 2.5: Dependence of C-terminal HDX for YPI (A) and the C-2 proton of TM85 (B) on the solution ionic strength as observed by 1H NMR. 1H NMR spectra are shown for YPI (C) and TM85 (D) at pD 6.07 and 6.24 respectively; calculated ionic strengths for NMR samples are reported (i is given in units of mol/L).

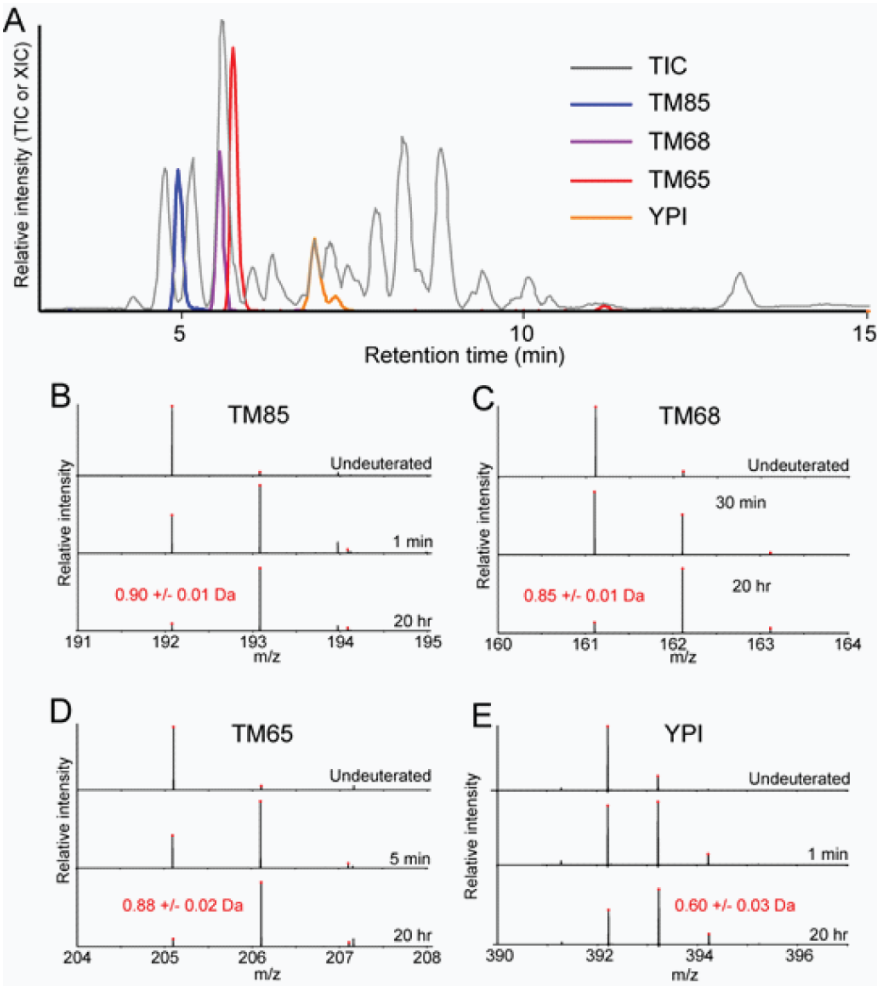

Figure 2.6: A) The LC chromatogram of an undeuterated pepsin digest of Cytochrome C (TIC shown in the gray trace). Extracted ion chromatograms (XIC) for the IERs are shown: TM85 (blue), TM68 (purple), TM65 (red), and YPI (orange). B-E) Mass spectra for each IER in the undeuterated state (top), or at two deuterium time points (middle and lower panel) with deuterium exchange times indicated on the right side. Numbers indicate the total mass shift at the longest (20 hour) time point (average +/- standard deviation from triplicate measurements).

Chapter 3

2nd Generation Imidazolium Internal Exchange Reporters

3.1 Introduction

Internal Exchange reporters (IERs) function by exchanging in solution alongside the protein being studied [134]. At a basic level, IERs should provide coverage of the entire time course of the HDX experiment and retain information about the exchange reaction after downstream processing. More specifically, IERs must also be observable at concentrations much lower than that of the proteins and be efficiently trapped and separated from peptides by liquid chromatography to simplify incorporation and identification. In Chapter 2 the 1^{st}generation imidazolium IERs that I developed in the Guttman lab were introduced. Although these compounds exceed the performance of peptide based reporters, our own experiences using these compounds and the feedback we received from collaborators revealed shortcomings that were possible to overcome through refinement.

The most pressing drawback associated with the use of the 1st generation imidazolium IERS (TM-65,68,85) is the lack of chromatographic retention. Compounds TM-65 and 68 can be efficiently trapped under typical conditions using C18 only, and TM-85 cannot be trapped efficiently under typical chromatographic conditions. Detection of TM-85 was only possible through a molar excess, more than 100X that of the protein and roughly 3000X that of the other reporters[90]. This is undesirable as any IER at high concentrations may interact with the protein and influence observed exchange. Another drawback associated with the 1^{st}generation reporters is that the mass of these compounds is below the typical m/z window for HDX-MS studies (300-2000 m/z). In some cases this can be overcome by simply adjusting the mass analyzer method. However, strong background ionization of commonly used reagents such as TCEP (251 m/z) can reduce sensitivity towards peptides [28]. In an effort to address these limitations and further expand the utility of imidazolium IERs, we designed and validated a series of improved reporters referred to as 2^{nd}generation imidazolium reporters.

3.2 Designing and Validation of 2nd Gen Imidazolium IERs

A series of N-benzyl and N-heptyl derivatives of the 1^{st}generation IERs was generated. The retention of these compounds under typical conditions was compared to TM-65 and TM-68 in a retention assay. The observed retention time for each of the compound incorporated was then plotted against a computationally derived logP value generated using ©Molinspiration cheminformatics online tools, this is shown in Figure 3.1. Fitting this relationship with a linear equation allowed for prediction of retention time for unknown imidazolium derivatives with an average deviation of $\pm 33s$. Using this relationship it was determined that N-heptyl derivatives would be too strongly retained to be useful under typical conditions. However, diverse N-benzyl derivatives could be generated with appropriate mass values and greater retention than the majority of peptides. Having the IERs elute after the peptides is particularly desirable as it minimizes overlap with

signals corresponding to peptides allowing the user more freedom to optimize methods to improve sensitivity or minimize deuterium loss[11, 50, 67].

Using a previously established synthetic approach 6 new candidates were acquired (Figure 3.2). The hydrophobic nature of these larger compounds rendered HDX-NMR analysis of exchange kinetics impractical. As a result, we devised an apparatus to enable highly reproducible continuous labeling HDX-MS (CHDX-MS) on a variety of platforms. This system allows for simultaneous analysis of multiple IERs at once with far greater sensitivity than HDX-NMR. For a detailed description of this apparatus please refer to the methods section. CHDX-MS studies were carried out on a Thermo Orbitrap. Individual runs were carried out in succession with blank samples in between to minimize carryover. The results of these studies demonstrated clearly that all 6 perspective candidates exhibit 1st order exchange kinetics (Figure 3.3). The exchange rates for each compound at pD 7.0 and 25°C as determined by this experiment are: TM-2-16 4.56E-4 s^{-1} (t1/2 = 25.3 min), TM-155 4.36E-5 s^{-1} (t1/2 = 4.42 hrs), TM-151 1.70E-3 s^{-1} (t1/2 = 6.78 min), TM-139 8.35E-4 s^{-1} (t1/2 = 13.8 min), TM-143 0.111 s^{-1} (t1/2 = 6.24 s), and TM-141 5.01E-3 s^{-1} (t1/2 = 2.31 min). The time point coverage corresponding to these compounds is visualized in Figure 3.4 where the shaded region represents the useful extent of deuteration, compounds outside of this range are within 10% of the maximal deuterium content or have not incorporated enough deuterium to be reliably measured. The uptake curves in Figure 3.4 show that TM-143 is capable to reporting on reaction conditions at the shortest typical time point of 3s for solution HDX-MS, and that the other compound offer overlapping coverage all the way up to 14400s or 4hrs.

3.2.1 Assessment of Chromatographic Performance

In an effort to assess the chromatographic performance of the potential 2nd generation IERs, undeuterated samples were subjected to the same downstream processing procedures used in the analysis of proteins. To accomplish this, the same custom automated system described in Chapter 2 was used. This system allows for precise and independent temperature control over the digestion and subsequent chromatographic separation. With the exception of compounds TM-141 and TM-139, the 2nd generation IERs performed as expected. Interestingly, TM-141 and TM-139 exhibited extensive and persistent carryover with the pepsin column in line. However, when the pepsin column was removed, the compounds behaved as expected. That is to say, that TM-141 and TM-139 eluted within 33 seconds of the expected retention time and did not carry over to a significant degree when the pepsin column was removed. From this observation we infer that these compounds are very strongly retained by the pepsin column conceivably through interaction with the resin POROS onto which the protease is immobilized. Attempts were made to minimize this interaction via modifying the pepsin wash protocol and loading buffer, but with no success. Alternative protease immobilization resins such as BEH and Nugel may overcome this issue[67]. We do not recommend the use of compounds TM-139 and TM-141 in conjunction with a POROS resin protease column. The removal of TM-139 does not significantly impact the potential quality of IER based corrections near physiological pH because TM-2-16 has a similar half-life. However, the removal of TM-141 reduces the quality of coverage for experiments below pD 7.2 at the 30s time point. Filling this gap in coverage is the subject of ongoing work discussed in Chapter 4.

3.2.2 Optimizing Reporter Concentration

Having identified candidates with suitable exchange kinetics and chromatographic behavior, it was necessary to determine how efficiently these compounds could be detected under typical conditions. As previously discussed, minimizing the concentration of IERs is necessary to avoid influencing deuterium uptake via interactions between the protein and reporters. The target range for IER concentration is ideally 100x less than that of the protein being studied. In this range, even strong unforeseen binding interactions between proteins and IERs are virtually undetectable. To determine if the 2nd generation IERs could be detected within this concentration range, un-deuterated samples containing 1.5μM equine cytochrome C, equine myglobin, and Hen Egg lysozyme in addition to the IERs and bradykinin were prepared. After several iterations, it was found that TM-143, TM-151, TM-155, and TM-2-16 could be detected within the linear range of a first generation Themo-Orbitrap-LTQ at reaction concentrations of 0.005μM, 0.003μM, 0.0004μM, and .013μM respectively (Figure 3.5). These results suggest that these IERs could be incorporated into a

wide variety of HDX-MS experiments without any risk of interacting with the protein analyte and influencing the observed exchange.

3.3 Suitability of 2nd Gen IERs for HDX-MS studies

In order to rigorously assess the performance of proposed 2nd generation IERs we incorporated the compounds into a comparative HDX-MS study carried out under two pH conditions. The exchange reaction buffers were phosphate buffered saline adjusted to pH 7.4 and pH 6.4 by using small amounts of HCl and NaOH to achieve final pH* values in D2O of 7.183 and 6.227 (pD 7.62, 6.65) respectively. Reaction deuterium content was calculated to be 84.6%. The exchange reactions included 3 proteins: Hen egg lysozyme, equine Cytochrome C, and equine Myoglobin, 4 imidazolium reporters; TM-143, TM-151, TM-155, and TM-2-16 in addition to the back-exchange reporter bradykinin. Exchange reactions were carried out in quadruplicate at 7 time points; 3s, 15s, 1min, 5min, 30min, 4hrs, and 20hrs. Maximally deuterated exchanges were also carried out in quadruplicate for each condition. Detailed information about sample preparation and handling can be found in the methods section.

Analysis, of the exchange reactions shows a clear difference in deuterium uptake by both peptides and reporters between the two conditions. Figure 3.6 panels A, B, and C (peptide uncorrected, pD corrected, IER corrected over time course) shows uncorrected uptake for the three peptide from Equine Cytochrome C (CYT C): AGIKKKTE, YLENPKKY, and IFAGIKKKTEREDL. Figure 3.6 panels D, E, and F shows the uptake of these same peptides with the low pD data time shifted along the X-axis to account for the difference between the high and low pD conditions by applying a correction factor pD_{corr} acquired from equation 3.1. The exchange time in seconds is simply divided by pD_{corr} to correct for differences in reaction pD. For example, the 60s time point at pD 6.65 is corrected to 6.43s using this approach.

$$pD_{corr} = 10^{(pD_{high} - pD_{low})} \tag{3.1}$$

This correction assumes that the increase observed deuterium uptake by the protein between low and high pH conditions is the result of changes to the intrinsic amide exchange rate (k_{ch}) alone. This method further assumes that the change in $k_{ch}$with regard to pD is consistent with 1st order kinetics, i.e., for a pH increase of 1.0 units k_{ch}increases by a multiple of 10. While this method is widely utilized, it's limitations are well understood[134, 28, 84, 50, 90]. For example in this data set the pD correction tends to over-represent the extent of exchange for the low pD data. This is likely due to error associated with pH measurement and conversion of pH* to pD: a limitation that is overcome by using imidazolium IERs[90, 67]. Time-shifting using the imidazolium IERS was accomplished by calculating the difference in exchange rate between the high and low pD data sets. The average ratio of observed exchange rates across the entire time course was applied as a correction factor to scale the time points in the low pD data set, in the same manner as the pD correction. Figure 3.6 panels G, H and I demonstrates how this method minimizes the error associated with pH measurement to accomplish better quality corrections.

Although, frequently unnecessary it is possible to use the uptake of the 2nd generation IERs to make robust time point specific corrections. This is only possible because the lack of back-exchange allows for accurate calculation of rates from single time point measurements, using 3.2 where $\#D$ is the observed extent of deuteration and D_{max} is the maximum observed deuterium content.

$$Rate = -ln(-(\frac{\frac{\#D - D_{max}}{D - max}}{time})) \tag{3.2}$$

The rate corresponding to the specific time point can then be used in the manner previously discussed to generate more accurate exchange corrections. To fully take advantage of this capability, the extent of exchange for the IER must be within 10% and 90% of the maximal deuterium content at each time point intended for correction. In this experiment it was possible to accomplish time point specific corrections for the entire time course using the IERs incorporated. In Figure 3.7 panel C the time point-specific correction of low pD measurements corresponding to the peptide LENPKKYIPGTKMIF from CYT C is displayed. although not evident from the data presented in Figure 3.7, a time point-specific exchange correction can in general provide a higher quality correction.

3.4 Methods

3.4.1 Reagents

D2O, deuterated ACN, and deuterated DMSO were purchased from Cambridge Isotope Labs (Tewksbury, MA, USA). benzyl bromide 98%, trimethyloxonium tetraflouroborate 95% potassium carbonate, 2,3-diaminonaphthalene 98%, and formic acid 88% in methanol were purchased from sigma Aldrich (St. Louis, MO, USA). 5-mehtylbenzimidazole 98%, and 5-nitrobenzimidazole 98+% were purchased through Alfa Aesar (Haverhill, MA, USA). Benzimdazole 98% was purchased from Acros Organics (Geel, Belgium). 1-methylbenzimdazole-5-carboxylic acid was purchased from Maybridge Chemicals (Altrincham, UK). Before use in alkylation reactions the solvents were dried via distillation over activated 3A molecular sieves. Chromatography solvents, absolute ethanol, concentrated HCl, and solid NaOH were purchased from Fisher Scientific (Hampton, NH, USA).

3.4.2 Continuous labeling HDX-MS (CHDX-MS)

CHDX-MS requires the quenched exchange reaction to flow directly into the ionization source at relatively high flow rates. As a result, volatile buffers are essential. For the CHDX-MS experiments we carried out, the exchange buffer was 200mM ammonium acetate and the quench buffer included 1% formic acid and 1% trifluoroacetic acid in optima H_2O. Both buffers were adjusted using solutions of sodium hydroxide or hydrochloric acid to achieve the desired solution pH value. The reaction buffer was made by adding 150μL of the acetate buffer to 1350μL of 99.99% D2O for a final buffer concentration of 20mM. The IER master mix was made by adding compounds TM-155, TM-151, TM-143, TM-141, TM-139, TM-2-16, along with TM-65, TM-68, and TM-85 as reference compounds to optima H_2O. Immediately before beginning the experiment, 1485μL of the buffered D_2Osolution was drawn up into a glass Pasteur pipette and mixed in a vessel containing 15μL of the IER master mix to form the reaction mixture. Half of the reaction mixture was promptly removed using a gastight 1ml syringe and the remaining 750μL was used to measure reaction pH* by a Thermo combined glass electrode.

To deliver sample to the spectrometer, a Harvard Instruments syringe pump was set up to drive a 1ml gastight Hamilton syringe and deliver $10 frac \mu L min$ of the CHDX-MS reaction mixture. The flow from this pump is directed through 280mm of PEEK tubing with an inner diameter of 0.25mm into a T-shaped PEEK junction. At this junction the reaction mixture is diluted 1:1 by an opposing flow of quench buffer delivered by a Shimadzu LC-10ADV solvent pump. The length and inner diameter of the PEEK tubing connecting both the syringe and solvent pumps to the T-shaped peek junction was matched to minimize back flow and pressure ripple. The out flow from the T-shaped junction to the spectrometer was directed through 140mm of PEEK tunning with an inner diameter of 0.5mm. The experiment was begun as soon as the D_2Obuffer was added to the IER master mix, signal did not appear until approximately 2 minutes after syringe pump began delivering the reaction mixture. To minimize carryover, the solvent pump continued to deliver quench between runs and a blank was run between every sample. Uptake data was analyzed via Microsoft excel following export as .csv from platform specific software.

3.4.3 HDX-MS

Equine Cytochrome C , Equine myoglobin, and Hen Egg Lysozyme (Sigma Aldrich) were resuspended in PBS (20 mM sodium phosphate 150 mM NaCl, 2 mM DTT) to an individual concentration of 15.0μM. A mixture of the 2nd gen IERs; TM-143, TM-151, TM-155, and TM-2-16 was added to protein stock to achieve concentrations of 0.05μM, 0.03μM, 0.004μM, and .13μM respectively. The PBS buffers for conditions 1 and 2 were adjusted with small additions of HCl and NaOH to pH 7.457 and 6.405, corresponding to pH* values in $D_2O$of 7.183 and 6.227 respectively. 10 μL of the protein solution was diluted 10-fold into a deuterated buffer containing 0.2 μg/mL of bradykinin and angiotensin II to serve as controls for assessing back-exchange[134]. The exchange reaction deuterium content was calculated to be 85%. Reactions were incubated at $23.5°C$ for 3 sec, 15 sec, 1 min, 5 min, 30 min, 4 hrs, or 20 hrs. Exchanged samples were added to an equal volume (100 μL) of ice-cold quench buffer (8 M Urea, 0.2% formic acid) for a final pH of 2.544. Samples were flash frozen in an ethanol-dry ice bath ($-60°C$) and subsequently stored at $-80°C$until LC-MS analysis. Undeuterated samples were prepared in the usual way[84]. Maximally deuterated exchanges were also carried

out in quadruplicate for both condition using two different methods. In method 1 (TDA) exchange reactions were prepared in the usual way, sealed with parafilm, and heated to $60°C$for 2 hours in a slotted heat block before being quenched and prepared for analysis. In method 2 (TDB) exchange reactions were prepared in the same way as TDA however, excess guanidinium chloride (3M) was added to facilitate more complete deuterium incorporation by the proteins in solution[59]. Reactions for both conditions were carried out by hand in a single day. The exact pH* during the deuterium reaction was measured using an identical sample in D_2O, without protein and used to calculate the pD as described for the NMR methods in Chapter 2. Frozen samples were thawed on a $5°C$block for 4 minutes prior to injection into a loading loop. The loaded sample was passed over a protease column containing porcine pepsin immobilized on POROS resin (2.1 x 50 mm) at $10°C$ with a flow of 0.1% trifluoroacetic acid (TFA) at 200 μL/min[67]. Digested peptic fragments were trapped onto a Waters BEH trap column (2.1 x 5 mm, 1.7 μm). After 7 minutes of loading, digestion, and trapping, peptides were resolved on an analytical column (Waters CSH 1 x 100 mm, 1.7μm, 130Å) using a gradient buffers A (0.1% FA, 0.025% TFA, 2% ACN; B) 0.1% FA in ACN) and B (99.9% ACN, 0.1%TFA). In this gradient B is held at 2% for 4min then increasing to 10% 4.5min, then to 33% via linear gradient at 13min, and to 50% at 14.5min, before increasing linearly again to 95% at 16min. After 16min the column was washed and allowed to equilibrate at 2%B for several minutes. The LC system was coupled to a Thermo Orbitrap performing full scans over the m/z range of 150 - 1500 with a resolution setting of 30,000. During the analytical separation step, a series of 250 μL injections were used to clean the pepsin column: 1) 0.1% Fos-12 with 0.1% TFA; 2) 2 M GndHCl in 0.1% TFA; 3) 10% acetic acid, 10% acetonitrile, 5% IPA[80, 51]. After each gradient the trapping column was washed with a series of 250 μL injections: 1) 10% FA; 2) 30% trifluoroethanol; 3) 80% MeOH; 4) 66% isopropanol, 34% ACN; 5) 80% ACN. During the trap washes the analytical column was cleaned with three rapid gradients[39]. These cleaning steps were necessary to ensured that the level of carry-over was below 5% for each peptide analyzed. Undeuterated samples were used to collect MS/MS spectra using data-dependent acquisition. Peptic peptides were identified by exact mass and tandem mass spectrometry (MS/MS) spectra using Byonic (Protein Metrics). Mass shifts were determined using HD-Examiner V2 (Sierra Analytics) and HX-Express v2.34[46]. The exchange kinetics for each IER were calculated by fitting the data to a single exponential.

3.4.4 Time shifting HDX-MS data

Time shifting of the pD 6.65 data was first achieved by assuming a ten-fold increase in the intrinsic amide exchange rate for a pH increase of 1.0 unit. By this criterion, the time axis of the pD 6.65 data set was shifted down by a factor of 10 raised to the difference in calulcated pD values for conditions 1 and 2 ($pD_{corr} = 10^{(7.62-6.65)} = 9.33$). Time-shifting using the 2nd gen imidazolium IERs was accomplished by first calculating the difference in IER exchange rates for the pD 7.62 and 6.65 data sets. This was accomplished by fitting the observed uptake overtime under each condition with a single exponential equation. The correction factor was then calculated by raising the difference between the high and low pD rates to the power of 10 (average IER factor of 7.25). This value was applied by dividing the low pD time point y the value of the correction factor. For example, the 60s time point was shifted down to 6.43s when using the pD correction and 8.3s when using the IER based correction.

For time point specific corrections to be effective it is necessary to compare the rates of a single standard within a deuteration range of 10-90% under both conditions. The rate is calculated using equation 3.2, where $\#D$ is the observed extent of deuteration and D_{max} is the maximum observed deuterium content. We note that miss-representation of absolute deuterium content can arise from FT-MS and the data processing method[11]. However, this did not appear to adversely affect the quality of correction factors generated using this approach.

3.4.5 Synthesis 1,3-dibenzylbenzimidazolium (TM-151)

To an oven dried round bottom flask containing a magnetic stir bar benzimidazole (0.84mmol, 1.0 eq) and potassium carbonate (1.26mmol, 1.5 eq) were added. The vessel was fitted with a rubber septum and flushed with Argon (g). Approximately 30mL of dried acetonitrile was added via cannula to the vessel via argon pressure. Next the mixture was set to stir and benzylbromide (4,23mmol, 5.0 eq) was added dropwise to the stirring solution. The vessel was then fitted with a liquid cooled reflux condenser and heated to reflux.

The mixture was allowed to stir at this temperature for approximately 12 hours or until all starting material appeared to be consumed by TLC. Excess solvent was removed under reduced pressure. The residue was resuspended in mobile phase (9:1 H2O:ACN w/ 0.1% TFA) and filtered using a syringe driven filter (0.22μM). The effluent was purified via reverse phase HPLC (C18, gradient elution: 15-95% ACN in H2O with 0.1% TFA), to yield 1,3-dibenzylbenzimidazolium (TM-151) as a white solid, 89%, 1H NMR (499.73 MHz, D2O, ppm): 9.37 (S, 1H), 7.79-7.77 (M, 2H), 7.61-7.59 (M, 2H), 7.46-7.42 (M,10H), 5.71 (S, 4H); MS (ESI) calcd for C21H19N2: 299.1543, found: 299.1550 M/Z

3.4.6 Synthesis 1,3-dibenzylimidazolium (TM-155)

See synthesis TM-151; no changes made to procedure. 1,3-dibenzylimidazolium (TM-155) isolated as transparent oil 99% 1H NMR (499.73 MHz, D2O, ppm): 8.95 (S, 1H), 7.52-7.44 (M,10H), 5.41 (S, 4H), 4.87 (S, 2H); MS (ESI) calcd for C17H17N2: 249.1386, found: 249.1392 M/Z

3.4.7 Synthesis 1,3-dibenzyl-5-nitrobenzimidazolium (TM-143)

See synthesis TM-151; no changes made to procedure. 1,3-dibenzy-5-nitrobenzimidazolium (TM-143) isolated as white solid 99% 1H NMR (499.73 MHz, D2O, ppm): 9.62 (S, 1H), 8.79-8.78 (D, 1H), 8.49-8.46 (D, 1H), 8.01-7.99 (D, 1H), 7.48-7.46 (M,10H), 5.79 (S, 2H), 5.76 (S, 2H); MS (ESI) calcd for C21H18N3O2: 344.1393, found: 344.1395 M/Z

3.4.8 Synthesis 1-methyl-3-benzylbenzimidazolium-5-benzylester (TM-141)

See synthesis TM-151; no changes made to procedure. 1,3-dibenzy-5-nitrobenzimidazolium (TM-141) isolated as white solid 99% 1H NMR (499.73 MHz, D2O, ppm): 9.46 (S, 1H), 8.34 (S, 1H), 8.25-8.23 (D, 1H), 7.94-7.92 (D, 1H), 7.44-7.462 (M,10H), 5.71 (S, 2H), 5.33 (S, 2H), 4.13 (S, 3H); MS (ESI) calcd for C23H21N2O2: 357.1597, found: 357.1591 M/Z

3.4.9 Synthesis 1,3-dibenzyl-5-methylbenzimidazolium (TM-139)

See synthesis TM-151; no changes made to procedure. 1,3-dibenzy-5-nitrobenzimidazolium (TM-139) isolated as white solid 99% 1H NMR (499.73 MHz, D2O, ppm): 9.307 (S, 1H), 7.65 (S, 1H), 7.63 (S, 1H), 7.57 (S, 1H), 7.46-7.41 (M,10H), 5.68-5.67 (D, 4H), 2.45 (S, 3H); MS (ESI) calcd for C22H21N2: 313.1699, found: 313.1699 M/Z

3.4.10 Synthesis 1,3-dimethylnaphthoimidazolium (TM-2-16)

To a round bottom flask containing a magnetic stir bar 2,3-napthalenediamine (0.63mmol, 1.0eq) was added. The solid was added to 10ml of absolute ethanol. Next 88% formic acid in methanol (250 microliter approx. 6eq) was added dropwise to the stirring solution. The vessel was then fitted with a liquid-cooled condensation column and heated to approximately $80°C$. The reaction was monitored by mass spectrometry, with a small portion of the reaction mixture being removed, neutralized, and filtered at regular intervals. Upon completion, the reaction vessel was allowed to cool before being poured into a saturated solution of sodium carbonate. The crude napthimidazole precipitated and was isolated via vacuum filtration. The filter Cake was washed 5 times with de-ionized water, and the identity of the crude product (TM-2-13) was confirmed by HR-MS (1H-Napthimidazole, HR-MS = 169.079 m/z). TM-2-13 was dried completely before use in the subsequent reaction. Solid TM-2-13 (0.31mmol, 1.0eq) was dissolved in dried methylene chloride (DCM), and the vessel was then sealed and flushed with argon (g). Next, solid trimethyloxonium tetrafluoroborate (1.55mmol, 5.0 eq) was added in small portions under a light flow of argon (g) to exclude atmosphere. After addition of the alkylating agent, the vessel was fitted with a rubber septum and the mixture formed a white fluffy precipitate, which over time became dark red and opaque. After allowing the mixture to stir at room temperature for approximately 48hrs. reaction monitoring was carried out via removing a small portion of the reaction mixture, diluting it with ice-cold 1:1 water and methanol, and filtering in preparation for MS analysis. When MS indicated completion, the reaction mixture was diluted with ice-cold 1:1 water and methanol and concentrated onto silica gel. The silica gel was transferred into a RediSep solid loading column

for chromatography. 1,3-dimethylimiazolium (TM-2-16) was isolated via flash chromatography (silica gel, gradient elution: 0-10% Methanol in DCM) as an off-white solid 98% 1H NMR (499.73 MHz, D2O, ppm): 9.03 (S, 1H), 7.96 (S, 2H), 7.91-7.89 (M, 2H), 7.48-7.46 (M, 2H), 3.88 (S, 6H); MS (ESI) calcd for C13H13N2: 197.1073, found: 197.1079 M/Z

3.5 conclusions

Here we demonstrate a series of 2nd generation imidazolium IERs. These compounds utilize the same well studied kinetics of the 1st generation standards but feature more extensive time point coverage and better chromatographic performance. Importantly, the improvment in chromatographic performance allows for the detection of the IERs at very low concentrations, more than 100X less than that of the protein analyte. At such low concentrations potential unforeseen interactions between the analyte and IERs have virtually no impact on the observed exchange. These improved imidazolium IERS are amenable to a wider variety of HDX-MS experiments.

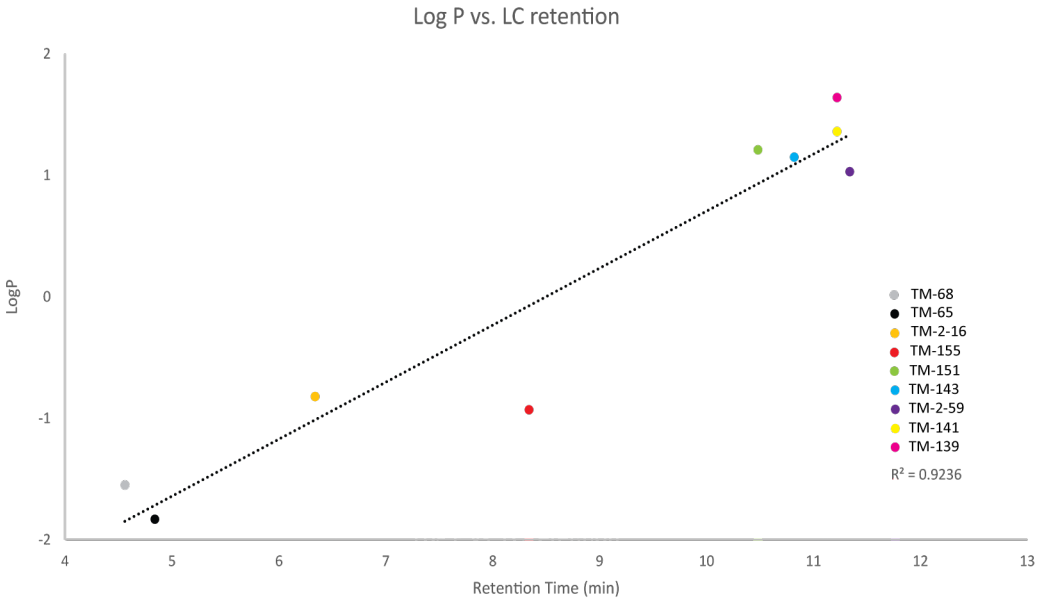

Figure 3.1: Computationally generated logP values for imidazolium IERs as a function of observed retention. Details pertaining to the chromatographic conditions can be found in the methods section. LogP values were generated using ©Molinspiration cheminformatics online tools.

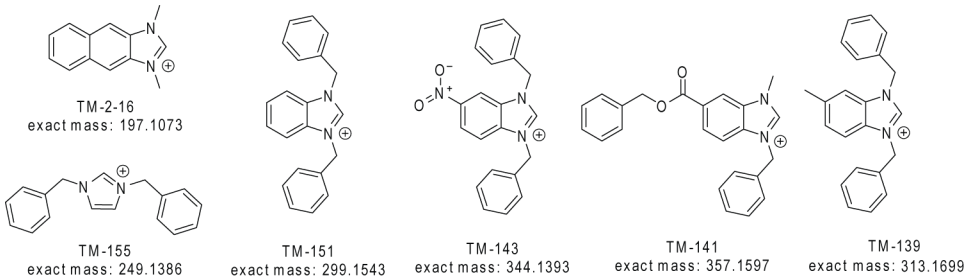

Figure 3.2: Structures with reference number and exact mass values for compounds TM-139, TM-141, TM-151, TM-155, TM-2-16.

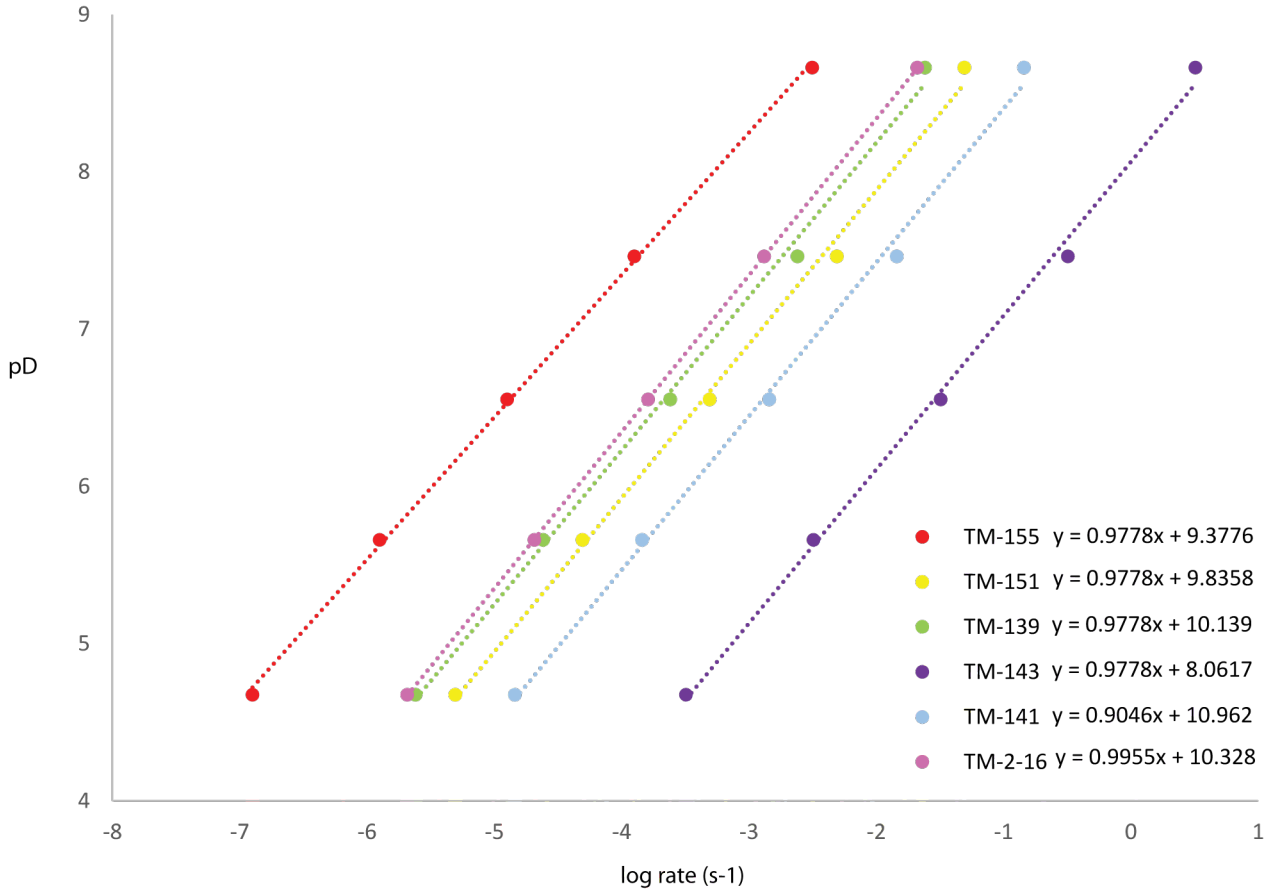

Figure 3.3: pD dependence of rate for compounds TM-139, TM-141, TM-151, TM-155, and TM-2-16. Rates were measured by CHDXMS.

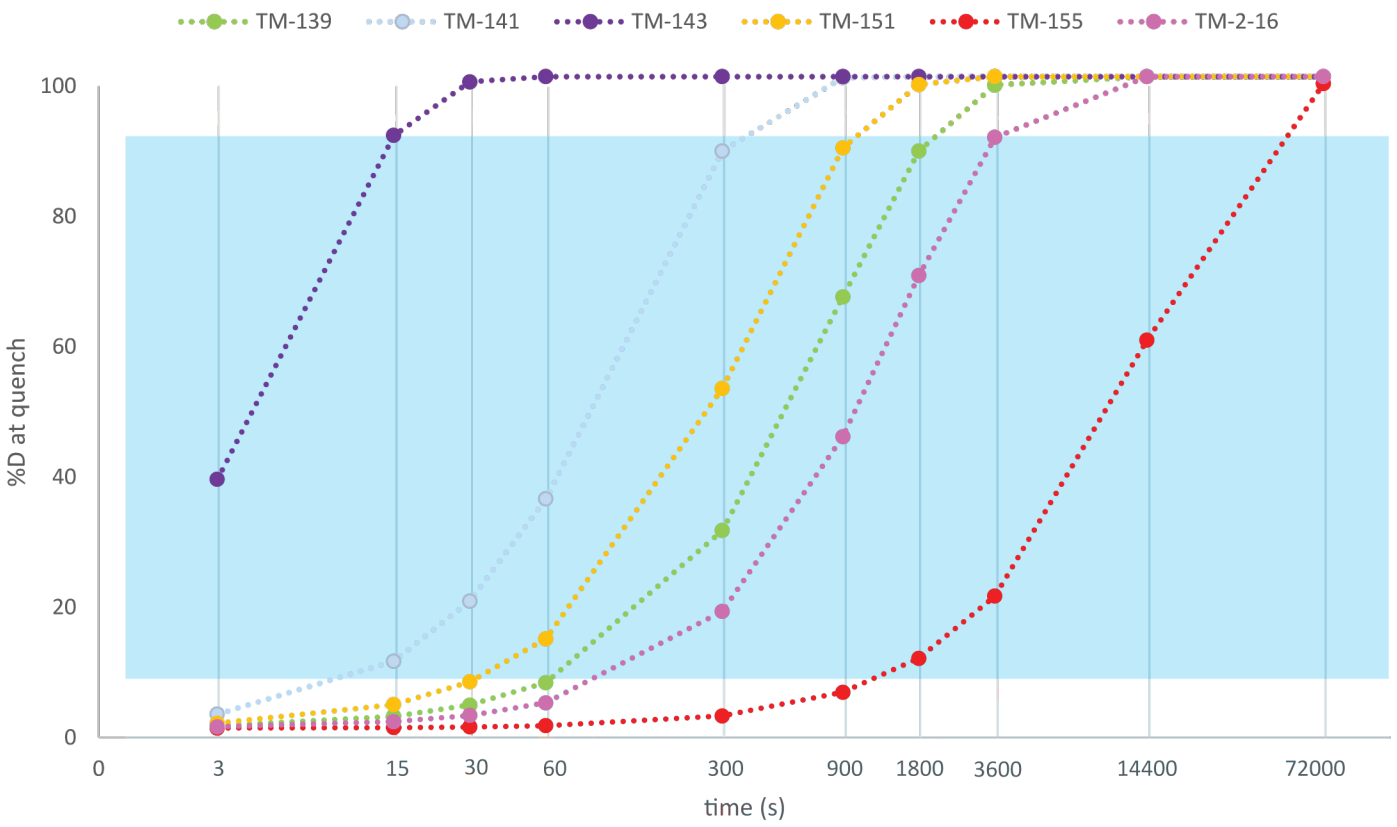

Figure 3.4: Time point coverage map for 2nd generation imidazolium IERs. The shaded region (blue) indicates extent of exchange where is it possible to calculate a rate from a single time point measurement with reasonable accuracy.

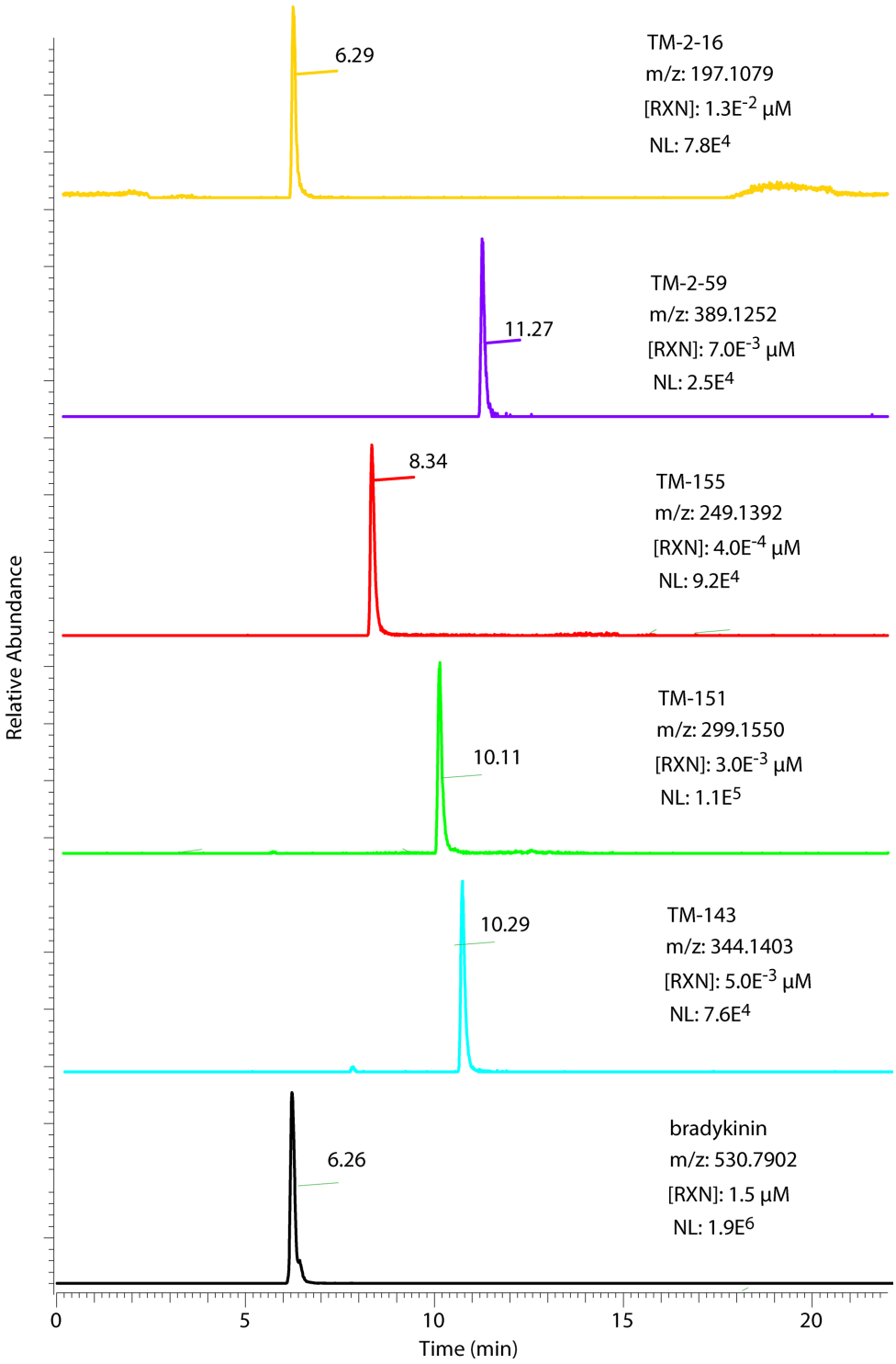

Figure 3.5: Observed retention times and reaction concentrations [RXN] for TM-139, TM-141, TM-151, TM-155, TM-2-16, TM-2-59 and Bradykinin.

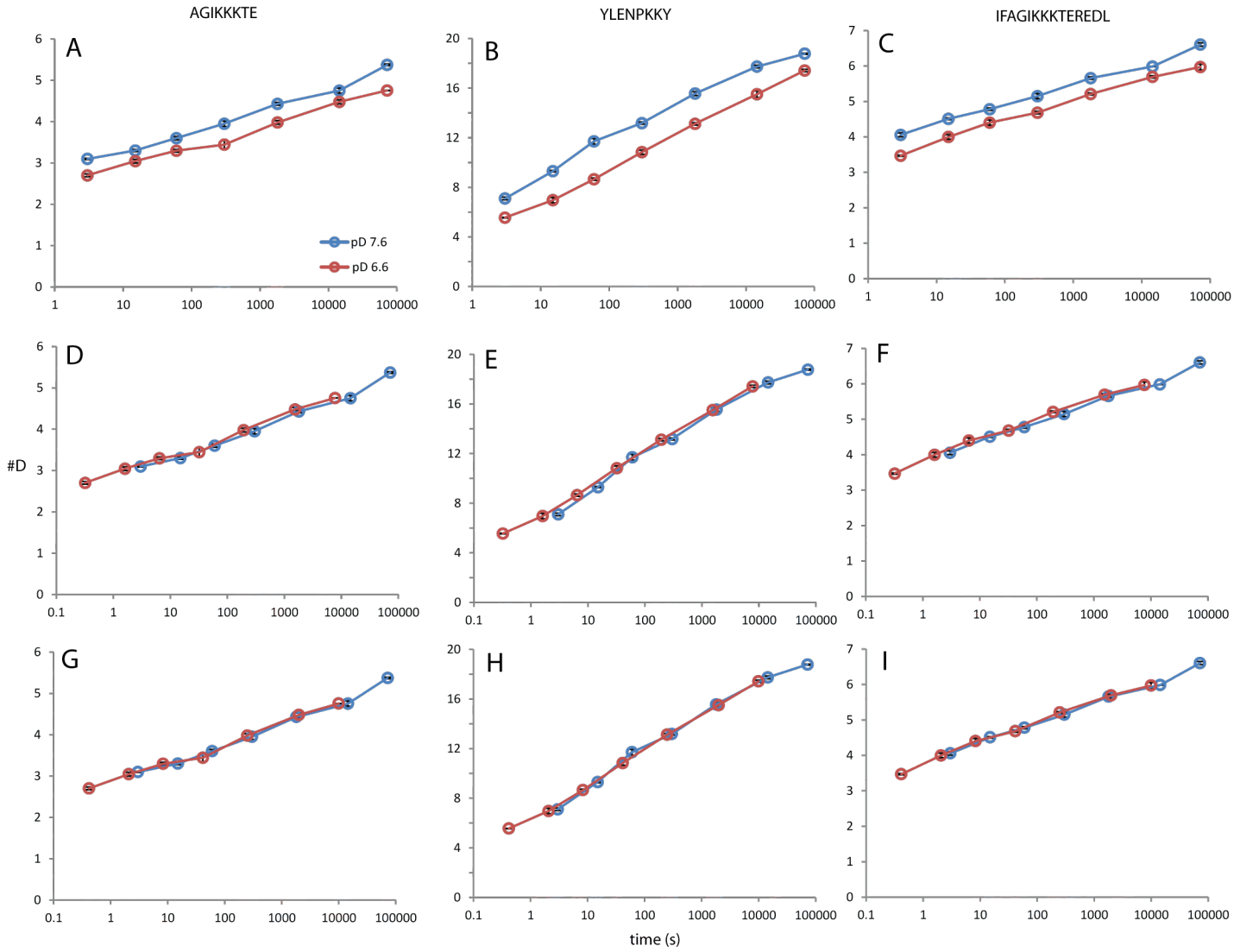

Figure 3.6: Panels A, B, and C show the observed deuterium uptake at pD 7.62 (blue) and 6.65 (red) for 3 peptic peptide from Equine Cytochrome C: AGIKKKTE, YLENPKKY, and IFAGIKKKTEREDL. Panels D, E, and F show these same peptides with the low pD time points shifted to account for the difference between the high and low pD conditions. Panels G, H, and I show these peptides with the low pD time points shifted by a factor proportional to the average difference in observed rates under the high and low pD conditions for the imidazolium IERs. Note that the reported pD values are calculated from the measured pH* using the method described in Chapter 2.

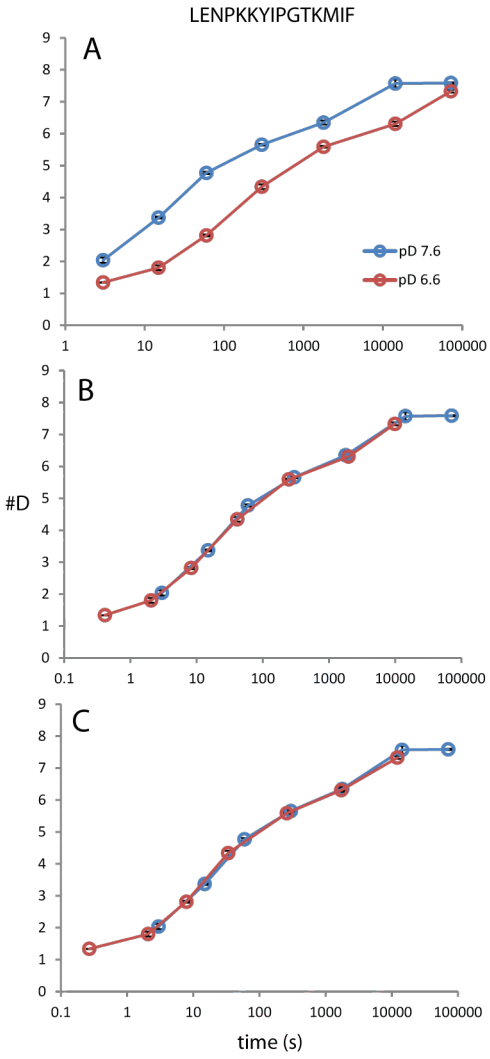

Figure 3.7: Panels A shows the observed deuterium uptake at pD 7.62 (red) and 6.65 (blue) for the Equine Cytochrome C deried peptic peptide LENPKKYIPGTKMIF. Panel B shows the low pD time points for this peptide shifted by a factor proportional to the average or global difference in observed rates under the high and low pD conditions for the imidazolium IERs. Panel C shows the low pD time points for this peptide shifted by a factor proportional to the difference in observed rates under the high and low pD conditions for an imidazolium IER between 10 and 90% exchanged at each time point.

Chapter 4

An IER Based Strategy for Standardizing % D

4.1 Introduction

For typical HDX-MS studies peptide deuterium uptake tends to vary by approximately 10%[60, 13]. Some advanced automated systems can achieve more precise measurements however, widespread use of these systems remains impractical[10]. The development of more pragmatic approaches to improving HDX-MS data quality has tangible benefits. For example, by improving precision beyond 10% HDX-MS can be utilized to study more subtle interactions or more complex systems, create higher resolution labeling maps, and help improve the statistical power of datasets[38]. Internal standard-based approaches have been shown to considerably improve data quality[129, 121, 90, 134]. However, these methods are generally only suitable for detecting changes in reaction buffer conditions or sample handling variations. Significantly less attention has been directed towards addressing variation in reaction deuterium content.

Observed deuterium uptake is linearly proportional to the reaction deuterium content or % D. Variation in % D typically arises from dispensing error, changes in reagent quality, or through exposure of the exchange reaction to atmospheric moisture[109, 84]. Often a change in % D for a few samples within a single experiment can be detected and corrected using a maximally deuterated control. Essentially the maximally deuterated control shows the highest possible degree of deuteration for a specific peptide. This value can be used to adjust the uptake of a matching peptide where variation in % D has impacted the extent of exchange. In Figure 4.1 the uptake of the Equine Cytochrome C derived peptic peptide MEYLENPKKYIPGTKMIFAGIKKK-TERED is shown under two conditions where reaction % D has been varied. In panel A the solid blue line represents the correction of the deuterium uptake under condition 2 through the use of a maximally deuterated control sample. Although very useful, the maximally deuterated control cannot be used to determine the actual reaction deuterium content. A consequence of this limitation is shown in Figure 4.1 panel B, where the uptake of the same peptide under the low % D condition is corrected using the maximal deuterium uptake for the back-exchange reporter peptide Bradykinin. The underrepresentation of deuterium denoted by the solid blue line occurs because the Equine Cytochrome C derived peptide and Bradykinin lose different amounts of deuterium over the numerous downstream processing steps following quench[28, 50, 134, 129, 60]. While Bradykinin is not typically used to correct for variation in reaction % D, doing so in this example is conceptually similar to correcting uptake for matched peptides collected at different sites or on different days. The inability of peptide-based controls to facilitate meaningful comparison of HDX-MS data-sets suggests that in the absence of additional tools, reproducibility will remain limited[60, 22].

Currently the only method intended to facilitate the detection and correction of variation in reaction deuterium content across disparate HDX-MS datasets was published in 2014 by Joey G. Sheff and David C. Schriemer[109]. This approach requires that known quantities of "light" and "heavy" (C13 labeled) caffeine be added to the $H_2O$and D_2Oreaction buffers prior to the incubation step. The caffeine standard does not retain any deuterium following quench, so the resulting ratio of caffeine isotopes can be used to estimate the reaction % D directly. Conceptually this estimate of % D could be used to standardize deuterium content across

data sets collected at different times or in different laboratories. However, the non-exchangeable caffeine standards can only detect dispensing errors. In other words, this approach cannot address % D variation arising from changes in reagent quality or exposure to atmospheric moisture. Additionally, the amounts of light and heavy caffeine have to be optimized to achieve a linear response from the mass spectrometer[109]. This can be challenging to achieve in certain instruments, particularly those with a limited dynamic range[11, 109]. Essentially, extensive system-specific back-exchange prevents peptide-based controls from measuring reaction deuterium content, and the alternative non-exchangeable reporter based strategy, is similarly limited by insensitivity towards reaction conditions and incompatibility with many workflows[114, 115, 134, 109]. In this Chapter we will discuss the development of an imidazolium based reporting strategy for standardizing reaction % D. Imidazolium reporters are particularly well suited to this purpose because the rate of exchange can be accelerated to allow for maximal deuteration within the shortest typical time point for an HDX-MS experiment of 3s, and the extremely slow and predictable back-exchange for these compounds allows for unambiguous detection of actual reaction deuterium content[28].

4.2 Designing an Imidazolium based % D reporter

Most exchange reactions are carried out at room temperature in buffered solutions ranging from pH 6.5 to 7.5, from this we understand that a versatile % D reporter should have a half-life less than 0.6s at pH 7.0. Given that imidazolium IERs exchange exclusively through base catalysis, it is possible to accurately predict the extent of deuterium loss under quench conditions and during downstream processing. This property of imidazolium allowed for the establishment of a lower limit on the half-life of a "useful" % D reporter, which is 0.215s. Beyond this lower limit, the half-life under typical chromatographic conditions is less than 40min, and as much as 12% of the deuterium content could be lost. This estimate considers the acceleration of exchange in the presence of the organic co-solvent acetonitrile (ACN). An in-depth discussion of this effect as it pertains to imidazolium can be found in Chapters 2 and 5. Additionally, a discussion of predicting D-loss by imidazolium under chromatographic conditions can be found in the subsection titled "Addressing Downstream Deuterium Loss".

4.2.1 Using Computational Methods to Accelerate Discovery

Although we have successfully targeted time point coverage using a conceptual understanding of how imidazolium structure influences the rate of C-2 exchange, using this same approach to pursue such a narrow temporal window may have taken many iterations. In an effort to accelerate the search for a suitable % D reporter, we attempted to develop a computational model to estimate exchange rates for unknown imidazolium derivatives. The model was conceptually similar to a Hammett plot, in that it related the changes to electronic structure induced by specific substituents to the rate of proton transfer. This was accomplished by using the computational chemistry platform Gaussian to generate single point energy (SPE) values for optimized 3D structures of protonated and de-protonated forms of well-studied imidazolium compounds. As de-protonation is understood to be the rate-limiting step in the proton transfer reaction at the C-2, the difference in SPE values corresponding to the protonated and de-protenated forms can be used as a qualitative indicator of C-2 acidity analogous to the measurement of C-2 ppm[2]. This assumption is supported by a reasonably strong linear relationship between the observed chemical shift for the C-2 proton in 10% $D_2O$and the computationally derived difference in SPE seen in Figure 4.2. This relationship facilitated the calculation of C-2 chemical shift values for unknown compounds. These computationally derived C-2 values were then used to estimate the rate of exchange for the unknown compound via the empirical relationship discussed in Chapter 2.

Initial tests of this method showed an average percent difference between predicted and observed rates within the training set of 39%, with the maximum deviation being 87% and the minimum being 1.9%. Despite this limitation, the approach was used to generate crude estimates of exchange rates for a series previously uncharacterized imidazolium derivatives. Among the initial series of unknown compounds was 1,3-dimethyl-5,6-dinitrobenzimidazolium (TM-162). The computationally estimated rate for TM-162 at pD 7.0 and 25C was 0.239 s^{-1} (t1/2=2.89 s) which did not meet the minimum rate requirement for a % D reporter. Moreover, the estimated log P of -3.8 suggested that TM-162 would be insufficiently retained under typical chromatographic conditions and therefore of limited utility. Nonetheless, TM-162 was synthesized in

an effort to refine the computational approach through expansion of the training set. The observed rate for TM-162 was measured at 0.249 s^{-1} (t1/2=2.78 s) under standard conditions. The surprising accuracy of this prediction suggested a bias towards nitro-containing compounds which may have been resolved through further expansion of the training set. Such refinement was found to be unnecessary as empirical data showed that the additions of N-benzyl groups to this structure would accelerate exchange by approximately 10-fold exceeding the minimum necessary rate for a % D reporter.

The synthesis of the benzyl derivative of TM-162, 1,3-dibenzyl-5,6-dinitrobenzimidazolium (TM-2-59) was accomplished over 2 steps via 4.3. Analysis of the compound's kinetics by CHDX-MS showed that the under standard conditions, the rate was 2.86 s^{-1} (t1/2= 0.242 s). This rate is just within the maximum for a "useful" % D reporter of 3.224 s^{-1} (t1/2= 0.215s). Additionally TM-2-59 has a relatively high estimated logP of 1.03, which suggested that it would be retained for 632±33s (10.54±0.55min) corresponding to an estimated loss of 10.28±2.56% deuterium content under the chromatographic conditions typically used in the Guttman lab (see Chapter 2, methods). However, due to the accuracy with which imidazolium D-loss can be predicted this proved to have little impact on the overall quality of the % D correction.

4.3 Suitability of TM-2-59 to Standardize % D

In order to assess the utility of an imidazolium reporter-based approach to correcting % D variation in HDX-MS we carried out a series of exchanges where reaction pH* was kept constant at 7.183 (pD 7.63), and deuterium content was varied in known intervals over 2 conditions. Reaction deuterium content for conditions 1 and 2 was 84.6% and 69.5% respectively. Conditions 1 and 2 were prepared using the same buffer at the same concentration. Condition 1 represents the maximum % D for a typical exchange reaction. In condition 2 the % D was reduced by adding water to the condition specific D2O stock. The small peptide bradykinin was included in each D2O stock as a back exchange reporter. The % D reporter TM-2-59 along with 2nd generation reporters TM-143, TM-151, TM-155, and TM-2-16 were added to a protein solution containing Equine Cytochrome C, Equine Myoglobin and Hen Egg Lysozyme. Exchange reactions corresponding to each condition were carried out side by side at $25°C$in quadruplicate at 3 time points: 3s, 1min, 4hrs (3s, 60s, and 14400s). Maximally deuterated samples were also generated for both conditions in the usual way[84, 67]. The deuterium uptake of the peptic peptides and imidazolium reporters was observed via Thermo LTQ-Orbitrap at 60K resolution, and the data was processed using Sierra Analytics HDexaminer version 2.34.

The imidazolium reporters were detectable at very low concentrations, more than 100X less than that of the individual proteins. Deuterium uptake by the analytes clearly reflected the reaction deuterium content corresponding to each condition (Table 4.4). Consistent with previous observations TM-151 reached maximal deuterium incorporation after 30 min at pH* 7.183 and 25C. From these measurements, reaction deuterium content for conditions 1 and 2 were calculated at 85.6% and 69.7% respectively. TM-2-16 was observed to reach full deuterium incorporation after 30 min. From these measurements, reaction deuterium content for conditions 1 and 2 were calculated at 87.2% and 69.65% respectively. The faster exchanging reporter TM-143 reached maximal deuterium incorporation after 15 seconds under these conditions. From these measurements, reaction deuterium content for conditions 1 and 2 were calculated at 84.8% and 68.4% respectively. The proposed % D reporter, TM-2-59, reached maximal deuterium incorporation within 3 seconds under both conditions. This is clear from the relatively minimal variation in the # D for this compound across the entire time course (4.5, panel A). Consistent with our expectation regarding back-exchange by TM-2-59 under chromatographic conditions, the compound reports reaction deuterium content at 74.5% and 58.3% for conditions 1 and 2 respectively. Although % D loss by TM-2-59 cannot be meaningfully reduced through modification of the chromatographic conditions, the extent of D-loss is significantly less than what is typically observed for peptide-based alternatives[90, 134]. Moreover, the comparatively simple exchange kinetics of imidazolium IERs makes it possible to accurately calculate the extent of downstream deuterium loss with reasonable accuracy.

4.3.1 Addressing Downstream Deuterium Loss

As previously discussed, peptide-based reporters are incapable of accurately measuring reaction deuterium content because of extensive system specific back-exchange. Unfortunately an imidazolium reporter capable of measuring % D across the entire HDX-MS time course must exchange so rapidly that some back-exchange

is likely. Unlike peptides, D-loss by imidazolium occurs almost exclusively during chromatography. This behavior is a consequence of the compounds 1st order exchange kinetics. For example, during the thawing phase where solution pH is approximately 2.5 and the temperature is $5°C$TM-2-59 has a half-life of 27.5hrs, a value which decreases only slightly during the trapping phase to 24.03hrs. As solution pH and temperature during the trapping phase are kept low, the slight acceleration in rate is a understood to arise primarily from the change in solvent composition[35, 54, 12, 47, 90, 61, 41, 98]. This observation is consistent with the effects of ACN on imidazolium exchange discussed in Chapter 2 and suggests that back-exchange by TM-2-59 or any imidazolium based reporter can be generally considered as function of chromatographic retention and solvent composition.

In an effort to test this assumption, the downstream processing of matched maximally deuterated samples was broken down into 3 phases, thawing, trapping, and chromatography. Each phase was then modified independently over 5 different experiments to systematically identify sources of D-loss. In Experiments 1-4, a Waters BEH C18 trapping column (2.1 × 5 mm, 1.7 μm) and a Waters BEH C18 analytical column (1x50mm, 1.7 μm, 130 Å) were used. Experiment 1 established the baseline for typical downstream process. In this experiment frozen samples were subjected to a standard 4min thawing phase followed by an IER-optimized 7min trapping phase and an IER-optimized LC gradient. In experiment 2 the thawing phase was unchanged, while the length of the trapping phase was reduced to 5min, and the LC gradient was changed to one optimized for general use was. This experiment was intended to show if the downstream optimization made for IERs have any impact on D-loss. Next in experiment 3 frozen samples were subjected to a standard 4min thawing phase followed by an extended 20min trapping phase and an IER-optimized LC gradient. By changing the length of the trapping phase only, we were able directly compare D-loss in experiments 1 and 3 to understand how the trap environment influences back exchange. In experiment 4 the thawing phase was changed from 4min at $5°C$to 60min at $0°C$, while the trapping and chromatography phases were matched to experiment 1. Experiment 3 allowed for the assessment of how changes to the thawing phase, which could arise from improper sample handling affect back-exchange. Lastly, in experiment 5 the the thawing, trapping, and chromatography phases were matched to experiment 1, but the dimensions of the analytical column were changed from 1 × 50mm to 1 × 100mm. By altering the column dimensions only between experiments 1 and 5, we were able to isolate the effect of retention time on the extent of D-loss.

Figure 4.6 summarizes the results of these studies by showing how these sample handling variations influenced D-loss for TM-143, TM-2-59 and Bradykinin. Between experiments 1 and 2, there is no significant change in the apparent % D reported by TM-143 or TM-2-59 and a modest 0.80% deviation in the reported %D for bradykinin. These observations suggest that the IER-optimized gradient has little effect on imidazolium back-exchange but may slightly increase D-loss in peptides. During the extended trapping phase in experiment 3 the change in % D reported by TM-143 and TM-2-59 changes very little compared to bradykinin, which loses an additional 25% D relative to experiment 2. These results suggest that trap time strongly affects back-exchange in peptides, but has little effect on imidazolium D-loss. Following the extended 1hr thawing phase in experiment 4, Bradykinin loses 19%D, while TM-2-59 shows a small loss of 0.838% D, and TM-143 shows no significant change compared to the average observed % D in experiments 1-3. This experiment reinforces the assertion that back-exchange rates for imidazolium compounds are very slow under the thaw conditions. Lastly in experiment 5, where only the retention of compounds was altered relative to experiment 1 via the change in the length of the analytical column there is a more significant loss of deuterium by TM-2-59 amounting to 3.8% D. This is in contrast to the absence of any significant change in the % D reported by TM-143 and the sizable reduction in D-loss for Bradykinin relative to experiments 3 and 4 (1.93% D). The observation that an increase in retention has a greater effect on imidazolium D-loss than extensive trapping or thawing strongly suggests that the vast majority of D-loss by imidazolium reporters occurs during the chromatography phase. The practical consequence of this observation is that the extent of imidazolium back exchange can be treated as a function of retention time and the mole fraction of ACN.

Using HDX-NMR data, a system of empirically derived equations was developed to facilitate the calculation of imidazolium D-loss during chromatography. First the rate correction factor (τ_{corr}) is calculated from equation 4.1 where χ is the mole fraction of ACN at a given time point in the LC-gradient and λ_{H_2O} is the decay constant for the imidazolium reference reporter determined by HDX-NMR.

$$\tau_{corr} = \frac{\frac{ln(2)}{10^{\lambda_{H_2O}}}}{\frac{ln(2)}{10^{(7.437\chi - 3.8965)}}} \tag{4.1}$$

The correction factor τ_{corr} is then applied in equation 4.2 to generate λ_{OR} which is the decay constant for the reporter in question under the solvent conditions specified in equation 4.1. In equation 4.2 the term τ_q is the half-life for the reporter in question under the thaw conditions, in this case pH 2.5 and $5°C$. We note that the value of τ_q may require adjustment if the difference between thaw and LC temperature is large, as temperature is also a strong modulator of imidazolium exchange rate[118, 96, 40, 90].

$$\lambda_{OR} = \frac{ln(2)}{\frac{\tau_q}{\tau_{corr}}} \tag{4.2}$$

The value λ_{OR} is time point specific and can be used in equation 4.3, where t_{OR} is the time point in question, N_0 refers to the amount of deuterated reporter at the previous time point and N_t refers to the amount of deuterated reporter present after t_{OR}.

$$N_t = N_0 e^{(-\lambda_{OR} \cdot t_{OR})} \tag{4.3}$$

Accurate calculation of N_t using this system of equations requires that the value of N_0 change throughout the LC gradient to account for the cumulative reduction in % D. To streamline the calculation of N_t a Microsoft Excel based tool has been created. Using this tool, TM-2-59 is estimated to lose 11.69% D from the starting point of 84.6% D in condition 1, and 9.61% D from the starting point of 69.5% D in condition 2. This closely corresponds to the observed deuterium loss by TM-2-59 relative to the other reporters, which can be seen in Table 4.4. It should be noted that the comparatively minor deviations in % D reporting by TM-143, TM-151, and TM-2-16 are likely not the result of back-exchange because, these compounds back-exchange too slowly for D-loss to be detected under the chromatographic conditions used. It is more likely that these smaller variations are the consequence of destructive interference arising from the insufficient resolution of the signals corresponding to the M+D ion and C^{13} containing M+H ion by the Thermo LTQ-Orbitrap instrument used in this study[11, 67]. In Figure 4.7 panel A, two isotopes of TM-2-16 are displayed. Here M+H is shown at 197.1077 m/z, and M+D highlighted in red is shown at 198.1138 m/z. Panels B, C, D and E show the M+D peak at 15K, 60K, 120K and 240K resolution respectively. By zooming in on this region it is possible to see the C^{13} containing M+H emerge from under the broad peak associated with the M+D ion as resolution increases. The data discussed in this Chapter was collected at 60K resolution where the effect of this destructive interference can be recognized by the reduction in apparent % D particularly under condition 2. Consequently the quality of % D correction is limited by this effect. However, It should be noted that this distortion can be minimized on Fourier-transform mass spectrometry (FT-MS) instruments like the Thermo LTQ-Orbitrap by adding a low resolution 15K scanning event to the acquisition method.

4.3.2 Standardizing Deuterium content using TM-2-59

The published approach to generating a correction factor (X_{corr}) based on the ratio of "light" and "heavy" caffeine can be modified for use with exchanging reporters (4.4). In equation 4.4 the term D_{obs} is the actual observed deuterium uptake for the species and D_{max} is the maximum deuterium content for an IER that exhibits no back exchange, in this case the average uptake of TM-143 under condition 1 (84.6% D, pD 7.6) during the 60s and 14400s time points was used.

$$X_{corr} = \frac{D_{obs}}{D_{obs} + (D_{max} - D_{obs})} \tag{4.4}$$

$$D_{corr} = \frac{D_{meas}}{X_{corr}} \tag{4.5}$$

The value X_{corr} is applied in equation 4.5, where D_{meas} is the raw uptake of the species in question and the D_{corr} is the corrected uptake for that species[109]. Figure 4.8 shows the uncorrected deuterium uptake for the Equine Cytochrome C derived peptide MEYLENPKKYIPGTKMIFAGIKKKTEREDL in broken lines. Here, the solid blue line represents the uptake for the same peptide scaled to the measured reaction deuterium content using this method. In Figure 4.8 panel A the correction was accomplished by using the uptake of TM-143 under condition 2 (69.5% D, pD 7.63) at the 60s and 1440s time points as D_{obs} and the average maximum deuterium content of TM-143 under condition 1 (84.6% D, pD 7.63) as D_{max}. Here the raw uptake for the peptide under condition 2 is adjusted from 33.4% at 60s and 46.6% at 14400s

to 41.4% and 57.8% respectively. This corresponds to an average of 1.06% error between the observed % D under condition 1 and corrected % D under condition 2. This example serves as a useful proof of concept, demonstrating that it is possible to make robust corrections to observed deuterium uptake for a peptide by scaling uptake to the reaction deuterium content measured by an exchangeable reporter molecule. In Figure 4.8 panel B the back-exchange corrected uptake of TM-2-59 is used to facilitate the scaling of deuterium uptake for the same peptide across the entire time course for the experiment. Here the raw deuterium uptake for the peptide under condition 2 is adjusted from 22.5% at 3s, 33.4% at 60s, and 46.6% at 14400s to 28.2%, 41.8%, and 58.3% respectively. Notably, the back-exchange correction of TM-2-59 appears to have little effect on the quality of the % D correction. This is evident from the average error between observed % D in condition 1 and the corrected % D under condition 2, which is 1.53%. This relatively small increase in error further suggests that imidazolium D-loss can be accurately calculated using the method described in addressing Downstream Deuterium Loss". Moreover, the quality of imidazolium based % D correction is likely to improve if the destructive interference effects associated with FT-MS instrument can be avoided [11].

4.4 Methods

4.4.1 Reagents

D2O, deuterated ACN, and deuterated DMSO were purchased from Cambridge Isotope Labs (Tewksbury, MA, USA). benzyl amine 99%, trimethyloxonium tetraflouroborate 95%, and formic acid 88% in methanol were purchased from sigma Aldrich (St. Louis, MO, USA). 1,2-difluoro-4,5-dinitrobenzene 95%, and 5,6-dinitrobenzimidazole 98+% were purchased through Enamine Building Blocks (Cincinnati, OH, USA). Before use in alkylation reactions the solvents were dried via distillation over activated 3A molecular sieves. Chromatography solvents, absolute ethanol, concentrated HCl, and solid NaOH were purchased from Fisher Scientific (Hampton, NH, USA).

4.4.2 Computational Approach to Reporter Discovery

Structures of well-studied imidazolium reporters TM-31, TM-39, TM-65, TM-68, TM-85, and TM-91 in addition to the unknown target molecule TM-162 were generated in cationic and ylide forms ChemDraw prime (PerkinElmer) then exported as .mol files. These structures were imported into the computational chemistry platform Gaussian (ver. 16, Rev. A. 03). Initial structural optimization for all structures was carried out using density functional theory (DFT, b3lyp/6-311+g(d,p)). The most reasonable low energy optimized outputs were selected for single point energy (SPE) calculation using 3 different models: mp2/6-31+g(d), hf/3-21g, and b3lyp/6-1+g(d). SPE values for individual structures were given in hartrees. The difference in SPE values corresponding to cationic and ylide structures was calculated for each model then related to the experimentally derived C-2 chemical shift for each compound. All NMR experiments were performed on a 499.73 MHz Agilent DD2 spectrometer equipped with a 5 mm triple-resonance 1 H(13C/15N), z-axis pulsed-field gradient probe head. Samples were all prepared in 10% D2O and observed at $23°C$. Residual solvent signal was suppressed using pre-saturation. A strong linear relationship was observed between the mp2/6-31+g(d) associated SPE values and the corresponding C-2 chemical shift thereby enabling the calculation of C-2 chemical shift (CG-C2) from computationally generated SPE values. The CG-C2 value was used to estimate C-2 exchange rate via the empirical relationship between C-2 ppm and exchange rate discussed in Chapter 2. We note that this model exhibits a clear bias with regard to the quality of rate estimation and recommend that the reader seek out more refined methods for estimating C-2 chemical shift like those recently published by Peng Gao and colleagues18.

4.4.3 Continuous labeling HDX-MS (CHDX-MS)

CHDX-MS requires the quenched exchange reaction to flow directly into the ionization source at relatively high flow rates. As a result, volatile buffers are essential. For the CHDX-MS experiments we carried out, the exchange buffer was 200mM ammonium acetate and the quench buffer included 1% formic acid and 1% trifluoroacetic acid in optima H2O. Both buffers were adjusted using solutions of sodium hydroxide or

hydrochloric acid to achieve the desired solution pH value. The reaction buffer was made by adding 150μL of the acetate buffer to 1350μL of 99.99% D2O for a final buffer concentration of 20mM. The IER master mix was made by adding compounds TM-155, TM-151, TM-143, TM-2-16, and TM-2-59 to optima H_2O. Immediately before beginning the experiment, 1485μL of the buffered D_2Osolution was drawn up into a glass Pasteur pipette and mixed in a vessel containing 15μL of the IER master mix to form the reaction mixture. Half of the reaction mixture was promptly removed using a gastight 1ml syringe and the remaining 750μL was used to measure reaction pH* by a Thermo combined glass electrode. Please refer to Chapter 3 for a detailed description of the CHDX-MS apparatus and associated data processing methods.

4.4.4 HDX-MS

To asses the utility of the proposed imidazolium reporter based strategy for standardizing deuterium content, phosphate buffered saline (PBS) D2O reaction buffers with different deuterium concentrations were created using a single PBS solution adjusted to pH 7.457 (pH* 7.183, pDcalc 7.63). The reaction buffers with calculated deuterium contents of 94.05% and 77.22% D, correspond to conditions 1 and 2 respectively. The deuterated buffer had 0.2 μg/mL of bradykinin and angiotensin II to serve as controls for assessing back-exchange[134]. The protein solution included Equine Cytochrome C, Equine Myglobin, Hen Egg Lysozyme (Sigma-Aldrich) resuspended in PBS (20 mM sodium phosphate, 150 mM NaCl, 2 mM DTT) to an individual concentration of 15μM. To this stock, a total of 5 imidazolium exchange reporters were added: TM-143 (.05 μM), TM-151 (.03 μM), TM-155 (.004 μM), TM-2-16 (.12 μM), and TM-2-59(.07 μM). Exchange reactions were prepared in quadruplicated by adding 10 μL of the protein solution to 90 μL of a deuterated buffer. Incubation was carried out at 23.5°C for 3 s, 1 min, or 4 h. Undeuterated samples were prepared in the usual way[84]. Maximally deuterated exchanges were also carried out in quadruplicate for each condition using two different methods. Detailed descriptions of maximally deuterated sample prep can be found in Chapter 3. All exchange reactions and undeuterated samples were prepared by hand in a single day. Following incubation, exchanged samples were added to an equal volume (100 μL) of ice-cold quench buffer (8 M urea, 0.2% formic acid) for a final pH of 2.5. Samples were flash frozen in an ethanol−dry ice bath $-60°C$and subsequently stored at $-80°C$until LC-MS analysis. The exact pH* during the deuterium reaction was measured using an identical sample in D2O, without protein, and used to calculate the pD using methods discussed in Chapter 2[19, 20, 44]. Frozen samples were thawed on a 5°Cblock for 4min prior to injection onto a loading loop. The loaded sample was passed over a custom packed pepsin column (2.1 × 50 mm) kept at 8°C with a flow of 0.1% trifluoroacetic acid (TFA) at 200 μL/min. Digested peptic fragments were trapped onto a Waters CSH trap column (2.1 × 5 mm, 1.7 μm). Waters BEH traps were also found to be effective. After a 7min phase, digested peptides and IERs were resolved on an analytical column (Waters CSH 1 × 100 mm mm, 1.7μm, 130Å) using a binary buffered mobile phase composed of buffer A (0.1% FA, 0.025% TFA, 2% ACN; B) 0.1% FA in ACN) and buffer B (99.9% ACN, 0.1% TFA). The ratio of these buffers was changed over an optimized steeped gradient, wherein buffer B is held at 2% for 4 min then increasing to 10% 4.5 min, then to 33% via linear gradient at 13 min, and to 50% at 14.5 min, before increasing linearly again to 95% at 16min. After 16min the column was washed and allowed to equilibrate at 2% B for several minutes. The LC system was coupled to a Thermo LTQ-Orbitrap performing full scans over the m/z range of 150− 1500 with a resolution setting of 60,000. During the analytical separation step, a series of 250 μL injections were used to clean the pepsin column. A complete description of the wash buffers and between-run LC cleaning protocol can be found in Chapter 3. Undeuterated samples were used to collect MS/MS spectra using data-dependent acquisition. Peptic peptides were identified by exact mass and tandem mass spectrometry (MS/MS) spectra using Byonic (Protein Metrics). Mass shifts were determined using HD-Examiner V2 (Sierra Analytics) and HX-Express v2.34.

4.4.5 Deuterium Content standardization

The correction factor X_{corr} is generated using equation 4.4. We note that back-exchange correction of D_{obs} is necessary for TM-2-59. a detailed discussion of how this correction is accomplished can found in the section "Addressing Downstream Deuterium loss". Next using equation 4.5 the raw uptake for a particular peptide (D_{meas}) is dived by X_{corr} to generate the value D_{corr}. The value D_{corr} is the uptake of the raw peptide adjusted to match the maximal deuterium content as determined by D_{ref}. The equations described

have been adapted from a previously published method for use with reporting controls[109]

4.4.6 Evaluation of Downstream Deuterium loss

In an effort to asses the effects of downstream processing on D-loss, 5 sets of maximally deuterated samples containing imidazolium IERs and bradykinin were prepared at pH 7.4 using totally deuterated method A (TDA). All samples were prepared in triplicate. Samples were flash frozen in an ethanol−dry ice bath $-60°C$and subsequently stored at $-80°C$until LC-MS analysis. The exact pH* during the deuterium reaction was measured using an identical sample in D2O, without protein, and used to calculate the pD using methods discussed in Chapter 2[19, 20, 44]. Measurements were carried out back-to-back in triplicate for all conditions except experiment 1, which was performed in duplicate due to sample loss caused by instrument error. Samples were processed using the automated methods and buffers described in Chapter 2. In experiment 1 frozen quenched samples were thawed at $5°C$for 4min, then injected into a refrigerated LC-system for a 7min trapping phase where buffer salts were removed and analytes were concentrated on a waters BEH C18 trap column (2.1 × 5 mm, 1.7 μm), following trapping LC separation of analytes was accomplished using a waters BEH C18 analytical column (1 × 50mm, 1.7 μm, 130 Å) and the IER-optimized gradient described in the subsection titled "HDX-MS". In experiment 2 frozen quenched samples were thawed at $5°C$for 4min, then injected into a refrigerated LC-system for a 5min trapping phase where buffer salts were removed and analytes were concentrated on a waters BEH C18 trap column (2.1 × 5 mm, 1.7 μm), following trapping LC separation of analytes was accomplished using a waters BEH C18 analytical column (1 × 50mm, 1.7 μm, 130 Å) and the standard gradient described in Chapter 2. In experiment 3 frozen quenched samples were thawed at $5°C$for 4min, then injected into a refrigerated LC-system for a 20min trapping phase where buffer salts were removed and analytes were concentrated on a waters BEH C18 trap column (2.1 × 5 mm, 1.7 μm), following trapping LC separation of analytes was accomplished using a waters BEH C18 analytical column (1 × 50mm, 1.7 μm, 130 Å) and the IER-optimized gradient described in the subsection titled "HDX-MS". In experiment 4 frozen quenched samples were thawed at $0°C$for 60min, then injected into a refrigerated LC-system for a 7min trapping phase where buffer salts were removed and analytes were concentrated on a waters BEH C18 trap column (2.1 × 5 mm, 1.7 μm), following trapping LC separation of analytes was accomplished using a waters BEH C18 analytical column (1 × 50mm, 1.7 μm, 130 Å) and the IER optimized gradient described in the subsection titled "HDX-MS". In experiment 5 frozen quenched samples were thawed at $5°C$for 4min, then injected into a refrigerated LC-system for a 7min trapping phase where buffer salts were removed and analytes were concentrated on a waters BEH C18 trap column (2.1 × 5 mm, 1.7 μm), following trapping LC separation of analytes was accomplished using a waters BEH C18 analytical column (1 × 100mm, 1.7 μm, 130 Å) and the IER-optimized gradient described in the subsection titled "HDX-MS". The results of these experiments are summarized in the Figure 4.6.

4.4.7 Calculating the extent of imidazolium D-loss

A Microsoft Excel based tool has been developed to allow for accurate calculation of D-loss by an imidazolium-based reporter. This tool will be made publicly available upon publication of this work.

4.4.8 Synthesis of 1,3-dimethyl-5,6-dinitrobenzimidazolium (TM-162)

To an oven dried round bottom flask containing a magnetic stir bar 5,6-dinitrobenzimidazole (0.23mmol, 1.0 eq)and trimethyloxonium tetraflouoborate (1.15mmol, 5.0 eq) were added. Next approximately 5ml methylene chloride (DCM) was added, and the vessel was fitted with a rubber septum and flushed with argon (g). The mixture was set to stir under an argon environment at room temperature for 48hrs. Excess solvent was removed under reduced pressure. The residue was resuspended in mobile phase (75:25 H2O:ACN w/ 0.1% TFA) and filtered using a syringe driven filter (0.22μM). The effluent was purified via reverse phase HPLC (C18, gradient elution: 20-95% ACN in H2O with 0.1% TFA), to yield 1,3-dimethyl-5,6-dinitrobenzimidazolium (TM-162) as a yellow orange oil, 95% 1H NMR (300.13 MHz, DMSO-D6, ppm): 10.05 (S, 1H), 9.16 (S, 2H), 4.15 (S, 6H); MS (ESI) calcd for C9H9N4O4: 237.0618, found: 237.0552 M/Z.

4.4.9 Synthesis of 1,3-dibenzyl-5,6-dinitrobenzimidazolium (TM-2-59)

To an oven-dried round bottom flask containing a magnetic stir bar solid 1,2-diflouro-4,5-dinitrobenzene (0.97mmol, 1.0eq) and anhydrous potassium carbonate (3.88mmol, 4.0eq) were added. The solids were set to stir in 3ml of anhydrous Dimethyl sulfoxide (DMSO). The vessel was sealed with a rubber septum and flushed with argon (g). Next, anhydrous benzyl amine was added dropwise via cannula under an argon environment. After 2hrs at roomtemperature, the reaction mixture was diluted with 20ml of ice water. The reaction vessel was cooled to $-20°C$ until precipitate formed. The supernatant was removed and the solids were washed with ice-cold brine before being dissolved in 2:1 hexanes:DCM and allowed to reach room temperature. The remaining dark red solids were removed via gravity filtration over filter paper. The effluent was then cooled to $-20°C$ overnight, and the supernatant was removed to reveal the intermediate 1,2-dibenzyl-4,5-dinitrobenzene (TM-2-53) as fine yellow crystals (MS: 379.1 M/Z, M+H). The solid TM-2-53 was used in the next reaction without further purification, with purity unknown, and an approximate yield of 14% . In a round bottom flask, solid TM-2-53 (0.13mmol, 1.0eq)was dissolved in 5ml of triethylorthoformate and set to stir. Next 300 μL of 21N hydrochloric acid (HCl) was added at once followed by 150 μL of 88% formic acid in H2O. The vessel was then fitted with a water cooled reflux condenser and heated to approximately $150°C$ and held for 2 hrs. After, the reaction vessel was allowed to cool and the reaction solvent was removed under reduced pressure. The residue was resuspended in 1:1 ACN:H2O (0.1% TFA) and purified by HPLC using a linear gradient from 30-70% ACN with 0.1% TFA over 20min to yield 1,3-dibenzyl-5,6-dinitrobenzimidazolium (TM-2-59) as a yellow oily solid 99% 1H NMR (699.96 MHz, DMSO-D6, ppm): 10.39 (S, 1H), 9.22 (S, 2H), 7.55-7.41 (M,10H), 5.87 (S, 4H); MS (ESI) calcd for C21H17N4O4: 389.1244, found: 389.1239 M/Z

4.5 Conclusions

In this Chapter we have demonstrated a novel IER based approach to standardizing reaction deuterium content. Using this approach, deuterium uptake by an Equine Cytochrome C derived peptide at 69.5% D was adjusted to match the uptake of the same peptide at 84.6% D at 3s, 60s, and 14400s with an average error of 1.53%. The correction of peptide deuterium uptake arising from the variation in reaction % D was made possible by the development of an imidazolium based % D reporter TM-2-59. This molecule has an observed exchange rate of 2.86 s^{-1} (t1/2= 0.242 s) at pH 7.0 and $25°C$allowing 99% deuteration within 3s. We note that the rapid exchange of this compound combined with it's relatively extensive chromatographic retention promotes the loss of approximately 10% D. However, this has little impact on the quality of the corrections made by this reporter because unlike peptide-based alternatives the extent of imidazolium back-exchange can be accurately predicted. That being said, efforts to develop an imidazolium based % D reporter which does not lose deuterium during chromatography are ongoing. This approach to detecting and correcting for variations in reaction deuterium content has considerable utility in both academic and industrial research. We believe that this method can be used to improve the reproducibility of HDX-MS analysis by facilitating a more robust comparison of HDX-MS datasets.

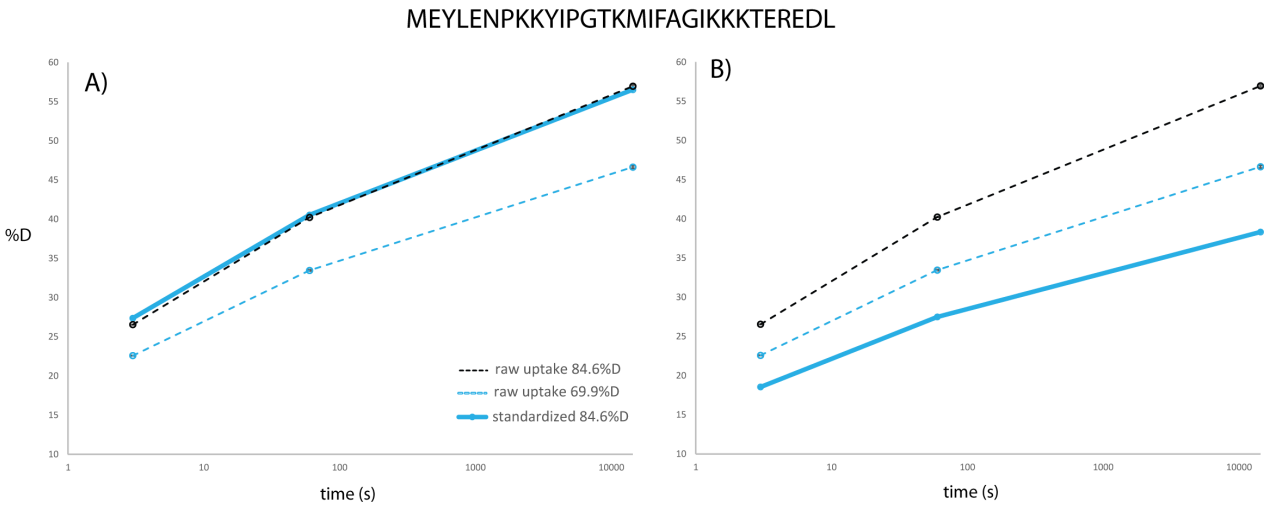

Figure 4.1: In panels A and B the raw uptake plots for the Equine Cytochrome C derived peptic peptide: MEYLENPKKYIPGTKMIFAGIKKKTERED under conditions 1 and 2 (84.6% D, pD 7.63, and 69.5% D, pD 7.63) are represented by the black and blue broken lines receptively. In panel A the solid blue line shows the uptake of the peptide under condition 2 adjusted to match the deuterium content in condition 1 using the widely utilized maximally deuterated control approach[84]. In Panel B the solid blue line shows uptake of the peptide under conditon 2 adjusted to condition 1 using the maximal deuterium uptake of Bradykinin. This was done to demonstrate the outcome of using this approach without matched peptides.

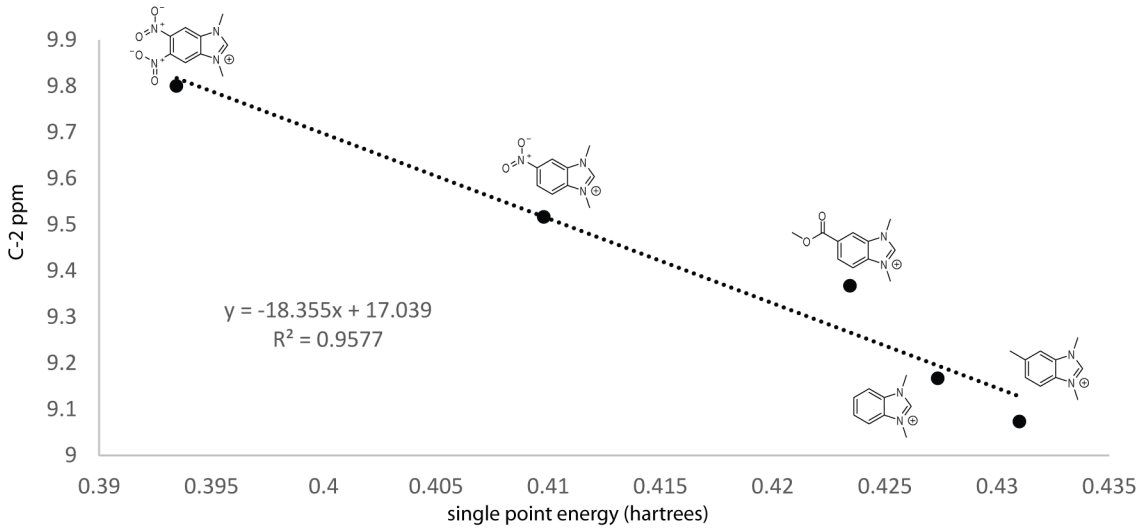

Figure 4.2: The difference in protonated and de-protonated single point energy (SPE) values as a function of observed C-2 ppm in 10% $D_2O$for TM-39, TM-65, TM-68, TM-85, and TM-162.

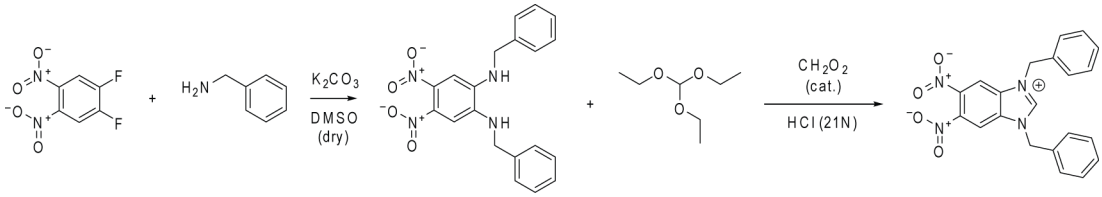

Figure 4.3: Scheme showing the two-step synthesis of TM-2-59.

	EXP 1 (84.6%D)	EXP 2 (69.5%D)
compound	avg max %D	avg max %D
bradykinin	68.2	56.5
peptide: MEY...	56.9	46.6
TM-2-59	74.5	58.3
TM-2-16	87.2	69.6
TM-151	85.6	69.7
TM-143	84.8	68.4

Figure 4.4: Tabulated % D values for compounds of interest under conditions 1 and 2 (84.6% D, pD 7.63, and 69.5% D, pD 7.63). The complete sequence for the peptide titled MEY... is MEYLENPKKYIPGTKMIFAGIKKKTERED. Note that TM-155 has been omitted from this table because it does not reach maximal deuteration within the longest time point of 14400s (4hrs).

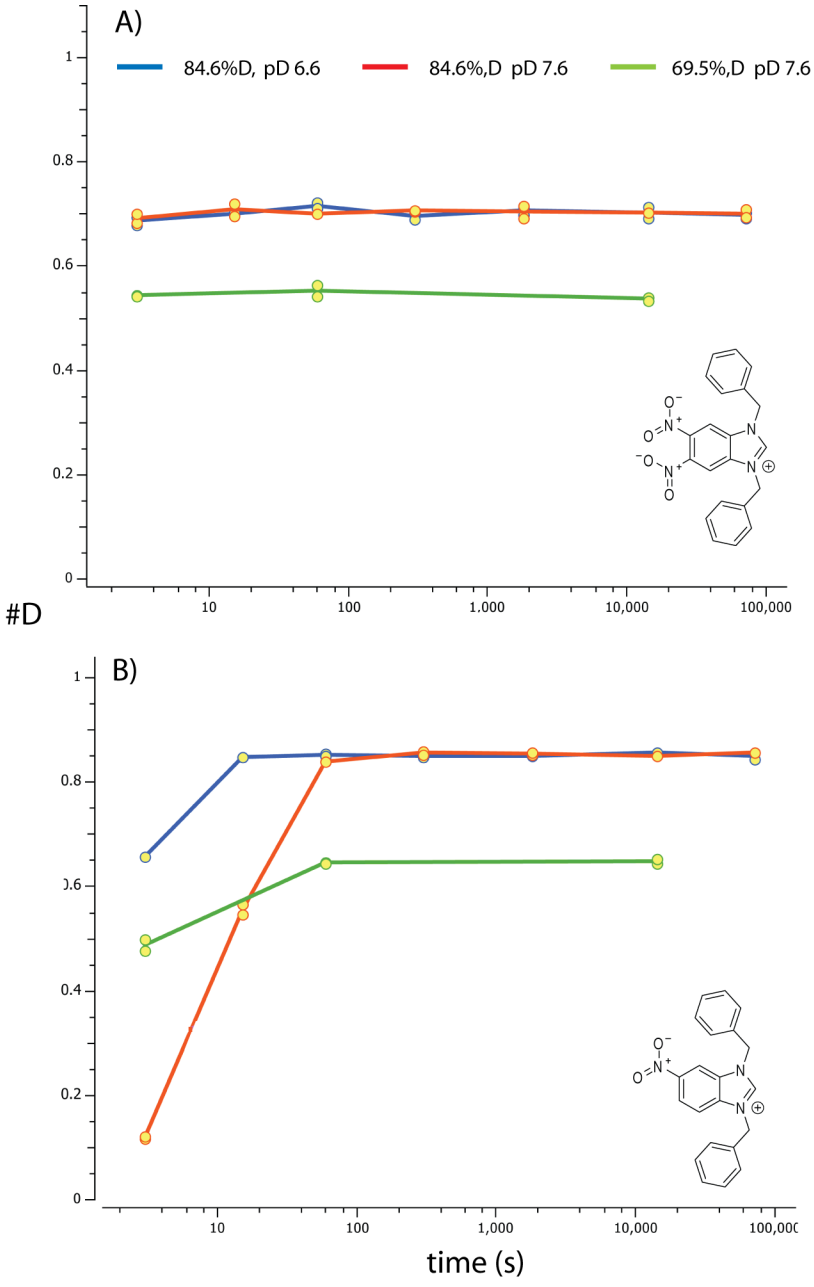

Figure 4.5: Raw deuterium uptake for TM-2-59 (panel A), and TM-143 (panel B). The deuterium uptake of the IERs at pD 7.63 and 84.6% D is shown in red. The deuterium uptake of the IERs at pD 6.63 and 84.6% D is shown in blue. The deuterium uptake of the IERs at pD 7.6 and 69.5% D is shown in green.

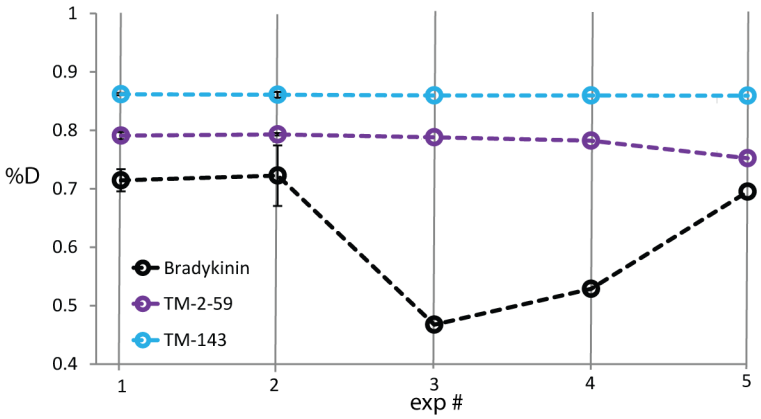

Figure 4.6: Experiments 1-5 (Exp #) show uptake with standard deviation error bars for TM-143, TM-2-59, and bradykinin following different downstream processing methods. In Experiment 1 frozen totally deuterated samples were subjected to the following processing steps; a 4min thawing phase at $5^{\circ}C$, followed by a 7min trapping phase and separation over a 1 x 50mm analytical UPLC column using an IER-optimized gradient. In experiment 2, the trapping phase was shortened to 5min and the gradient was changed to one optimized for general use in the Guttman lab. In experiment 3, all conditions were matched to experiment 1, except the length of the trapping phase which was extended to 20min. In experiment 4, all conditions were matched to experiment 1, except the thawing phase was changed to 60min at $0^{\circ}C$. In experiment 5, all conditions were matched to experiment 1, except the length of the analytical UPLC column was increased to 1 x 100mm.

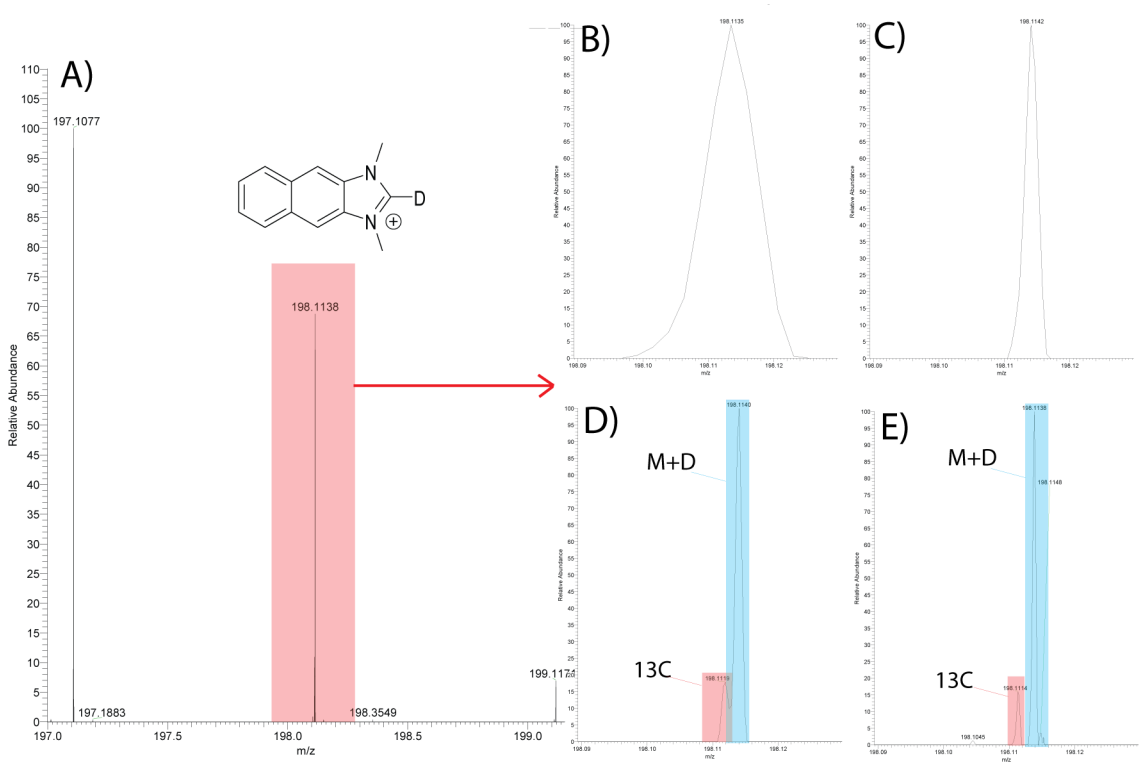

Figure 4.7: Panel A shows two isotopes of TM-2-16; the M+H is shown at 197.1077 m/z, and the M+D, highlighted in red is shown at 198.1138 m/z. Panels B, C, D and E show the M+D peak at 15K, 60K, 120K and 240K resolution respectively. By zooming in on this region it is possible to see the C^{13} containing M+H emerge from under the broad peak associated with the M+D ion as resolution increases. The C^{13} containing M+H ion is visible at 198.1119 m/z in panel D (120K) and 198.1114 m/z in panel E (240K).

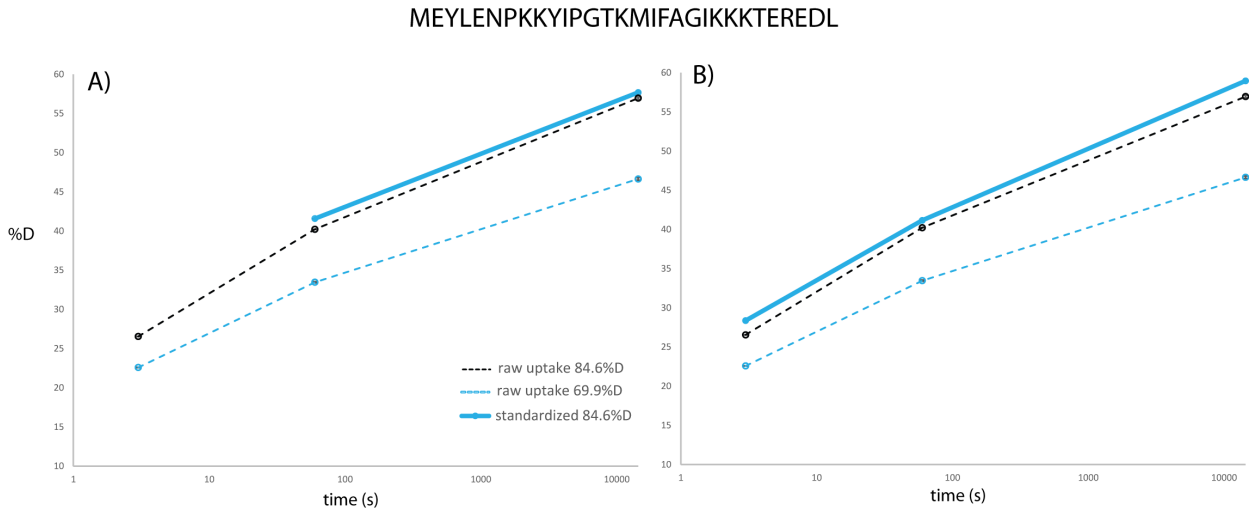

Figure 4.8: In panels A and B the raw uptake for the Equine Cytochrome C derived peptic peptide: MEYLENPKKYIPGTKMIFAGIKKKTERED under conditions 1 and 2 (84.6% D, pD 7.63, and 69.5% D, pD 7.63) is represented by the black and blue broken lines receptively. In Panel A the solid blue line represents the scaling peptide deuterium uptake under condition 2 at 60s and 14400s using TM-143 as reference for the reaction deuterium content under condition 1. In Panel B the solid blue line represents the scaling peptide deuterium uptake under condition 2 at 3s, 60s, and 14400s using the back-exchange corrected uptake of TM-2-59 as reference for the reaction deuterium content under condition 1. The slight overrepresentation of D uptake in both corrections is likely the result of FT-MS distortion[11].

Chapter 5

Ongoing Work

5.1 Expanding the Capabilities of Imidazolium IERS

In Chapter 3 the development and validation of improved imidazolium IERs were discussed. Later in Chapter 4 we demonstrated the potential of imidazolium IERs to act as % D reporters in the HDX-MS experiment. The data presented in these Chapters demonstrates the remarkable adaptability of imidazolium reporters. In this Chapter ongoing efforts to further expand the utility of these reporters are discussed. Areas of focus include; expansion of time point coverage, developing reporter based strategies for immobilized HDX-MS, improving % D reporter performance, and developing a novel mass spectrometry imaging method for measuring tissue pH variation.

5.1.1 Expansion of Time Point Coverage

During the development of the 2nd generation IERs, described in Chapter 3, several compounds exhibiting desirable exchange kinetics were found to be unsuitable due to their poor chromatographic performance. Specifically, compounds TM-141 and TM-139 were found to interact strongly with the POROS resin used in the protease column. Attempts were made to mitigate this interaction with no success. Given the popularity of this resin it was decided that these compounds should be excluded from further experiments. Removing TM-141 led to a reduction in time point coverage at the 30s time point below pD 7.2. While this lapse in coverage has little effect on the quality of correction in multi-time point experiments, it does limit overall utility. To fill this gap in coverage 1,3-dibenzyl-5-triflouromethylbenzimidazolium (TM-3-35) was synthesized. From CHDX-MS the compounds rate at pD 7.0 and 25°$C$is 0.0265 s^{-1} (t1/2 = 26s), which should allow coverage of 30s time point under a variety of conditions (Figure 5.1). If TM-3-35 exhibits desirable chromatographic performance, it will be used as a direct replacement for TM-141/

Additionally 3 slow exchanging reporters have been synthesized to help expand coverage to extended time points at elevated pH. Initially 1,3-diheptylimidzolium (TM-2-145) and 1-heptly-3-benzylimidazolium (TM-2-161) were synthesized. Subsequent evaluation of the chromatographic performance of these compounds revealed that they were unsuitable for HDX-MS. Both TM-2-145 and TM-2-161 interacted strongly with PEEK surfaces causing extensive and persistent carryover. Following these observations 1-methyl-3-benzylimidazolium (TM-3-27) was synthesized. This compound exhibits desirable chromatographic performance. In Figure 5.2 the structures of available imidazolium IERs are separated into three groups. In the red box are structures that exhibit desirable chromatographic performance and can be readily incorporated into a wide variety of bottom-up HDX-MS workflows. In the green box are structures that either tend to carry over or are too poorly retained under typical chromatographic conditions to be used in many bottom-up HDX-MS workflows. The structures in the blue box have not been fully evaluated.

5.1.2 IERs for Immobilized HDX-MS

Although less common, there is developing interest in expanding the utility of HDX-MS to allow for the study of proteins that either cannot be studied in solution or that need to be studied within a highly

complex environment[23, 132, 127, 67]. Typically these studies utilize biotin-labeled proteins which upon interaction with streptavidin-coated surfaces or beads can be isolated from the complex mixture. This pull-down approach does not allow for the use of currently available reporting controls, which is especially problematic as the complex nature of these experiments makes them especially error-prone. In the near future we intend to develop imidazolium IERs capable of reporting on exchange reaction conditions in these complex experiments.

Figure 5.3 displays a generalized biotin-labeled imidazolium-based IER. The structure of the potential IER is comprised of 3 distinct groups joined by linkages A and B. Each of these groups performs a necessary function in the immobilized HDX-MS workflow. For example, during the labeling step the benzimidazolium group will begin to exchange at the C-2 position at a rate dependent on the pH, temperature and ionic strength of the solution. Next, the Biotin group will enable the IER to be co-isolated with the labeled protein by associating strongly with streptavidin coated surface during the enrichment step. Lastly, the variable linker contains a di-sulfide region that can be cleaved by the reducing agent TCEP, which is commonly added to the HDX-MS quench buffer. The reduction of the di-sulfide region would facilitate the release of the protein and IER from the streptavidin coated surface, enabling downstream analysis.

One challenging aspect of designing a biotin-containing imidazolium IER is minimizing the impact of other exchangeable groups on the pH-dependent behavior of the C-2. The influence of the weakly acidic biotin on the exchange behavior of the C-2 may be mitigated by Increasing linker length. However, the formation of linkages A and B must also be carefully considered, as the presence of an exchangeable amide in such close proximity will influence C-2 exchange. We are confident that it will be possible to utilize ether or ester linkages in conjunction with variable-length di-sulfide-containing linkers to generate functional biotin-labeled imidazolium IERs.

5.1.3 Improving % D Reporter Performance

The concept of using a reporter to standardize reaction deuterium content (% D) was first introduced in 2014 by Joey Sheff and colleagues[109]. While interesting, the approach had several limitations that prevented more widespread use. In Chapter 4 we demonstrated a novel reporter-based method for detecting and correcting variations in % D. The proposed alternative relies on the deuterium uptake of 1,3-dibenzyl-5,6-dinitrobenzimidazolium (TM-2-59) to represent actual deuterium content for each sample in the experiment. This enables direct and robust comparison of % D between samples as well as the highly accurate correction of % D variation. Unfortunately, the predictable downstream deuterium loss by TM-2-59 complicates the calculation of a correction factor (X_{corr}), and ultimately limits the quality of % D correction. To overcome this limitation, it is necessary to develop a % D reporter with reduced back exchange. In the absence of viable alternatives to the imidazolium scaffold, it was determined that the most practical means of accomplishing this goal was to reduce the chromatographic retention of the % D reporter.

From our knowledge of D-loss by imidazolium under chromatographic conditions, we understand that a reporter with a logP between -2.0 and -0.76 limits D-loss in the functional rate range to less than 5%. In an effort to pursue new targets within this range, 1,3-dimethyl-6,7-perimidinum was synthesized over 3 steps (Figure 5.4). Surprisingly, this compound exchanges considerably more slowly than expected with a rate of 0.012 s_{-1} (t1/2 = 56s) at pD 7.0 and 25°$C$by CHDX-MS. Although this compound is clearly not suitable to act as a % D reporter, the synthetic approach is novel and may enable access to other more suitable candidates. In the near future we intend to refine this synthetic approach in an effort to explore napthimidazolium and perimidinium-based reporters.

5.1.4 Mass Spectrometry Imaging of Tissue pH by In-Situ HDX-MS

Matrix assisted laser desorption/ionization (MALDI) is a widespread technique that is frequently coupled with time-of-flight mass analysis (MALDI-TOF-MS) for imagining various biomolecules in tissues. Recently, more advanced instruments and methods have enabled MALDI imaging at the single-cell level. The remarkable spatial resolution and adaptability of the technique makes it particularly valuable for the study of cellular communication. There are numerous examples of how MALDI imaging has advanced our understanding of these processes. Recently we have been refining an imidazolium reporter-based method for resolving tissue pH by MALDI-TOF-MS.

Our Initial experiments were carried out on a Bruker Autoflex instrument using index plates. First small amounts of H_2Obuffers with known pH values were added to specific region on the plate and allowed to dry completely. Next a dilute aqueous solution of TM-3-35, TM-151, and TM-141 was applied to the surface in a light even coat and allowed to dry completely. These particular reporters were chosen because it is necessary to have a reporter between 20% and 80% exchanged in addition to a reliable measurement of % D after a single 5min time point at room temperature under physiologically relevant pH. Following the application of the reporters, the surface was placed in a D_2Orich humidification chamber and very lightly misted with 99.9% D_2O. The surface was kept damp in the humidification chamber for 5min before being removed and being sprayed with several light coats of a low pH α-Cyano-4-hydroxycinnamic acid matrix (CHCA). The application of the matrix halts the exchange process by dropping the surface pH and also promotes the ionization of the IERs on the surface.

Our preliminary experiments show that on-surface exchanges are highly precise and accurate to within 0.02 pH units. These results suggest that the proposed reporter-based approach may be suitable for spatially resolving pH differences in immobilized tissue slices. In the immediate future we intend to develop an automated spray applicator protocol to facilitate the rapid and robust evaluation of pH in tissue samples immobilized on glass slides. Through refinement of this approach we hope to gain a deeper understanding of how tissues regulate pH to perform specific biological functions.

5.2 Closing Remarks

The work discussed in this document would not have been possible with the guidance of Dr. Guttman, the expertise available in the department of Medicinal Chemistry, and the friendship and support of my fellow students. I have deeply enjoyed my time in the Guttman lab and I feel indebted to the wonderful people who helped me bring this project to where it is now.

Thank you all for your support and encouragement.
-Taylor

5.3 Supplementary

5.4 Amide exchange processes in solution

The chemical process of backbone amide exchange is broadly described in solution using proton transfer theory [25]. This process is highly sensitive to exchange reaction conditions and the local electronic environment [87, 69]. The numerous and complex relationships between reaction parameters and amide exchange kinetics have been extensively studied by numerous investigators [63, 35, 133, 87, 6, 97, 36]. Here we will attempt to distill the core concepts underlying these relationships and illuminate some of the more subtle aspects of $k_{ch}$with regard to unstructured backbone amides . While not covered in detail here, it is also important to be aware of the exchange processes beyond the amide, such as at side chain positions, which have recently been reviewed in detail [50].

Amide exchange in an aqueous medium proceeds through three mechanisms: acid, base, and water catalysis [88]. Acid catalysis proceeds through two distinct mechanisms shown in Schemes 1 and 2. Scheme 1 describes O-protonation (acid-imidic exchange), which is understood to be the predominant pathway of acid catalysis for backbone amides [97, 36, 50, 83]. This process begins with the transfer of a deuteron from the solvent to the peptide carbonyl oxygen. The imidic nitrogen is then deprotonated, which is followed by transfer of a deuteron from the solvent back to the nitrogen. Scheme 2 displays the pathway for N-protonation or the direct deuteration of the amide. This pathway begins with the transfer of a deuteron to the neutral amide, followed by removal of the hydrogen that leads to the deuteration of the amide. It should be noted that the N-protonation pathway is understood to be energetically disfavored for backbone amides, with the possible exception being the N-terminal amide [97].

The process of base-catalyzed amide exchange on the other hand, is understood to proceed through a single pathway (Scheme 3). Base catalysis begins with the direct removal of a hydrogen atom from the amide and the resulting highly basic nitrogen then receives a deuteron from the solvent. Deuterium oxide in its unionized form is also capable of initiating the protonation/deprotonation steps in these three mechanisms to mediate hydrogen/deuterium exchange, albeit at a much slower rate. The second order rates for acid k_{D^+}, base k_{OD^-}, and water k_{D_2O} catalyzed exchange can be calculated using proton transfer theory, provided the reaction conditions are well characterized. These values are summed using equation 1 to yield the observed rate of exchange for a particular amide (k_{-ch}). For solution HDX-MS, the rate of water catalyzed exchange k_{D_2O} is considered negligible and can be ignored which simplifies equation 1 to equation 2. Furthermore, due to the tendency of amide exchange to proceed primarily through base catalysis above pH 2.3-2.6, the contribution of acid catalysis k_{D^+} to the observed rate amide exchange (k_{-ch}) is considered minimal. This allows for the use of equation 3 to describe k_{-ch} near physiological pH (pH 5-10)[16]. Accurate estimation of k_{-ch} is central to informative measurements from HDX-MS experiments [93, 91]. Therefore, extraordinary care has been taken to understand how structural influences and solution conditions combine to impact amide exchange rates [63, 35, 133, 87, 6, 97, 36, 83, 131].

The value of k_{-ch} is unique for each type of amino acid and varies for each amide within a sequence depending on its position within the sequence and neighboring residues. This is because the side chain chemistry of a particular amino acid influences the buildup of charge on the amide during the proton transfer process [87, 6, 42]. The term "side chain effects" is often used to describe the structural influences responsible for the distinct exchange behavior of amino acids. These structural nuances have more far-reaching effects within a polypeptide sequence. Often referred to as "nearest neighbor effects" or "sequence effects", the arrangement of amino acids relative to one another has a significant impact on k_{ch}[87, 6, 93, 88, 35]. Additionally, the proximity of a particular residue to the N- or C-terminus also greatly impacts the exchange behavior. Although N- and C-terminal effects have little influence on intrinsic exchange behavior in full proteins, these effects become pronounced in small unstructured peptides [6, 93, 88, 108]. The positive charge at the N-terminus accelerates k_{OD^-} of the neighboring amino acid, sometimes to the point where the second amino acid (first backbone amide) exchanges so quickly that it cannot be probed by HDX-MS [93]. As a result, N- and C-terminal effects are frequently considered when gathering higher resolution HDX data [50]. The Englander group has compiled a set of spreadsheets for calculating k_{-ch} for amides in the context of their sequence and buffer conditions, which are available at: http://hx2.med.upenn.edu/download.html. Alternatively, the online tool: Server Program for Hydrogen Exchange Rate Estimation (Sphere) can also calculate predicted k_{-ch} for a given peptide sequence and condition: https://protocol.fccc.edu/re-

search/labs/roder/sphere/sphere.html

5.4.1 pH

Controlling solution pH is fundamental to the HDX-MS experiment. In fact, the sensitivity of amide exchange rates to pH is what enables the retention of deuterium for analysis by MS. Proteins are typically labeled around neutral pH or under near-physiological conditions (pH 5-10). Within this pH range k_{ch} is relatively fast, enabling the probing of diverse protein motions on a reasonable time scale [49, 45, 16]. In order to actually observe the localization of deuterium and gain any kind of structural insight from the HDX-MS experiment, it is necessary to slow the exchange process or "quench" the reaction, otherwise the sample handling steps with H_2O-based buffers will result in loss of the deuterium label . Although the quench step serves additional purposes, the slowing of amide exchange is accomplished here by acidifying the exchange reaction buffer to a range where the rates of acid and base catalysis are minimized [31, 35, 29, 36, 32, 121]. The "V-shaped" plot in 5.5 is a useful approximation of the pH dependency of amide exchange. The negative sloping region on the left side of the plot represents the region where amide exchange proceeds primarily through acid catalysis and the corresponding positive sloping region on the right, represents the region where amide exchange proceeds primarily through base catalysis. The minimum in the center represents the region where both acid and base catalyzed exchange rates are at their lowest values, referred to as the pH_{min}. Although pH_{min}varies for individual amino acids, it is generally approximated at pH 2.5 for proteins, and is what most HDX-MS researchers target for their quench pH [29, 121].

Amide exchange in the deuterium rich labeling buffer is primarily catalyzed by the acidic D_3O^+ and basic OD^- species in solution. Equation 2 provides a way to calculate the impact that the relative quantities of these two species have on the observed rate of amide exchange k_{ch} in the HDX-MS experiment. Within the physiologically relevant pH range, an increase of 1 pD unit will result in an approximately ten-fold increase in k_{ch}. This assumption is generally robust despite the tendency for the second order rate constants of acid and base catalysis to vary with some solution parameters beyond the apparent pD [88, 35]. That being said, special care should be given to the precise measurement of D_3O^+ and OD^- concentrations within labeling and quench buffers, as the ratio of these species has a direct impact on deuterium uptake. The use of glass electrodes to measure the pD of the labeling and quench buffers is ubiquitous. It is necessary to correct the pH measured in a D2O rich solution (pHread or 'pH*') to account for the variation in ionic activities of H^+ and D^+ [18]. There are several methods for calculating pD from pH*, each of which features different assumptions regarding the variations on the pH scale [50, 77, 44, 19]. It should also be noted that pH* varies with the concentration of deuterium in solution ($\%D$) [77]. As a result, the use of a different approach to convert pH* can result in a slightly different pD. For this reason, it is recommended that investigators simply report pH* associated with HDX-MS experiments to avoid confusion [84].

5.4.2 temperature

Temperature is another major factor that affects $k_{ch}$and should be controlled throughout the HDX-MS experiment. We note that temperature will likely also affect the solution structure and dynamics of a protein, but here we focus only on the effects related to k_{ch}. Solution temperature is directly tied to the ionization constant of deuterium oxide k_{D_2O}in a given buffer system, which therefore effects the concentration of $D_3O^+$and OD^-in solution [35, 18, 110, 78]. A theoretical value for k_{ch}at a specific temperature can be computed using a modified Arrhenius equation (5.1) [68, 35, 97]. In this equation T refers to the experimental temperature in kelvin, $k_{ch}(293)$ is the reference rate for the target at 293K, Ea refers to the activation energy for the target, and R refers to the appropriate molar gas constant.

$$k_{ch}(T) = k_{ch}(293) * exp\frac{-Ea}{R} * \left(\frac{1}{T} - \frac{1}{293}\right) \tag{5.1}$$

Accordingly, k_{ch}increases ten-fold with every $22°C$ increase in temperature (5.6). This relationship appears to be maintained even below freezing, as observed from exchange studies of ultra-low temperature HDX or the observed deuterium loss in solid frozen samples 79, 80. While this relationship between temperature and $k_{ch}$is adequate for planning and interpreting most solution HDX-MS experiments, there are several assumptions associated with this treatment that should be noted, particularly if experiments are to

be compared across different temperatures. The activation energies for acid, base and water catalyzed amide exchange are often reported as 14, 17 and 19 $\frac{kcal}{mol}$ respectively [6, 93, 50]. Although these fixed values are appropriate for most amide rate predictions, the actual acid, base, and water catalyzed activation energies can be moderately offset by solution parameters, like dissolved salts [14, 1, 21, 1, 21, 74, 14, 42]. Furthermore, temperature dependent changes to $k_{D_2O}$are not uniform for all buffer systems [21, 95, 72, 21, 119]. This inconsistency can result in a temperature dependent change in pH, which is unique to a particular buffer system. For example, phosphate shows minimal variation while TRIS, ACES, acetate, and citrate show more significant variation in pH with temperature and should be pH adjusted at their intended temperatures.

5.4.3 pressure

Pressure is not commonly a factor in probing protein conformational dynamics, because the labeling step in solution HDX-MS experiments is typically conducted at atmospheric pressure. However elevated pressures are common during downstream processes like digestion and chromatographic separation. Like temperature, system pressure exerts an influence on k_{D_2O}, and the resulting change in pH impacts amide intrinsic exchange[68] 87. Under certain conditions it is possible to use established empirical relationships to model the effects of pressure, but in many cases this approach is not adequate for describing the full impact of pressure on k_{ch}[35, 54, 12, 47]. In general, the ionization of weak electrolytes, like phosphoric acid increases with pressure [68, 79]. As a result, the effects of pressure on the rate of amide intrinsic exchange in some common buffer systems can be generalized [69, 43]. It is possible to move beyond this generalization to provide a semi-quantitative estimate for the pressure dependence of pH for specific buffered systems using Plank's equation [79, 43, 66]. This approach brings to light the more complex relationship between buffer pH and pressure. For example, phosphate buffer is understood to drop by almost half a pH unit per 100 MPa, while the pH of a MOPS buffer increases by approximately the same amount (5.7) [12, 43, 101, 7]. Though its effect are minor compared to pH and temperature, handling of HDX-MS samples at elevated pressures may contribute to offsets solution conditions and k_{ch}.

5.4.4 solution ionic strength

The identities and concentrations of salts added to the labeling buffer are understood to effect deuterium uptake and this phenomenon has been extensively investigated [35, 87, 6, 31, 88, 74, 42, 62]. These experiments have clearly demonstrated that ions in solution exert a direct influence on k_{ch}through altering the local electronic enviroment of the amide. These data demonstrate that charged residues exhibit a greater response to KCl than neutral residues, and that the response of a negatively charged residue differs from that of a positively charged residue. This selective and directional modulation of $k_{ch}$is often attributed to the exclusion of deuterium oxide and its ionization products by salt ions interacting preferentially with charged regions of the sequence [68, 74, 81]. While there is strong empirical evidence to support this model, it is also clear that dissolved salts like NaCl and KCl alter the activities of other charged species in the solvent, which manifests as a change in buffer pH. Therefore, the effect of salt content on buffer pH should be considered for studies conducted at high ionic strength.

On a related note, glass electrode pH probes are unreliable for the interpretation of H_3O^+activity at higher ionic strength [64]. As a result, many investigators use empirically determined activity values for water to improve estimates of pH in the bulk solution at elevated ionic strength [64, 74, 103, 78, 42]. Although this is common practice, it should be noted that the effect of salts like NaCl and KCl on activity is not uniform for all buffer systems [21, 72, 52] 85. Therefore, the use of empirically determined activity values from non-comparable buffer systems may misrepresent the actual pH of the bulk solution. 5.8 shows the effect of salt concentration for several different chloride salts on the pH of citric acid and triethanolamine/trienthanolammonium chloride buffers (TEA). Note that the addition of NaCl (square) results in a decrease in pH in the citric acid buffered system, while the addition of the same salt to the TEA buffer resuts in an increase in pH. Although there is little evidence to suggest that such a discrepancy could lead to significant misinterpretation of k_{ch}, performing HDX-MS experiments involving high salt concentrations in well studied systems where appropriate empirically determined activity values are available will allow for a more accurate estimate of pH in the bulk solution, thereby enabling a more informed interpretation of salt effects on deuterium uptake. Though not necessarily related to ionic strength, it has also been noted that the solution

viscosity can affect k_{ch}in ways that may need to be considered for certain studies [92, 104].

5.4.5 solvent composition

Organic solvents are often involved in HDX-MS during sample processing and are also occasionally necessary in the deuterium labeling step to facilitate probing of ligand interactions. It is common for studies of protein-ligand interactions to include low amounts of organic solvent (e.g. DMSO) to aid in the solubilization of hydrophobic small molecules. Despite the extensive use of organic solvents in HDX-MS, there are few studies of the effects of organic co-solvents on kch [35, 29, 75].

It is widely accepted that organic co-solvents influence kch indirectly through several mechanisms: 1) the addition of the organic component reduces the concentration of water, thereby reducing the number of interactions between the analyte and the aqueous components that catalyze exchange; 2) miscible organic solvents depress $k_{\mathrm{D_2O}}$in certain systems, resulting in fewer ionization products to suppress k_{ch}; 3) the organic component reduces the dielectric constant of the solution, which shifts the equilibrium to favor neutral products reducing the availability of catalytic ions to suppress k_{ch}[70, 35, 87, 50, 75]. Using these assumptions, the depression of amide exchange in the presence of organic co-solvents has been predicted for a variety of solvent systems (5.9). However, there have been examples suggesting that an organic solvent may accelerate k_{ch}98, [90, 61, 41, 98]. Interestingly, there is a considerable body of literature to suggest that the acceleration of amide HDX in the presence of an organic co-solvent is expected for certain systems due to an increase in pH or change in buffer capacity [94, 112, 128, 82, 37, 8, 94, 105]. These discrepancies may arise from the inability to uniformly relate proton activity measured in an aqueous reference to that of a non-aqueous or mixed (hydroorganic) solvent using a universal pH scale [112]. This is because pH scale length depends on an activity coefficient, which is a system-specific parameter that depends not only upon the particular organic modifier and the pH of the aqueous component, but also upon the nature of the buffering system, i.e., the concentration and identities of the buffering agents [94, 65]. At the very least these findings indicate that organic co-solvents can influence k_{ch}in different ways, and additional care should be taken to ensure the utilization of organic co-solvents is consistent, especially in comparative HDX-MS studies.

5.4.6 isotope effects

The hydrogen isotope effect only has a small effect on kch and is rarely considered in the HDX-MS experiment. For base-catalyzed exchange the slight isotope effect is primarily attributed to the rate-limiting step which is breaking of the N-H or N-D bond to form the imidate ion (Scheme 3). This is corroborated by the rate of hydrogen exchange being higher than that of deuterium and tritium exchange, which is consistent with the primary kinetic isotope effect [17]. For the acid catalyzed reaction there is an associated slight inverse isotope effect that is attributed to the slightly higher acidity of the D_3O^+ion compared to the H_3O^+ion [110]. Though isotopic effects have relatively little impact on kch, it has been noted that the stabilities, activities, and dynamics within native proteins can be offset by changing from $H_2O$to D_2O[100]. This can at least be partially explained by the isotope effect of deuterium leading to slightly weaker hydrogen bonding [24, 76].

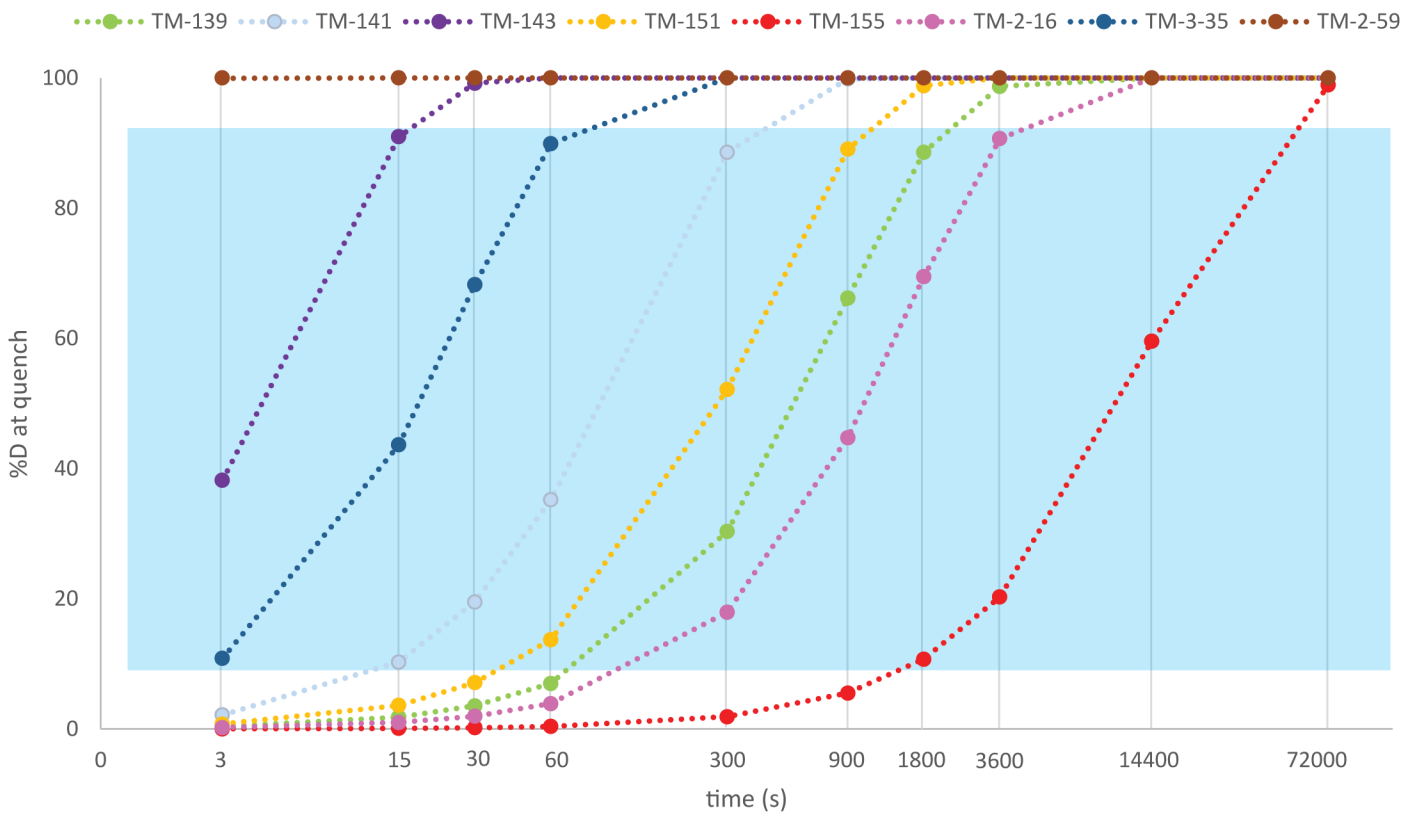

Figure 5.1: Updated time point coverage map including % D reporter TM-2-59 and TM-3-35. The shaded region (blue) indicates extent of exchange where is it possible to calculate a rate from a single time point measurement with reasonable accuracy.

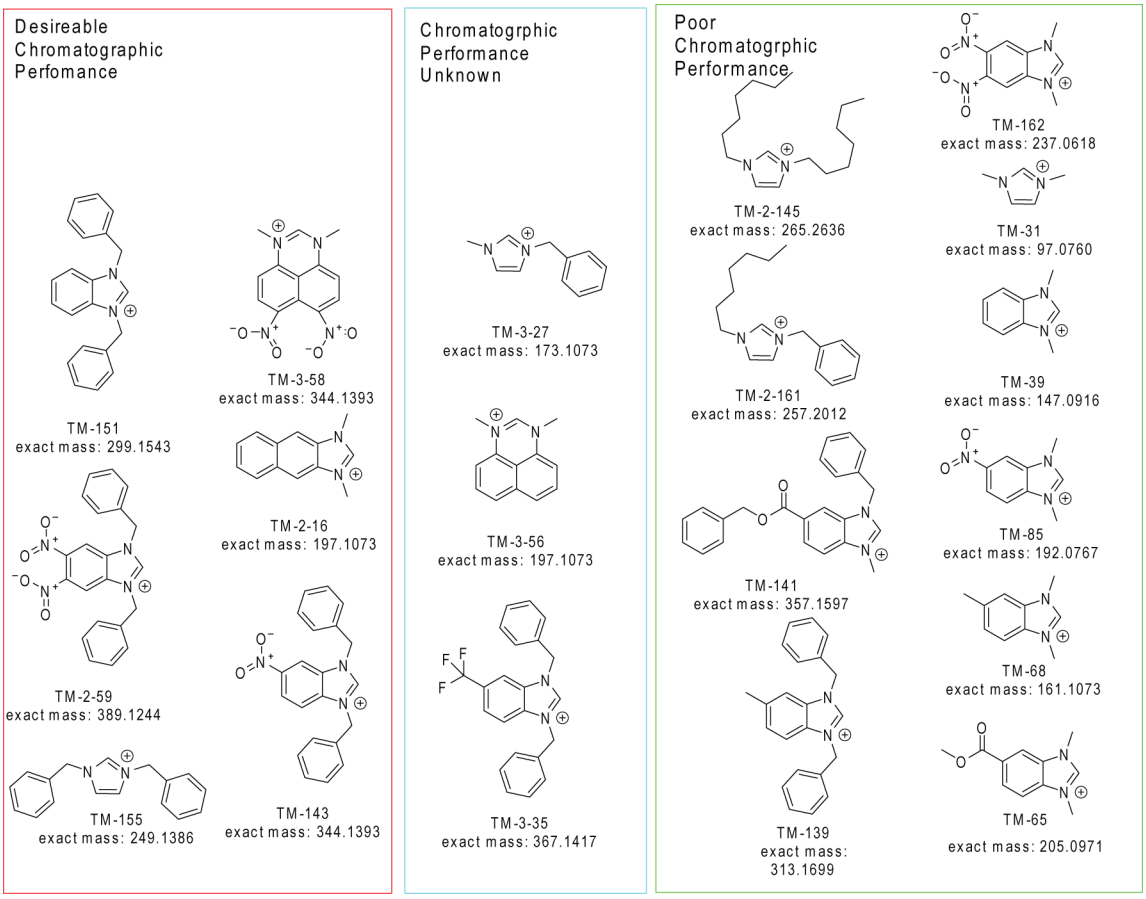

Figure 5.2: the structures of available imidazolium IERs are separated into three groups. In red are structures which exhibit desirable chromatographic performance, in green are structures which exhibit poor chromatographic performance, those in blue have not been fully evaluated

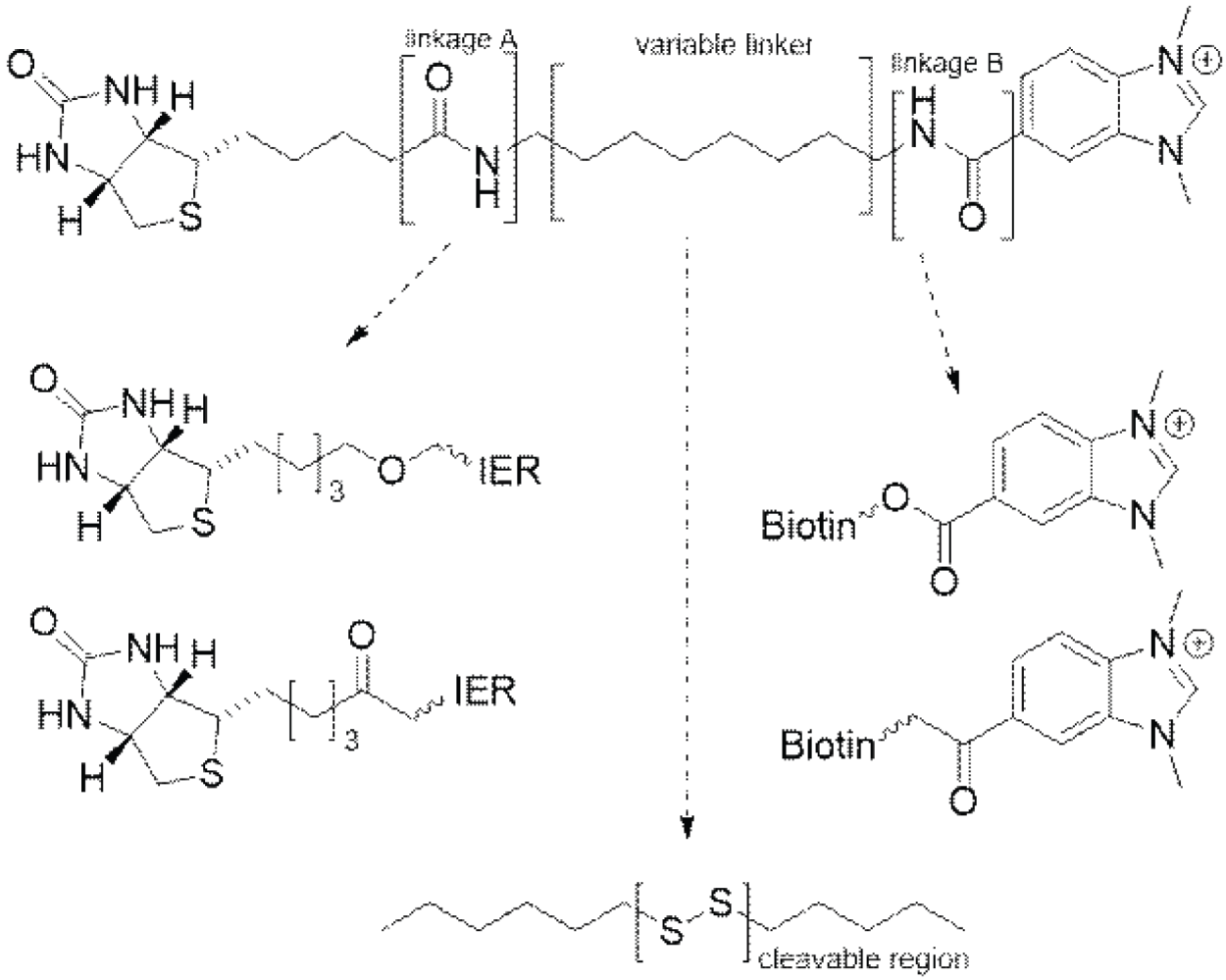

Figure 5.3: Diagram showing generalized structure for imidazolium IER compatible with HDX-MS studies involving a biotin-streptavidin isolation or immobilization strategy.

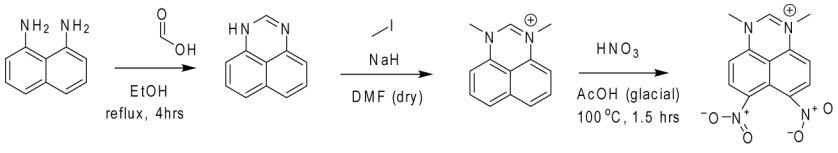

Figure 5.4: Scheme showing 3 step synthesis of TM-3-58.

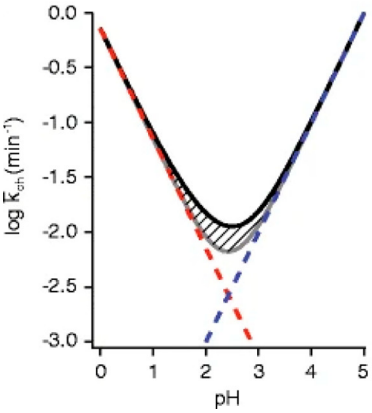

Figure 5.5: Rate of exchange of an unstructured amide is shown as a function of pH. The gray line is the summed rate from the acid and base catalyzed exchange contributions, which are individually depicted with the red and blue dashed lines, respectively. The black line above the hatch marks is the net rate accounting for the contribution of water catalysis. Reproduced with permission from [121]. Copyright 2012 American Chemical Society.

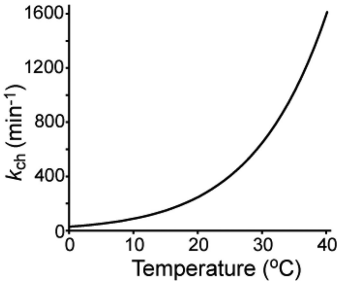

Figure 5.6: $k_{ch}$of polyalanine is plotted as a function of temperature based on calculations from Bai et al. [6]

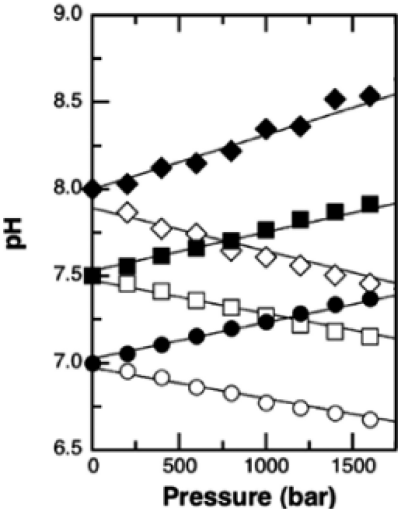

Figure 5.7: Relationship between solution pressure and pH for phosphate (white) and MOPS (black) buffer are shown. Circles, squares, and diamonds reflect a starting solution pH of 7.0, 7.5, and 8.0, respectively. Reproduced with permission from [101]. Copyright 2005 Elsevier

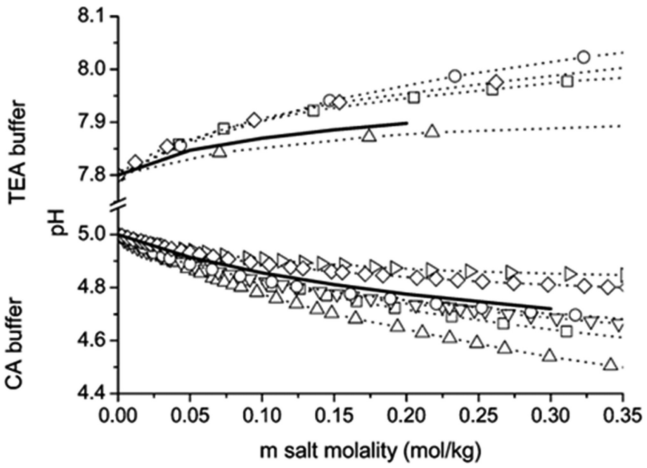

Figure 5.8: Relationship between the salt concentration and pH for triethanolamine (TEA) buffer and citrate buffer (CA) are shown. The salts used in the study were tetramethylammonium chloride ( ), choline chloride ( ), cesium chloride ( ), potassium chloride ( ) sodium chloride ( ), and lithium chloride ( ). Solid lines are predictions based upon extended Debye–Huckel equation using ionic size parameter 4 × 10–10 m. Reproduced with permission from [119]. Copyright 2006 American Chemical Society.

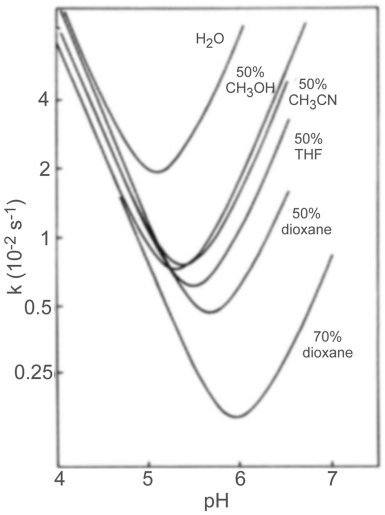

Figure 5.9: Predicted relationship between kch and pH at different levels of organic solvent. The general shift in the position of the "V" shaped curves results from offsets to solution conditions and the lower concentration of water available for catalyzing amide exchange. Reproduced with permission from [29]. Copyright 1985 Elsevier.

Bibliography

[1] Y. Abe et al. "Effect of salt concentration on the pKa of acidic residues in lysozyme". In: *Journal of Biochemistry* 118.5 (Nov. 1995), pp. 946–952. ISSN: 0021-924X. DOI: 10.1093/jb/118.5.946.

[2] Tina L. Amyes et al. "Formation and Stability of N-Heterocyclic Carbenes in Water: The Carbon Acid pKa of Imidazolium Cations in Aqueous Solution". In: *Journal of the American Chemical Society* 126.13 (Apr. 1, 2004). Number: 13, pp. 4366–4374. ISSN: 0002-7863. DOI: 10.1021/ja039890j. URL: https://doi.org/10.1021/ja039890j (visited on 09/05/2019).

[3] M. D. Archer and R. P. H. Gasser. "Electrolyte solutions in dimethyl sulphoxide. Part 2.—Caesium iodide". In: *Trans. Faraday Soc.* 62.0 (1966). Number: 0, pp. 3451–3458. ISSN: 0014-7672. DOI: 10.1039/TF9666203451. URL: http://xlink.rsc.org/?DOI=TF9666203451 (visited on 10/03/2019).

[4] Orazio Attanasi, Giuseppe Bartoli, and Paolo E. Todesco. "Base-catalyzed hydrogen-deuterium exchange in some 5- and 6-substituted benzothiazoles. Activity of the sulphur and nitrogen heteroatoms in the transmission of the substituent effects". In: *Journal of Heterocyclic Chemistry* 13.5 (Oct. 1, 1976). Number: 5, pp. 1021–1024. ISSN: 1943-5193. DOI: 10.1002/jhet.5570130516. URL: https://onlinelibrary.wiley.com/doi/abs/10.1002/jhet.5570130516 (visited on 10/16/2018).

[5] Remigiusz Bąchor et al. "Hydrogen-deuterium exchange of -carbon protons and fragmentation pathways in N-methylated glycine and alanine-containing peptides derivatized by quaternary ammonium salts". eng. In: *Journal of mass spectrometry: JMS* 49.6 (June 2014), pp. 529–536. ISSN: 1096-9888. DOI: 10.1002/jms.3371.

[6] Yawen Bai et al. "Primary structure effects on peptide group hydrogen exchange". In: *Proteins: Structure, Function, and Bioinformatics* 17.1 (1993). Number: 1 _eprint: https://onlinelibrary.wiley.com/doi/pdf/10.1002/prot.340170110, pp. 75–86. ISSN: 1097-0134. DOI: 10.1002/prot.340170110. URL: https://onlinelibrary.wiley.com/doi/abs/10.1002/prot.340170110 (visited on 06/04/2020).

[7] V. M. Balasubramaniam et al. "Recommended laboratory practices for conducting high-pressure microbial inactivation experiments". en. In: *Innovative Food Science & Emerging Technologies* 5.3 (Sept. 2004), pp. 299–306. ISSN: 1466-8564. DOI: 10.1016/j.ifset.2004.04.001. URL: https://www.sciencedirect.com/science/article/pii/S1466856404000347 (visited on 09/14/2022).

[8] J Barbosa et al. "Chromatographic behavior of ionizable compounds in liquid chromatography. Part 2. Standardization of potentiometric sensors and effect of pH and ionic strength on the retention of analytes using acetonitrile–water mobile phases". In: *Analytica Chimica Acta* 389.1 (May 14, 1999), pp. 43–52. ISSN: 0003-2670. DOI: 10.1016/S0003-2670(99)00132-4. URL: http://www.sciencedirect.com/science/article/pii/S0003267099001324 (visited on 01/10/2021).

[9] J. H. Bradbury, B. E. Chapman, and F. A. Pellegrino. "Hydrogen-deuterium exchange kinetics of the C-2 protons of imidazole and histidine compounds". In: *Journal of the American Chemical Society* 95.18 (Sept. 1, 1973). Number: 18, pp. 6139–6140. ISSN: 0002-7863. DOI: 10.1021/ja00799a063. URL: https://doi.org/10.1021/ja00799a063 (visited on 01/10/2020).

[10] William Burkitt and Gavin O'Connor. "Assessment of the repeatability and reproducibility of hydrogen/deuterium exchange mass spectrometry measurements". In: *Rapid communications in mass spectrometry: RCM* 22.23 (Dec. 2008). Number: 23, pp. 3893–3901. ISSN: 0951-4198. DOI: 10.1002/rcm.3794.

[11] Kyle M. Burns et al. “Platform dependencies in bottom-up hydrogen/deuterium exchange mass spectrometry”. In: *Molecular & cellular proteomics: MCP* 12.2 (Feb. 2013). Number: 2, pp. 539–548. ISSN: 1535-9484. DOI: 10.1074/mcp.M112.023770.

[12] J. V. Carter, D. G. Knox, and A. Rosenberg. “Pressure effects on folded proteins in solution. Hydrogen exchange at elevated pressures”. eng. In: *The Journal of Biological Chemistry* 253.6 (Mar. 1978), pp. 1947–1953. ISSN: 0021-9258.

[13] Michael J. Chalmers et al. “A two-stage differential hydrogen deuterium exchange method for the rapid characterization of protein/ligand interactions”. In: *Journal of biomolecular techniques : JBT* 18.4 (2007). Type: Journal Article, pp. 194–204. ISSN: 1524-0215. URL: https://pubmed.ncbi.nlm.nih.gov/17916792%20https://www.ncbi.nlm.nih.gov/pmc/articles/PMC2062560/.

[14] Morten Christoffersen, Simon Bolvig, and Erik Tüchsen. “Salt Effects on the Amide Hydrogen Exchange of Bovine Pancreatic Trypsin Inhibitor”. In: *Biochemistry* 35.7 (Jan. 1996). Number: 7, pp. 2309–2315. ISSN: 0006-2960, 1520-4995. DOI: 10.1021/bi951711q. URL: https://pubs.acs.org/doi/10.1021/bi951711q (visited on 08/08/2019).

[15] S. J. Coales, J. C. Tomasso, and Y. Hamuro. “Effects of electrospray capillary temperature on amide hydrogen exchange”. In: *Rapid Commun Mass Spectrom* 22.9 (2008). Type: Journal Article, pp. 1367–71. ISSN: 0951-4198 (Print) 0951-4198. DOI: 10.1002/rcm.3512.

[16] Stephen J. Coales et al. “Expansion of time window for mass spectrometric measurement of amide hydrogen/deuterium exchange reactions”. en. In: *Rapid Communications in Mass Spectrometry* 24.24 (2010). _eprint: https://onlinelibrary.wiley.com/doi/pdf/10.1002/rcm.4814, pp. 3585–3592. ISSN: 1097-0231. DOI: 10.1002/rcm.4814. URL: https://onlinelibrary.wiley.com/doi/abs/10.1002/rcm.4814 (visited on 09/14/2022).

[17] Gregory P. Connelly et al. “Isotope effects in peptide group hydrogen exchange”. In: *Proteins: Structure, Function, and Bioinformatics* 17.1 (1993). _eprint: https://www.onlinelibrary.wiley.com/doi/pdf/10.1002/prot.34 pp. 87–92. ISSN: 1097-0134. DOI: https://doi.org/10.1002/prot.340170111. URL: https://onlinelibrary.wiley.com/doi/abs/10.1002/prot.340170111 (visited on 01/11/2021).

[18] A. K. Covington, R. A. Robinson, and Roger G. Bates. “The Ionization Constant of Deuterium Oxide from 5 to 50°”. In: *The Journal of Physical Chemistry* 70.12 (Dec. 1, 1966). Number: 12, pp. 3820–3824. ISSN: 0022-3654. DOI: 10.1021/j100884a011. URL: https://doi.org/10.1021/j100884a011 (visited on 10/08/2019).

[19] Arthur K. Covington et al. “Use of the glass electrode in deuterium oxide and the relation between the standardized pD (paD) scale and the operational pH in heavy water”. In: *Analytical Chemistry* 40.4 (Apr. 1, 1968). Publisher: American Chemical Society, pp. 700–706. ISSN: 0003-2700. DOI: 10.1021/ac60260a013. URL: https://doi.org/10.1021/ac60260a013 (visited on 01/27/2021).

[20] Arthur K. Covington et al. “Use of the glass electrode in deuterium oxide and the relation between the standardized pD (paD) scale and the operational pH in heavy water”. In: *Analytical Chemistry* 40.4 (2002). Type: Journal Article, pp. 700–706. ISSN: 0003-2700 1520-6882. DOI: 10.1021/ac60260a013.

[21] F. E. Critchfield and J. B. Johnson. “Effect of Neutral Salts on pH of Acid Solutions”. In: *Analytical Chemistry* 31.4 (Apr. 1959). Number: 4, pp. 570–572. ISSN: 0003-2700, 1520-6882. DOI: 10.1021/ac50164a034. URL: https://pubs.acs.org/doi/abs/10.1021/ac50164a034 (visited on 10/02/2019).

[22] David J. Cummins et al. “Two-Site Evaluation of the Repeatability and Precision of an Automated Dual-Column Hydrogen/Deuterium Exchange Mass Spectrometry Platform”. In: *Analytical Chemistry* 88.12 (June 21, 2016). Number: 12, pp. 6607–6614. ISSN: 0003-2700, 1520-6882. DOI: 10.1021/acs.analchem.6b01650. URL: http://pubs.acs.org/doi/10.1021/acs.analchem.6b01650 (visited on 02/20/2019).

[23] D. Donnarumma et al. “The role of structural proteomics in vaccine development: recent advances and future prospects”. In: *Expert Rev Proteomics* 13.1 (2016). Type: Journal Article, pp. 55–68. ISSN: 1744-8387 (Electronic) 1478-9450 (Linking). DOI: 10.1586/14789450.2016.1121113. URL: https://www.ncbi.nlm.nih.gov/pubmed/26714563.

[24] Y. M. Efimova et al. “Stability of globular proteins in H2O and D2O”. eng. In: *Biopolymers* 85.3 (Feb. 2007), pp. 264–273. ISSN: 0006-3525. DOI: 10.1002/bip.20645.

[25] M. Eigen. “Proton Transfer, Acid-Base Catalysis, and Enzymatic Hydrolysis. Part I: ELEMENTARY PROCESSES”. en. In: *Angewandte Chemie International Edition in English* 3.1 (1964). _eprint: https://onlinelibrary.wiley.com/doi/pdf/10.1002/anie.196400011, pp. 1–19. ISSN: 1521-3773. DOI: 10.1002/anie.196400011. URL: https://onlinelibrary.wiley.com/doi/abs/10.1002/anie.196400011 (visited on 09/14/2022).

[26] Martin Lorenz Eisinger et al. “Ligand-induced conformational dynamics of the Escherichia coli Na+/H+ antiporter NhaA revealed by hydrogen/deuterium exchange mass spectrometry”. eng. In: *Proceedings of the National Academy of Sciences of the United States of America* 114.44 (Oct. 2017), pp. 11691–11696. ISSN: 1091-6490. DOI: 10.1073/pnas.1703422114.

[27] Johannes Elferich et al. “Determination of Histidine pK a Values in the Propeptides of Furin and Proprotein Convertase 1/3 Using Histidine Hydrogen−Deuterium Exchange Mass Spectrometry”. In: (2015). Type: Journal Article. DOI: 10.1021/acs.analchem.5b01721. URL: https://pubs.acs.org/sharingguidelines.

[28] John R. Engen and Thomas E. Wales. “Analytical Aspects of Hydrogen Exchange Mass Spectrometry”. eng. In: *Annual Review of Analytical Chemistry (Palo Alto, Calif.)* 8 (2015), pp. 127–148. ISSN: 1936-1335. DOI: 10.1146/annurev-anchem-062011-143113.

[29] J. J. Englander, J. R. Rogero, and S. W. Englander. “Protein hydrogen exchange studied by the fragment separation method”. In: *Analytical Biochemistry* 147.1 (May 15, 1985), pp. 234–244. ISSN: 0003-2697. DOI: 10.1016/0003-2697(85)90033-8.

[30] S. W. Englander. “Hydrogen exchange and mass spectrometry: A historical perspective”. In: *J Am Soc Mass Spectrom* 17.11 (2006). Type: Journal Article, pp. 1481–1489. ISSN: 1044-0305 (Print) 1044-0305. DOI: 10.1016/j.jasms.2006.06.006.

[31] S. W. Englander and A. Poulsen. “Hydrogen-tritium exchange of the random chain polypeptide”. In: *Biopolymers* 7.3 (1969). _eprint: https://onlinelibrary.wiley.com/doi/pdf/10.1002/bip.1969.360070309, pp. 379–393. ISSN: 1097-0282. DOI: https://doi.org/10.1002/bip.1969.360070309. URL: https://onlinelibrary.wiley.com/doi/abs/10.1002/bip.1969.360070309 (visited on 02/06/2021).

[32] S. W. Englander et al. “Hydrogen exchange: the modern legacy of Linderstrøm-Lang.” In: *Protein Science : A Publication of the Protein Society* 6.5 (May 1997). Number: 5, pp. 1101–1109. ISSN: 0961-8368. URL: https://www.ncbi.nlm.nih.gov/pmc/articles/PMC2143687/ (visited on 07/10/2018).

[33] S. W. Englander et al. “Protein Folding-How and Why: By Hydrogen Exchange, Fragment Separation, and Mass Spectrometry”. In: *Annu Rev Biophys* 45 (2016). Type: Journal Article, pp. 135–52. ISSN: 1936-1238 (Electronic) 1936-122X (Linking). DOI: 10.1146/annurev-biophys-062215-011121. URL: https://www.ncbi.nlm.nih.gov/pubmed/27145881.

[34] S. Walter Englander. “A Hydrogen Exchange Method Using Tritium and Sephadex: Its Application to Ribonuclease”. In: *Biochemistry* 2 (1963), pp. 798–807. ISSN: 0006-2960. URL: https://www.ncbi.nlm.nih.gov/pmc/articles/PMC3443402/ (visited on 09/14/2022).

[35] S. Walter Englander and Neville R. Kallenbach. “Hydrogen exchange and structural dynamics of proteins and nucleic acids”. In: *Quarterly Reviews of Biophysics* 16.4 (Nov. 1983). Number: 4, pp. 521–655. ISSN: 1469-8994, 0033-5835. DOI: 10.1017/S0033583500005217. URL: https://www.cambridge.org/core/journals/quarterly-reviews-of-biophysics/article/hydrogen-exchange-and-structural-dynamics-of-proteins-and-nucleic-acids/96B9DCAD3584DAE7A5AB5729244BCD69 (visited on 10/02/2019).

[36] M A Eriksson, T Härd, and L Nilsson. “On the pH dependence of amide proton exchange rates in proteins.” In: *Biophysical Journal* 69.2 (Aug. 1995). Number: 2, pp. 329–339. ISSN: 0006-3495. URL: https://www.ncbi.nlm.nih.gov/pmc/articles/PMC1236257/ (visited on 10/16/2018).

[37] Sonia Espinosa, Elisabeth Bosch, and Martí Rosés. "Retention of Ionizable Compounds on HPLC. 12. The Properties of Liquid Chromatography Buffers in Acetonitrile−Water Mobile Phases That Influence HPLC Retention". In: *Analytical Chemistry* 74.15 (Aug. 1, 2002). Publisher: American Chemical Society, pp. 3809–3818. ISSN: 0003-2700. DOI: 10.1021/ac020012y. URL: https://doi.org/10.1021/ac020012y (visited on 02/03/2021).

[38] Piotr G. Fajer, George M. Bou-Assaf, and Alan G. Marshall. "Improved Sequence Resolution by Global Analysis of Overlapped Peptides in Hydrogen/Deuterium Exchange Mass Spectrometry". In: *Journal of The American Society for Mass Spectrometry* 23.7 (2012). Type: Journal Article, pp. 1202–1208. ISSN: 1879-1123. DOI: 10.1007/s13361-012-0373-3. URL: https://doi.org/10.1007/s13361-012-0373-3.

[39] Jing Fang et al. "False EX1 signatures caused by sample carryover during HX MS analyses". In: *International journal of mass spectrometry* 302.1 (Apr. 30, 2011). Number: 1-3, pp. 19–25. ISSN: 1387-3806. DOI: 10.1016/j.ijms.2010.06.039. URL: https://www.ncbi.nlm.nih.gov/pmc/articles/PMC3106990/ (visited on 03/17/2020).

[40] M. Fang et al. "High-throughput hydrogen deuterium exchange mass spectrometry (HDX-MS) coupled with subzero-temperature ultrahigh pressure liquid chromatography (UPLC) separation for complex sample analysis". In: *Anal Chim Acta* 1143 (2021). Type: Journal Article, pp. 65–72. ISSN: 0003-2670. DOI: 10.1016/j.aca.2020.11.022.

[41] Ezio Fasoli, Amaris Ferrer, and Gabriel L Barletta. "Hydrogen/deuterium exchange study of subtilisin Carlsberg during prolonged exposure to organic solvents". In: *Biotechnology and bioengineering* 102.4 (Mar. 1, 2009), pp. 1025–1032. ISSN: 1097-0290. DOI: 10.1002/bit.22147. PMID: 18985614. URL: https://pubmed.ncbi.nlm.nih.gov/18985614.

[42] Federico Fogolari et al. "pKaShift Effects on Backbone Amide Base-Catalyzed Hydrogen Exchange Rates in Peptides". In: *Journal of the American Chemical Society* 120.15 (1998). Type: Journal Article, pp. 3735–3738. ISSN: 0002-7863. DOI: 10.1021/ja963133m. URL: https://dx.doi.org/10.1021/ja963133m.

[43] Elisa Gayán et al. "Effect of pressure-induced changes in the ionization equilibria of buffers on inactivation of Escherichia coli and Staphylococcus aureus by high hydrostatic pressure". eng. In: *Applied and Environmental Microbiology* 79.13 (July 2013), pp. 4041–4047. ISSN: 1098-5336. DOI: 10.1128/AEM.00469-13.

[44] Paul K. Glasoe and F. A. Long. "USE OF GLASS ELECTRODES TO MEASURE ACIDITIES IN DEUTERIUM OXIDE1,2". In: *The Journal of Physical Chemistry* 64.1 (Jan. 1, 1960). Publisher: American Chemical Society, pp. 188–190. ISSN: 0022-3654. DOI: 10.1021/j100830a521. URL: https://doi.org/10.1021/j100830a521 (visited on 01/27/2021).

[45] Devrishi Goswami et al. "Time window expansion for HDX analysis of an intrinsically disordered protein". In: *Journal of the American Society for Mass Spectrometry* 24.10 (Oct. 2013). Number: 10, pp. 1584–1592. ISSN: 1044-0305. DOI: 10.1007/s13361-013-0669-y. URL: https://www.ncbi.nlm.nih.gov/pmc/articles/PMC3773365/ (visited on 10/16/2018).

[46] Miklos Guttman et al. "Analysis of overlapped and noisy hydrogen/deuterium exchange mass spectra". In: *Journal of the American Society for Mass Spectrometry* 24.12 (Dec. 2013). Number: 12, pp. 1906–1912. ISSN: 1879-1123. DOI: 10.1007/s13361-013-0727-5.

[47] SD Hamann. "Chemical equilibria in condensed systems". In: *High Pressure Physics and Chemistry, Volume 2* 2 (1963). Type: Journal Article, p. 131.

[48] Yoshitomo Hamuro. "Determination of Equine Cytochrome c Backbone Amide Hydrogen/Deuterium Exchange Rates by Mass Spectrometry Using a Wider Time Window and Isotope Envelope". In: *Journal of The American Society for Mass Spectrometry* 28.3 (Mar. 1, 2017). Number: 3, pp. 486–497. ISSN: 1879-1123. DOI: 10.1007/s13361-016-1571-1. URL: https://doi.org/10.1007/s13361-016-1571-1 (visited on 05/18/2019).

[49] Yoshitomo Hamuro. "Determination of Equine Cytochrome c Backbone Amide Hydrogen/Deuterium Exchange Rates by Mass Spectrometry Using a Wider Time Window and Isotope Envelope". In: *Journal of The American Society for Mass Spectrometry* 28.3 (Mar. 2017). Number: 3, pp. 486–497. ISSN: 1044-0305, 1879-1123. DOI: 10.1007/s13361-016-1571-1. URL: http://link.springer.com/10.1007/s13361-016-1571-1 (visited on 09/15/2019).

[50] Yoshitomo Hamuro. "Tutorial: Chemistry of Hydrogen/Deuterium Exchange Mass Spectrometry". In: *Journal of the American Society for Mass Spectrometry* 32.1 (Jan. 6, 2021). Publisher: American Society for Mass Spectrometry. Published by the American Chemical Society. All rights reserved., pp. 133–151. ISSN: 1044-0305. DOI: 10.1021/jasms.0c00260. URL: https://doi.org/10.1021/jasms.0c00260 (visited on 01/12/2021).

[51] Yoshitomo Hamuro and Sook Yen. "Determination of Backbone Amide Hydrogen Exchange Rates of Cytochrome c Using Partially Scrambled Electron Transfer Dissociation Data". In: *J. Am. Soc. Mass Spectrom* 29 (2018). Type: Journal Article, pp. 989–1001. ISSN: 1336101818923. DOI: 10.1007/s13361-018-1892-3.

[52] H. S. Harned and B. B. Owen. *The Physical Chemistry of Electrolytic Solutions*. Reinhold Publishing Corporation, 1950. URL: https://books.google.com/books?id=CPwgAAAAMAAJ.

[53] Naoka Hayashi et al. "Imidazole C-2 Hydrogen/Deuterium Exchange Reaction at Histidine for Probing Protein Structure and Function with MALDI Mass Spectrometry". In: *Biochemistry* 53.11 (Mar. 25, 2014). Number: 11, pp. 1818–1826. ISSN: 0006-2960. DOI: 10.1021/bi401260f. URL: https://www.ncbi.nlm.nih.gov/pmc/articles/PMC4465451/ (visited on 09/22/2019).

[54] T. K. Hitchens and R. G. Bryant. "Pressure dependence of amide hydrogen-deuterium exchange rates for individual sites in T4 lysozyme". eng. In: *Biochemistry* 37.17 (Apr. 1998), pp. 5878–5887. ISSN: 0006-2960. DOI: 10.1021/bi972950b.

[55] Andrew N. Hoofnagle, Katheryn A. Resing, and Natalie G. Ahn. "Practical methods for deuterium exchange/mass spectrometry". eng. In: *Methods in Molecular Biology (Clifton, N.J.)* 250 (2004), pp. 283–298. ISSN: 1064-3745. DOI: 10.1385/1-59259-671-1:283.

[56] Andrew N. Hoofnagle, Katheryn A. Resing, and Natalie G. Ahn. "Protein analysis by hydrogen exchange mass spectrometry". eng. In: *Annual Review of Biophysics and Biomolecular Structure* 32 (2003), pp. 1–25. ISSN: 1056-8700. DOI: 10.1146/annurev.biophys.32.110601.142417.

[57] Damian Houde and Steven A. Berkowitz. "The Role of Hydrogen Exchange Mass Spectrometry in Assessing the Consistency and Comparability of the Higher-Order Structure of Protein Biopharmaceuticals". In: *Hydrogen Exchange Mass Spectrometry of Proteins*. John Wiley & Sons, Ltd, 2016, pp. 225–246. ISBN: 978-1-118-70374-8. DOI: 10.1002/9781118703748.ch13. URL: https://onlinelibrary.wiley.com/doi/abs/10.1002/9781118703748.ch13 (visited on 10/03/2019).

[58] Damian Houde and Stephen J Demarest. "Fine Details of IGF-1R Activation, Inhibition, and Asymmetry Determined by Associated Hydrogen /Deuterium-Exchange and Peptide Mass Mapping". In: *Structure* 19.6 (2011). Type: Journal Article, pp. 890–900. ISSN: 0969-2126. DOI: https://doi.org/10.1016/j.str.2011.03.014. URL: https://www.sciencedirect.com/science/article/pii/S0969212611001389.

[59] Jeffrey W. Hudgens, Richard Y.-C. Huang, and Emma D'Ambro. "Method Validation and Standards in Hydrogen Exchange Mass Spectrometry". In: *Hydrogen Exchange Mass Spectrometry of Proteins*. John Wiley & Sons, Ltd, 2016, pp. 55–72. ISBN: 978-1-118-70374-8. DOI: 10.1002/9781118703748.ch4. URL: https://onlinelibrary.wiley.com/doi/abs/10.1002/9781118703748.ch4 (visited on 10/03/2019).

[60] Jeffrey W. Hudgens et al. "Interlaboratory Comparison of Hydrogen–Deuterium Exchange Mass Spectrometry Measurements of the Fab Fragment of NISTmAb". In: *Analytical Chemistry* 91.11 (June 4, 2019). Number: 11, pp. 7336–7345. ISSN: 0003-2700. DOI: 10.1021/acs.analchem.9b01100. URL: https://doi.org/10.1021/acs.analchem.9b01100 (visited on 09/06/2019).

[61] G. A. Hutcheon, M. C. Parker, and B. D. Moore. "Measuring enzyme motility in organic media using novel H-D exchange methodology". In: *Biotechnology and Bioengineering* 70.3 (Nov. 5, 2000), pp. 262–269. ISSN: 0006-3592.

[62] A. Hvidt and S. O. Nielsen. "Hydrogen exchange in proteins". eng. In: *Advances in Protein Chemistry* 21 (1966), pp. 287–386. ISSN: 0065-3233. DOI: 10.1016/s0065-3233(08)60129-1.

[63] Aase Hvidt and K. Linderstrøm-Lang. "Exchange of hydrogen atoms in insulin with deuterium atoms in aqueous solutions". In: *Biochimica et Biophysica Acta* 14 (Jan. 1954), pp. 574–575. ISSN: 00063002. DOI: 10.1016/0006-3002(54)90241-3. URL: http://linkinghub.elsevier.com/retrieve/pii/0006300254902413 (visited on 10/16/2018).

[64] J A Illingworth. "A common source of error in pH measurements". In: *Biochemical Journal* 195.1 (Apr. 1, 1981), pp. 259–262. ISSN: 0264-6021. DOI: 10.1042/bj1950259. URL: https://doi.org/10.1042/bj1950259 (visited on 01/26/2021).

[65] J. Inczédy et al. *Compendium of Analytical Nomenclature: Definitive Rules 1997*. Type: Book. Blackwell Science, 1998. ISBN: 978-0-86542-615-3. URL: https://books.google.com/books?id=vF5jQgAACAAJ.

[66] Neil S. Isaacs. *Liquid phase high pressure chemistry*. John Wiley & Sons Incorporated, 1981. ISBN: 0-471-27849-1.

[67] Ellie I. James et al. "Advances in Hydrogen/Deuterium Exchange Mass Spectrometry and the Pursuit of Challenging Biological Systems". In: *Chemical Reviews* 122.8 (Apr. 27, 2022). Publisher: American Chemical Society, pp. 7562–7623. ISSN: 0009-2665. DOI: 10.1021/acs.chemrev.1c00279. URL: https://doi.org/10.1021/acs.chemrev.1c00279 (visited on 07/20/2022).

[68] Pernille Foged Jensen and Kasper D. Rand. "Gas-Phase Fragmentation of Peptides to Increase the Spatial Resolution of the Hydrogen Exchange Mass Spectrometry Experiment". In: *Hydrogen Exchange Mass Spectrometry of Proteins*. John Wiley & Sons, Ltd, 2016, pp. 127–147. ISBN: 978-1-118-70374-8. DOI: 10.1002/9781118703748.ch8. URL: https://onlinelibrary.wiley.com/doi/abs/10.1002/9781118703748.ch8 (visited on 10/03/2019).

[69] Pernille Foged Jensen and Kasper D. Rand. "Hydrogen Exchange". In: *Hydrogen Exchange Mass Spectrometry of Proteins*. John Wiley & Sons, Ltd, 2016, pp. 1–17. ISBN: 978-1-118-70374-8. DOI: 10.1002/9781118703748.ch1. URL: https://onlinelibrary.wiley.com/doi/abs/10.1002/9781118703748.ch1 (visited on 10/03/2019).

[70] Pernille Foged Jensen et al. "Affinity capture of biotinylated proteins at acidic conditions to facilitate hydrogen/deuterium exchange mass spectrometry analysis of multimeric protein complexes". In: *Analytical Chemistry* 85.15 (Aug. 6, 2013). Number: 15, pp. 7052–7059. ISSN: 1520-6882. DOI: 10.1021/ac303442y.

[71] Viswanatham Katta and Brain T. Chait. "Hydrogen/deuterium exchange electrospray ionization mass spectrometry: a method for probing protein conformational changes in solution". en. In: *Journal of the American Chemical Society* 115.14 (July 1993), pp. 6317–6321. ISSN: 0002-7863, 1520-5126. DOI: 10.1021/ja00067a054. URL: https://pubs.acs.org/doi/abs/10.1021/ja00067a054 (visited on 09/14/2022).

[72] C. D. Kennedy. "Ionic strength and the dissociation of acids". In: *Biochemical Education* 18.1 (Jan. 1, 1990). Number: 1, pp. 35–40. ISSN: 1879-1468. DOI: 10.1016/0307-4412(90)90017-I. URL: https://iubmb.onlinelibrary.wiley.com/doi/10.1016/0307-4412(90)90017-I (visited on 09/29/2019).

[73] T. R. Keppel et al. "An efficient and inexpensive refrigerated LC system for H/D exchange mass spectrometry". In: *J Am Soc Mass Spectrom* 22.8 (2011). Type: Journal Article, pp. 1472–6. ISSN: 1044-0305. DOI: 10.1007/s13361-011-0152-6.

[74] Peter S. Kim and Robert L. Baldwin. "Influence of charge on the rate of amide proton exchange". In: *Biochemistry* 21.1 (Jan. 1982). Publisher: American Chemical Society, pp. 1–5. ISSN: 0006-2960. DOI: 10.1021/bi00530a001. URL: https://doi.org/10.1021/bi00530a001 (visited on 09/14/2022).

[75] I. M. Klotz and B. H. Frank. "DEUTERIUM–HYDROGEN EXCHANGE IN AMIDE N–H GROUPS". eng. In: *Journal of the American Chemical Society* 87 (June 1965), pp. 2721–2728. ISSN: 0002-7863. DOI: 10.1021/ja01090a033.

[76] B. A. Krantz et al. "D/H amide kinetic isotope effects reveal when hydrogen bonds form during protein folding". eng. In: *Nature Structural Biology* 7.1 (Jan. 2000), pp. 62–71. ISSN: 1072-8368. DOI: 10.1038/71265.

[77] Artur Kr żel and Wojciech Bal. “A formula for correlating pKa values determined in D2O and H2O”. In: *Journal of Inorganic Biochemistry* 98.1 (Jan. 1, 2004), pp. 161–166. ISSN: 0162-0134. DOI: 10.1016/j.jinorgbio.2003.10.001. URL: http://www.sciencedirect.com/science/article/pii/S0162013403004008 (visited on 01/27/2021).

[78] Woon Ki Lim, Jörg Rösgen, and S. Walter Englander. “Urea, but not guanidinium, destabilizes proteins by forming hydrogen bonds to the peptide group”. In: *Proceedings of the National Academy of Sciences of the United States of America* 106.8 (Feb. 2009), pp. 2595–2600. ISSN: 0027-8424. DOI: 10.1073/pnas.0812588106. URL: https://www.ncbi.nlm.nih.gov/pmc/articles/PMC2650309/ (visited on 09/14/2022).

[79] D. A. Lown, H. R. Thirsk, and Lord Wynne-Jones. “Effect of pressure on ionization equilibria in water at 25°C”. en. In: *Transactions of the Faraday Society* 64.0 (Jan. 1968). Publisher: The Royal Society of Chemistry, pp. 2073–2080. ISSN: 0014-7672. DOI: 10.1039/TF9686402073. URL: https://pubs.rsc.org/en/content/articlelanding/1968/tf/tf9686402073 (visited on 09/14/2022).

[80] Ranajoy Majumdar et al. “Minimizing carry-over in an online pepsin digestion system used for the H/D exchange mass spectrometric analysis of an IgG1 monoclonal antibody”. In: *Journal of the American Society for Mass Spectrometry* 23.12 (Dec. 2012). Number: 12, pp. 2140–2148. ISSN: 1879-1123. DOI: 10.1007/s13361-012-0485-9.

[81] G. S. Manning. “The molecular theory of polyelectrolyte solutions with applications to the electrostatic properties of polynucleotides”. eng. In: *Quarterly Reviews of Biophysics* 11.2 (May 1978), pp. 179–246. ISSN: 0033-5835. DOI: 10.1017/s0033583500002031.

[82] Yizhak Marcus. “Effect of Ions on the Structure of Water: Structure Making and Breaking”. In: *Chemical Reviews* 109.3 (Mar. 11, 2009). Publisher: American Chemical Society, pp. 1346–1370. ISSN: 0009-2665. DOI: 10.1021/cr8003828. URL: https://doi.org/10.1021/cr8003828 (visited on 01/10/2021).

[83] R. Bruce Martin. “O-protonation of amides in dilute acids”. en. In: *Journal of the Chemical Society, Chemical Communications* 13 (Jan. 1972). Publisher: The Royal Society of Chemistry, pp. 793–794. ISSN: 0022-4936. DOI: 10.1039/C39720000793. URL: https://pubs.rsc.org/en/content/articlelanding/1972/c3/c39720000793 (visited on 09/14/2022).

[84] Glenn R. Masson et al. “Recommendations for performing, interpreting and reporting hydrogen deuterium exchange mass spectrometry (HDX-MS) experiments”. In: *Nature methods* 16.7 (June 28, 2019). Number: 7, pp. 595–602. ISSN: 1548-7091. DOI: 10.1038/s41592-019-0459-y. URL: https://www.ncbi.nlm.nih.gov/pmc/articles/PMC6614034/ (visited on 09/11/2019).

[85] M. Miyagi et al. “Histidine hydrogen-deuterium exchange mass spectrometry for probing the microenvironment of histidine residues in dihydrofolate reductase”. In: *PLoS One* 6.2 (2011). Type: Journal Article, e17055. ISSN: 1932-6203. DOI: 10.1371/journal.pone.0017055.

[86] Hossein Mohammadiarani et al. “Interpreting Hydrogen-Deuterium Exchange Events in Proteins Using Atomistic Simulations: Case Studies on Regulators of G-Protein Signaling Proteins”. eng. In: *The Journal of Physical Chemistry. B* 122.40 (Oct. 2018), pp. 9314–9323. ISSN: 1520-5207. DOI: 10.1021/acs.jpcb.8b07494.

[87] R. S. Molday, S. W. Englander, and R. G. Kallen. “Primary structure effects on peptide group hydrogen exchange”. In: *Biochemistry* 11.2 (Jan. 18, 1972). Publisher: American Chemical Society, pp. 150–158. ISSN: 0006-2960. DOI: 10.1021/bi00752a003. URL: https://doi.org/10.1021/bi00752a003 (visited on 01/11/2021).

[88] Robert S. Molday and Roland G. Kallen. “Substituent effects on amide hydrogen exchange rates in aqueous solution”. In: *Journal of the American Chemical Society* 94.19 (Sept. 1972). Number: 19, pp. 6739–6745. ISSN: 0002-7863. DOI: 10.1021/ja00774a029. URL: http://pubs.acs.org/doi/abs/10.1021/ja00774a029 (visited on 02/11/2019).

[89] Jamie A Moroco and John R Engen. “Replication in bioanalytical studies with HDX MS: aim as high as possible”. In: *Bioanalysis* 7.9 (May 2015). Number: 9, pp. 1065–1067. ISSN: 1757-6180. DOI: 10.4155/bio.15.46. URL: https://www.ncbi.nlm.nih.gov/pmc/articles/PMC4837975/ (visited on 09/06/2019).

[90] Taylor A. Murphree et al. “Imidazolium Compounds as Internal Exchange Reporters for Hydrogen/Deuterium Exchange by Mass Spectrometry”. In: *Analytical Chemistry* 92.14 (July 21, 2020). Number: 14 Publisher: American Chemical Society, pp. 9830–9837. ISSN: 0003-2700. DOI: 10.1021/acs.analchem.0c01328. URL: https://doi.org/10.1021/acs.analchem.0c01328 (visited on 09/18/2020).

[91] Mohammed A Al-Naqshabandi and David D Weis. “Quantifying Protection in Disordered Proteins Using Millisecond Hydrogen Exchange-Mass Spectrometry and Peptic Reference Peptides”. eng. In: *Biochemistry* 56.31 (Aug. 2017), pp. 4064–4072. ISSN: 1520-4995. DOI: 10.1021/acs.biochem.6b01312. URL: https://doi.org/10.1021/acs.biochem.6b01312 (visited on 09/14/2022).

[92] Z. E. Nazari et al. “Rapid Conformational Analysis of Protein Drugs in Formulation by Hydrogen/Deuterium Exchange Mass Spectrometry”. In: *J Pharm Sci* 105.11 (2016). Type: Journal Article, pp. 3269–3277. ISSN: 0022-3549. DOI: 10.1016/j.xphs.2016.07.006.

[93] David Nguyen et al. “Reference Parameters for Protein Hydrogen Exchange Rates”. In: *Journal of the American Society for Mass Spectrometry* 29.9 (Sept. 1, 2018). Publisher: American Society for Mass Spectrometry. Published by the American Chemical Society. All rights reserved., pp. 1936–1939. ISSN: 1044-0305. DOI: 10.1021/jasms.8b05911. URL: https://pubs.acs.org/doi/abs/10.1021/jasms.8b05911 (visited on 01/11/2021).

[94] Benton Brooks Owen. “DIRECT MEASUREMENT OF THE PRIMARY, SECONDARY AND TOTAL MEDIUM EFFECTS OF ACETIC ACID”. In: *Journal of the American Chemical Society* 54.5 (May 1, 1932). Number: 5, pp. 1758–1769. ISSN: 0002-7863. DOI: 10.1021/ja01344a006. URL: https://doi.org/10.1021/ja01344a006 (visited on 10/02/2019).

[95] Juan M. Padró et al. “Effect of temperature and solvent composition on acid dissociation equilibria, I: Sequenced (s)(s)pKa determination of compounds commonly used as buffers in high performance liquid chromatography coupled to mass spectroscopy detection”. In: *Analytica Chimica Acta* 725 (May 6, 2012), pp. 87–94. ISSN: 1873-4324. DOI: 10.1016/j.aca.2012.03.015.

[96] J. Pan et al. “Subzero temperature chromatography and top-down mass spectrometry for protein higher-order structure characterization: method validation and application to therapeutic antibodies”. In: *J Am Chem Soc* 136.37 (2014). Type: Journal Article, pp. 13065–71. ISSN: 1520-5126 (Electronic) 0002-7863 (Linking). DOI: 10.1021/ja507880w. URL: https://www.ncbi.nlm.nih.gov/pubmed/25152011.

[97] Charles L. Perrin. “Proton exchange in amides: Surprises from simple systems”. In: *Accounts of Chemical Research* 22.8 (Aug. 1, 1989). Publisher: American Chemical Society, pp. 268–275. ISSN: 0001-4842. DOI: 10.1021/ar00164a002. URL: https://doi.org/10.1021/ar00164a002 (visited on 01/11/2021).

[98] Gregory F. Pirrone et al. “Use of MALDI-MS Combined with Differential Hydrogen-Deuterium Exchange for Semiautomated Protein Global Conformational Screening”. eng. In: *Analytical Chemistry* 89.16 (Aug. 2017), pp. 8351–8357. ISSN: 1520-6882. DOI: 10.1021/acs.analchem.7b01590.

[99] Simo P. Porras et al. “Medium Effect (Transfer Activity Coefficient) of Methanol and Acetonitrile on -Cyclodextrin/Benzoate Complexation in Capillary Zone Electrophoresis”. In: *Analytical Chemistry* 75.7 (Apr. 1, 2003). Number: 7, pp. 1645–1651. ISSN: 0003-2700. DOI: 10.1021/ac026407z. URL: https://doi.org/10.1021/ac026407z (visited on 10/03/2019).

[100] Charulata B. Prasannan, Antonio Artigues, and Aron W. Fenton. “Monitoring allostery in D2O: a necessary control in studies using hydrogen/deuterium exchange to characterize allosteric regulation”. eng. In: *Analytical and Bioanalytical Chemistry* 401.3 (Aug. 2011), pp. 1083–1086. ISSN: 1618-2650. DOI: 10.1007/s00216-011-5133-x.

[101] R. Jason Quinlan and Gregory D. Reinhart. “Baroresistant buffer mixtures for biochemical analyses”. eng. In: *Analytical Biochemistry* 341.1 (June 2005), pp. 69–76. ISSN: 0003-2697. DOI: 10.1016/j.ab.2005.03.002.

[102] J. J. Rosa and F. M. Richards. “An experimental procedure for increasing the structural resolution of chemical hydrogen-exchange measurements on proteins: application to ribonuclease S peptide”. eng. In: *Journal of Molecular Biology* 133.3 (Sept. 1979), pp. 399–416. ISSN: 0022-2836. DOI: 10.1016/0022-2836(79)90400-5.

[103] Jörg Rösgen et al. “Statistical Thermodynamic Approach to the Chemical Activities in Two-Component Solutions”. In: *The Journal of Physical Chemistry B* 108.6 (Feb. 2004). Publisher: American Chemical Society, pp. 2048–2055. ISSN: 1520-6106. DOI: 10.1021/jp036325u. URL: https://doi.org/10.1021/jp036325u (visited on 09/14/2022).

[104] Farai I. Rusinga and David D. Weis. “Automated Strong Cation-Exchange Cleanup To Remove Macromolecular Crowding Agents for Protein Hydrogen Exchange Mass Spectrometry”. eng. In: *Analytical Chemistry* 89.2 (Jan. 2017), pp. 1275–1282. ISSN: 1520-6882. DOI: 10.1021/acs.analchem.6b04057.

[105] K. Sarmini and E. Kenndler. “Ionization constants of weak acids and bases in organic solvents”. eng. In: *Journal of Biochemical and Biophysical Methods* 38.2 (Jan. 1999), pp. 123–137. ISSN: 0165-022X. DOI: 10.1016/s0165-022x(98)00033-5.

[106] Jae C. Schwartz, Michael W. Senko, and John E. P. Syka. “A two-dimensional quadrupole ion trap mass spectrometer”. In: *Journal of the American Society for Mass Spectrometry* 13.6 (June 2002). Number: 6, pp. 659–669. ISSN: 1044-0305. DOI: 10.1016/S1044-0305(02)00384-7.

[107] J. G. Sheff, M. Rey, and D. C. Schriemer. “Peptide-column interactions and their influence on back exchange rates in hydrogen/deuterium exchange-MS”. In: *J Am Soc Mass Spectrom* 24.7 (2013). Type: Journal Article, pp. 1006–15. ISSN: 1879-1123 (Electronic) 1044-0305 (Linking). DOI: 10.1007/s13361-013-0639-4. URL: https://www.ncbi.nlm.nih.gov/pubmed/23649779.

[108] Joey G. Sheff, Martial Rey, and David C. Schriemer. “Peptide–Column Interactions and Their Influence on Back Exchange Rates in Hydrogen/Deuterium Exchange-MS”. In: *Journal of the American Society for Mass Spectrometry* 24.7 (July 1, 2013). Publisher: American Society for Mass Spectrometry. Published by the American Chemical Society. All rights reserved., pp. 1006–1015. ISSN: 1044-0305. DOI: 10.1021/jasms.8b04561. URL: https://pubs.acs.org/doi/abs/10.1021/jasms.8b04561.

[109] Joey G. Sheff and David C. Schriemer. “Toward Standardizing Deuterium Content Reporting in Hydrogen Exchange-MS”. In: *Analytical Chemistry* 86.24 (Dec. 16, 2014). Number: 24, pp. 11962–11965. ISSN: 0003-2700, 1520-6882. DOI: 10.1021/ac5034424. URL: http://pubs.acs.org/doi/10.1021/ac5034424 (visited on 02/11/2019).

[110] David William Shoesmith and Woon Lee. “The ionization constant of heavy water (D2O) in the temperature range 298 to 523 K”. In: *Canadian Journal of Chemistry* 54.22 (Nov. 1976). Publisher: NRC Research Press, pp. 3553–3558. ISSN: 0008-4042. DOI: 10.1139/v76-511. URL: https://cdnsciencepub.com/doi/10.1139/v76-511 (visited on 09/14/2022).

[111] Modupeola A. Sowole and Lars Konermann. “Effects of protein-ligand interactions on hydrogen/deuterium exchange kinetics: canonical and noncanonical scenarios”. eng. In: *Analytical Chemistry* 86.13 (July 2014), pp. 6715–6722. ISSN: 1520-6882. DOI: 10.1021/ac501849n.

[112] Xavier Subirats, Martí Rosés, and Elisabeth Bosch. “On the Effect of Organic Solvent Composition on the pH of Buffered HPLC Mobile Phases and the p K_a of Analytes—A Review”. In: *Separation & Purification Reviews* 36.3 (Aug. 2007). Number: 3, pp. 231–255. ISSN: 1542-2119, 1542-2127. DOI: 10.1080/15422110701539129. URL: http://www.tandfonline.com/doi/abs/10.1080/15422110701539129 (visited on 02/11/2019).

[113] Shisheng Sun et al. “Inhibition of protein carbamylation in urea solution using ammonium-containing buffers”. English (US). In: *Analytical biochemistry* 446.1 (Feb. 2014). Publisher: Academic Press Inc., pp. 76–81. ISSN: 0003-2697. DOI: 10.1016/j.ab.2013.10.024. URL: https://jhu.pure.elsevier.com/en/publications/inhibition-of-protein-carbamylation-in-urea-solution-using-ammoni-4 (visited on 09/14/2022).

[114] Ronald T. Toth et al. “Correction to Empirical Correction for Differences in Chemical Exchange Rates in Hydrogen Exchange-Mass Spectrometry Measurements”. In: *Analytical Chemistry* 89.24 (Dec. 19, 2017). Number: 24, pp. 13673–13673. ISSN: 0003-2700. DOI: 10.1021/acs.analchem.7b04690. URL: https://doi.org/10.1021/acs.analchem.7b04690 (visited on 09/04/2019).

[115] Ronald T. Toth et al. “Empirical Correction for Differences in Chemical Exchange Rates in Hydrogen Exchange-Mass Spectrometry Measurements”. In: *Analytical Chemistry* 89.17 (Sept. 5, 2017). Number: 17, pp. 8931–8941. ISSN: 0003-2700. DOI: 10.1021/acs.analchem.7b01396. URL: https://doi.org/10.1021/acs.analchem.7b01396 (visited on 10/16/2018).

[116] Erik Tüchsen and Clare Woodward. "Mechanism of surface peptide proton exchange in bovine pancreatic trypsin inhibitor salt effects and O-protonation". In: *Journal of Molecular Biology* 185.2 (Sept. 20, 1985). Number: 2, pp. 421–430. ISSN: 0022-2836. DOI: 10.1016/0022-2836(85)90413-9. URL: http://www.sciencedirect.com/science/article/pii/0022283685904139 (visited on 10/02/2019).

[117] Santosh G. Valeja, Mark R. Emmett, and Alan G. Marshall. "Polar Aprotic Modifiers for Chromatographic Separation and Back-Exchange Reduction for Protein Hydrogen/Deuterium Exchange Monitored by Fourier Transform Ion Cyclotron Resonance Mass Spectrometry". In: *Journal of The American Society for Mass Spectrometry* 23.4 (Apr. 1, 2012), pp. 699–707. ISSN: 1879-1123. DOI: 10.1007/s13361-011-0329-z. URL: https://doi.org/10.1007/s13361-011-0329-z (visited on 01/10/2021).

[118] John D. Venable et al. "Subzero temperature chromatography for reduced back-exchange and improved dynamic range in amide hydrogen/deuterium exchange mass spectrometry". eng. In: *Analytical Chemistry* 84.21 (Nov. 2012), pp. 9601–9608. ISSN: 1520-6882. DOI: 10.1021/ac302488h.

[119] Alina E. Voinescu et al. "Similarity of salt influences on the pH of buffers, polyelectrolytes, and proteins". eng. In: *The Journal of Physical Chemistry. B* 110.17 (May 2006), pp. 8870–8876. ISSN: 1520-6106. DOI: 10.1021/jp0600209.

[120] Thomas E. Wales, Michael J. Eggertson, and John R. Engen. "Considerations in the analysis of hydrogen exchange mass spectrometry data". In: *Methods in molecular biology (Clifton, N.J.)* 1007 (2013), pp. 263–288. ISSN: 1064-3745. DOI: 10.1007/978-1-62703-392-3_11. URL: https://www.ncbi.nlm.nih.gov/pmc/articles/PMC3713502/ (visited on 05/18/2019).

[121] Benjamin T. Walters et al. "Minimizing Back Exchange in the Hydrogen Exchange-Mass Spectrometry Experiment". In: *Journal of The American Society for Mass Spectrometry* 23.12 (Dec. 1, 2012), pp. 2132–2139. ISSN: 1879-1123. DOI: 10.1007/s13361-012-0476-x. URL: https://doi.org/10.1007/s13361-012-0476-x (visited on 01/10/2021).

[122] Michael J. Watson et al. "Simple Platform for Automating Decoupled LC-MS Analysis of Hydrogen/Deuterium Exchange Samples". eng. In: *Journal of the American Society for Mass Spectrometry* 32.2 (Feb. 2021), pp. 597–600. ISSN: 1879-1123. DOI: 10.1021/jasms.0c00341.

[123] H. Wei et al. "Using hydrogen/deuterium exchange mass spectrometry to study conformational changes in granulocyte colony stimulating factor upon PEGylation". In: *J Am Soc Mass Spectrom* 23.3 (2012). Type: Journal Article, pp. 498–504. ISSN: 1044-0305 (Print) 1044-0305. DOI: 10.1007/s13361-011-0310-x.

[124] David D. Weis et al. "Identification and characterization of EX1 kinetics in H/D exchange mass spectrometry by peak width analysis". eng. In: *Journal of the American Society for Mass Spectrometry* 17.11 (Nov. 2006), pp. 1498–1509. ISSN: 1044-0305. DOI: 10.1016/j.jasms.2006.05.014.

[125] G. M. West et al. "Protein conformation ensembles monitored by HDX reveal a structural rationale for abscisic acid signaling protein affinities and activities". In: *Structure* 21.2 (2013). Type: Journal Article, pp. 229–35. ISSN: 0969-2126 (Print) 0969-2126. DOI: 10.1016/j.str.2012.12.001.

[126] Y. Wu, J. R. Engen, and W. B. Hobbins. "Ultra performance liquid chromatography (UPLC) further improves hydrogen/deuterium exchange mass spectrometry". In: *J Am Soc Mass Spectrom* 17.2 (2006). Type: Journal Article, pp. 163–7. ISSN: 1044-0305 (Print) 1044-0305. DOI: 10.1016/j.jasms.2005.10.009.

[127] D. Yang et al. "Efficient Qualitative and Quantitative Determination of Antigen-induced Immune Responses". In: *J Biol Chem* 291.31 (2016). Type: Journal Article, pp. 16361–74. ISSN: 0021-9258 (Print) 0021-9258. DOI: 10.1074/jbc.M116.736660.

[128] Jia-Zhen Yang and Wei-Guo Xu. "Medium Effect of an Organic Solvent on the Activity Coefficients of HCl Consistent with Pitzer's Electrolyte Solution Theory". In: *Journal of Solution Chemistry* 34.1 (Jan. 1, 2005). Number: 1, pp. 71–76. ISSN: 1572-8927. DOI: 10.1007/s10953-005-2073-0. URL: https://doi.org/10.1007/s10953-005-2073-0 (visited on 10/02/2019).

[129] Hui-Min Zhang et al. “Fast reversed-phase liquid chromatography to reduce back exchange and increase throughput in H/D exchange monitored by FT-ICR mass spectrometry”. In: *Journal of the American Society for Mass Spectrometry* 20.3 (2009). Type: Journal Article, pp. 520–524. ISSN: 1879-1123 1044-0305. DOI: 10.1016/j.jasms.2008.11.010. URL: https://pubmed.ncbi.nlm.nih.gov/19095461%20https://www.ncbi.nlm.nih.gov/pmc/articles/PMC2673454/.

[130] J. Zhang, D. Goswami, and Z. Zhang. “New Insight into Differences in Intrinsic HDX Rates at Different pH and Temperature”. In: *67th ASMS Conference on Mass Spectrometry and Allied Topics*. Type: Conference Proceedings.

[131] Jianyu Zhang et al. “Hydrogen deuterium exchange defines catalytically linked regions of protein flexibility in the catechol O-methyltransferase reaction”. eng. In: *Proceedings of the National Academy of Sciences of the United States of America* 117.20 (May 2020), pp. 10797–10805. ISSN: 1091-6490. DOI: 10.1073/pnas.1917219117.

[132] Q. Zhang et al. “Rapid screening for potential epitopes reactive with a polycolonal antibody by solution-phase H/D exchange monitored by FT-ICR mass spectrometry”. In: *J Am Soc Mass Spectrom* 24.7 (2013). Type: Journal Article, pp. 1016–25. ISSN: 1044-0305. DOI: 10.1007/s13361-013-0644-7.

[133] Z. Zhang and D. L. Smith. “Determination of amide hydrogen exchange by mass spectrometry: a new tool for protein structure elucidation”. In: *Protein Science: A Publication of the Protein Society* 2.4 (Apr. 1993), pp. 522–531. ISSN: 0961-8368. DOI: 10.1002/pro.5560020404.

[134] Zhongqi Zhang, Aming Zhang, and Gang Xiao. “Improved Protein Hydrogen/Deuterium Exchange Mass Spectrometry Platform with Fully Automated Data Processing”. In: *Analytical Chemistry* 84.11 (June 5, 2012). Number: 11, pp. 4942–4949. ISSN: 0003-2700, 1520-6882. DOI: 10.1021/ac300535r. URL: http://pubs.acs.org/doi/abs/10.1021/ac300535r (visited on 10/16/2018).